

One-loop analysis of the reaction $\pi N \rightarrow \pi\pi N$

Nadia Fettes^{a#1}, Véronique Bernard^{b#2}, Ulf-G. Meißner^{a#3}

^a*Institut für Kernphysik (Theorie), Forschungszentrum Jülich
D-52425 Jülich, Germany*

^b*Laboratoire de Physique Théorique, Université Louis Pasteur
3-5, rue de l'Université, F-67084 Strasbourg Cedex, France*

Abstract

Single pion production off nucleons is studied in the framework of heavy baryon chiral perturbation theory to third order in the chiral expansion. Using total and some older differential cross section data to pin down the low-energy constants, most of the recent differential cross sections and angular correlation functions can be described as well as total cross sections at higher energies. We show that the contributions from the one loop graphs are essentially negligible and that the dominant terms at second and third order are related to pion-nucleon scattering graphs with one pion added. We also discuss the possibility of extracting the pion-pion S-wave scattering lengths from the unpolarized data.

Keywords: *Inelastic pion production, chiral symmetry, effective field theory*

PACS nos.: 25.80.Hp , 12.39.Fe , 11.30.Rd

^{#1}E-mail address: N.Fettes@fz-juelich.de

^{#2}E-mail address: bernard@lpt1.u-strasbg.fr

^{#3}E-mail address: Ulf-G.Meissner@fz-juelich.de

1 Introduction

1.1 General introductory remarks

Single pion production off nucleons has been at the center of numerous experimental and theoretical investigations for many years. One of the original motivations of these works was the observation that the elusive pion–pion threshold S–wave interaction could be deduced from the pion–pole graph contribution of the pion production reaction. A whole series of precision experiments at PSI, Los Alamos, TRIUMF and CERN (and other laboratories) has been performed over the last decade and there is still on–going activity. On the theoretical side, chiral perturbation theory has emerged as a precision tool in low energy hadron physics. It not only allows to investigate low–energy pion–pion scattering to high accuracy, see e.g. refs.[1, 2], but also elastic pion–nucleon scattering and inelastic pion production can be studied in the threshold region, for a review see [3]. Another important aspect of inelastic pion production is the excitation of resonances, some of which couple much stronger to the $\pi\pi N$ final–state than to the pion–nucleon continuum. In what follows, we will be concerned with the low energy region which allows to address questions connected to the chiral structure of QCD. Since there already exist a few studies based upon various approximations, we first give an overview of the theoretical status and discuss in which respects these existing calculations can be improved.

1.2 Short review of existing calculations and objectives

Beringer considered the reaction $\pi N \rightarrow \pi\pi N$ to lowest order in relativistic baryon chiral perturbation theory [4]. Low–energy theorems for the threshold amplitudes \mathcal{D}_1 and \mathcal{D}_2 ^{#4} were derived in [5]. These are free of unknown parameters and not sensitive to the $\pi\pi$ –interaction beyond tree level. A direct comparison with the threshold data in the $\pi^+p \rightarrow \pi^+\pi^+n$ channel, which is only sensitive to \mathcal{D}_1 , leads to a very satisfactory description, whereas in case of the process $\pi^-p \rightarrow \pi^0\pi^0n$, which is only sensitive to \mathcal{D}_2 , sizeable deviations were found from the total cross sections near threshold. These were originally attributed to the strong pionic final–state interactions in the $I_{\pi\pi} = 0$ channel. However, this conjecture turned out to be incorrect when a complete higher order calculation of the threshold amplitudes $\mathcal{D}_{1,2}$ was performed [6]. In that paper, the relation between the threshold amplitudes \mathcal{D}_1 and \mathcal{D}_2 and the $\pi\pi$ S–wave scattering lengths a_0^0 and a_0^2 was investigated in the framework of heavy baryon chiral perturbation theory to second order in the pion mass (which is the only small parameter at threshold). The pion loop and pionic counterterm corrections only start contributing to the $\pi\pi N$ threshold amplitudes at third order in the chiral expansion. One of these counterterms, proportional to the low–energy constant ℓ_3 , eventually allows to measure the scalar quark condensate, i.e. the strength of the spontaneous chiral symmetry breaking in QCD. At that order, the largest contributions to $\mathcal{D}_{1,2}$ stem from insertions of the dimension two chiral pion–nucleon Lagrangian, which is characterized by a few low–energy constants called c_i . In particular this is the case for the amplitude \mathcal{D}_2 . It appeared therefore natural to extend the same calculation above threshold and to compare to the large body of data for the various reaction channels. It was already shown by Beringer [4] that taking simply the relativistic Born terms does not suffice to describe the total cross section data for incoming pion energies up to 400 MeV in most channels. In ref.[7] the relativistic pion–nucleon Lagrangian including all dimension two operators

^{#4}These are related to the more commonly used \mathcal{A}_{10} and \mathcal{A}_{32} by $\mathcal{A}_{32} = \sqrt{10}\mathcal{D}_1$ and $\mathcal{A}_{10} = -2\mathcal{D}_1 - 3\mathcal{D}_2$, see also section 3.1.

was used, their coefficients being fixed from pion–nucleon scattering data and (sub)threshold parameters. This parameter–free calculation lead to a satisfactory description of most existing total and differential cross section data as well as angular correlation functions. While being rather successful, that calculation could not give a definite answer to the questions concerning the importance of loop effects (and thus the sensitivity to the pion–pion interaction beyond tree level) and the convergence of the chiral expansion. Also, the amplitudes calculated from the tree graphs in ref.[7] are, of course, purely real. How severe this approximation is can only be judged after a one loop calculation above threshold has been performed. A first attempt to include third order contributions above threshold in the framework of heavy baryon chiral perturbation theory was described in ref.[8]. There, the pertinent one loop graphs and insertions from the dimension three Lagrangian in the formulation of ref.[9] were calculated. However, only three of the five physical channels were considered and the finite pieces of the unknown dimension three low–energy constants were not determined but rather varied within given generous bounds. It was claimed that the contribution from the chiral dimension three amplitudes are large and play an essential role in the description of the data. Note that one of the low–energy constants (LECs) varied in ref.[8] was shown to have a fixed coefficient in ref.[10]. Also, no explicit formulae for the various third order contributions were given, so that it is not possible to check the consistency of the amplitudes constructed there with the threshold amplitudes obtained in [6]. For these reasons, we do not consider the results obtained in ref.[8] as conclusive. In addition, there exist some model calculations which are only partly constrained by chiral symmetry, see e.g. [11, 12]. The one closest in spirit to a chiral expansion is the one of ref.[13], in which Beringer’s Born terms were supplemented by explicit Δ and Roper (tree) contributions. Clearly, the inclusion of the resonances as done in that paper is not based on a consistent power counting scheme but rather it is argued that phenomenology demands the extension of the effective Lagrangian to include these higher mass states.

Our objective is to perform a complete third order calculation using the *minimal* effective pion–nucleon Lagrangian. In addition, we will use all available information about the appearing LECs, in particular from the comprehensive study of elastic pion–nucleon scattering described in ref.[10]. Throughout, we will work in the so–called standard scenario of spontaneous chiral symmetry breaking, i.e. assuming a large scalar quark condensate. While the extension to the small condensate case is in principle straightforward, we do not consider it in what follows. In particular, our study allows to address the following questions:

- i) How sensitive are the data in the threshold region to the $\pi\pi$ interaction beyond leading order? Previous investigations seem to indicate that a better method to access the $\pi\pi$ interaction is the use of Chew–Low techniques (see e.g. [14]) rather than a direct use of the chirally expanded $\pi\pi N$ threshold amplitudes (see e.g. refs.[6, 15]).
- ii) How quickly does the chiral series converge? The previous analyses have not yet given a unique answer to this, although the study of ref.[8] seems to indicate a slow convergence. On the other hand, the results obtained in the relativistic tree level calculation in ref.[7] could be taken as an indication that loop effects are not very important.
- iii) At third order, new LECs appear. These can be determined from a fit to cross section data. Are their values of natural size? If that is the case, it would also be interesting to develop an understanding of the numerical values as it was done for the dimension two LECs in ref.[16]. Furthermore, in ref.[6] resonance saturation was used to pin down the order three LEC contribution to the threshold amplitude D_2 and this procedure can be made more precise when all LECs are determined from above threshold data.

- iv) Can the existing data be described consistently in chiral perturbation theory? So far, mostly total cross section data and some angular distributions have been studied (with the exception of the detailed angular correlation functions in the $\pi^- p \rightarrow \pi^- \pi^+ n$ channel). With the new TRIUMF data [15] and the more recent ones from CHAOS [17] on $\pi^\pm p \rightarrow \pi^\pm \pi^+ n$ [15, 17], this data base has considerably increased and allows for detailed tests on chiral pion–nucleon dynamics. In particular, we now have differential cross sections with respect to the invariant dipion mass squared $M_{\pi\pi}^2$, the squared momentum transfer to the nucleon and the scattering angle between the two negative pions in the dipion restframe [17].

1.3 Organization of the paper

This paper is organized as follows. In section 2 we briefly review the effective Lagrangian underlying the calculation. Section 3 contains some formal aspects including the definition of the T-matrix and of the pertinent observables. The chiral expansion of the invariant amplitudes is performed in section 4. Section 5 contains the results and discussions thereof. In the appendix, we give the explicit expressions for the amplitudes.

2 Effective Lagrangian

At low energies, the relevant degrees of freedom are hadrons, in particular the Goldstone bosons linked to the spontaneous chiral symmetry breaking (for a review, see e.g. [3]). We consider here the two flavor case and thus deal with the iso-triplet of pions, collected in the unitary matrix $U(x) = u^2(x)$. It is straightforward to build an effective Lagrangian to describe their interactions, called $\mathcal{L}_{\pi\pi}$. This Lagrangian admits a dual expansion in small (external) momenta and quark (meson) masses as detailed below. Matter fields such as nucleons can also be included in the effective field theory based on the familiar notions of non-linearly realized chiral symmetry. The pertinent effective Lagrangian called $\mathcal{L}_{\pi N}$ consists of terms with exactly one nucleon in the initial and the final state. The various terms contributing to a process under consideration are organized according to their chiral dimension, which counts the number of derivatives and/or meson mass insertions. Here, we work to third order in the corresponding small parameter q (which is a generic symbol for an external momentum or pion mass). Consequently, the effective Lagrangian consists of the following pieces:

$$\mathcal{L}_{\text{eff}} = \mathcal{L}_{\pi\pi}^{(2)} + \mathcal{L}_{\pi\pi}^{(4)} + \mathcal{L}_{\pi N}^{(1)} + \mathcal{L}_{\pi N}^{(2)} + \mathcal{L}_{\pi N}^{(3)} , \quad (2.1)$$

where the superscript (i) gives the chiral dimension. The relevant terms of the meson Lagrangian read

$$\mathcal{L}_{\pi\pi}^{(2)} = \frac{F^2}{4} \langle \nabla^\mu U \nabla_\mu U^\dagger + \chi_+ \rangle , \quad \chi_+ = u^\dagger \chi u^\dagger + u \chi^\dagger u \quad (2.2)$$

$$\begin{aligned} \mathcal{L}_{\pi\pi}^{(4)} = & \frac{\ell_1}{4} \langle \nabla_\mu U \nabla^\mu U^\dagger \rangle^2 + \frac{\ell_2}{4} \langle \nabla_\mu U \nabla_\nu U^\dagger \rangle \langle \nabla^\mu U \nabla^\nu U^\dagger \rangle + \frac{\ell_3}{16} \langle \chi_+ \rangle^2 \\ & + \frac{\ell_4}{16} \left\{ 2 \langle \nabla_\mu U \nabla^\mu U^\dagger \rangle \langle \chi_+ \rangle + 2 \langle \chi^\dagger U \chi^\dagger U + \chi U^\dagger \chi U^\dagger \rangle - 4 \langle \chi^\dagger \chi \rangle - \langle \chi_+ \rangle^2 \right\} + \dots \end{aligned} \quad (2.3)$$

where the $SU(2)$ matrix-valued field $U(x)$ collects the iso-triplet pions,

$$U(x) = \frac{1}{F} \left[\sqrt{F^2 - \vec{\pi}(x)^2} + i\vec{\tau} \cdot \vec{\pi}(x) \right], \quad (2.4)$$

with F the pion decay constant in the chiral limit and $\nabla_\mu = \partial_\mu + \dots$ is the pion covariant derivative. Here, we only need the partial derivatives since we are not concerned with left- or right-handed external vector currents. This representation of the pion fields, the so-called σ -model gauge, is of particular convenience for calculations in the nucleon sector. The quantity χ contains the light quark mass $m_u = m_d = \hat{m}^{\#5}$ and external scalar and pseudoscalar sources. The ellipsis in eq.(2.3) stands for other terms of order q^4 which do not contribute in our case. The fourth order terms in the meson Lagrangian serve to cancel some of the divergences of the loop diagrams and contain the mesonic low-energy constants $\ell_{1,2,3,4}$. The latter encode information about the chiral corrections to the $\pi\pi$ scattering lengths. The finite pieces ℓ_i^r of the low-energy constants ℓ_i in eq.(2.3) are renormalization scale dependent and are related to the $\bar{\ell}_i$ of ref.[18] via (since both of these sets are used in the literature, it is pertinent to give these relations)

$$\bar{\ell}_i = 16 \alpha_i \pi^2 \ell_i^r(\lambda) - 2 \ln \frac{M_\pi}{\lambda}, \quad \alpha_1 = 6, \quad \alpha_2 = 3, \quad \alpha_3 = -4, \quad \alpha_4 = 1, \quad (2.5)$$

and their actual values will be discussed later. Here, λ is the scale of dimensional regularization. Let us now discuss in some more detail the terms appearing in the various parts of the pion-nucleon Lagrangian, i.e. in $\mathcal{L}_{\pi N}^{(1,2,3)}$. We make use of baryon chiral perturbation theory in the heavy mass formulation [19, 20] (HBCHPT). The nucleons are considered as extremely heavy. This allows to decompose the nucleon Dirac spinor into “large” (H) and “small” (h) components

$$\Psi(x) = e^{-imv \cdot x} \{H(x) + h(x)\}, \quad (2.6)$$

with v_μ the nucleon four-velocity, $v^2 = 1$, and the velocity eigenfields are defined via $\not{v} H = H$ and $\not{v} h = -h$.^{#6} Eliminating the “small” component field h (which generates $1/m$ corrections), the leading order chiral πN Lagrangian reads

$$\mathcal{L}_{\pi N}^{(1)} = \bar{H}(iv \cdot D + g_A S \cdot u)H. \quad (2.7)$$

Here, $D_\mu = \partial_\mu + \Gamma_\mu$ denotes the nucleon chiral covariant derivative, S_μ is a covariant generalization of the Pauli spin vector, g_A the nucleon axial vector coupling constant (in the chiral limit)^{#7} and $u_\mu = iu^\dagger \nabla_\mu U u^\dagger$. To leading one-loop accuracy, i.e. order $\mathcal{O}(q^3)$, one has to consider tree graphs from

$$\mathcal{L}_{\text{eff}} = \mathcal{L}_{\pi N}^{(1)} + \mathcal{L}_{\pi N}^{(2)} + \mathcal{L}_{\pi N}^{(3)} \quad (2.8)$$

and one-loop graphs with dimension one insertions only. The pertinent terms of $\mathcal{L}_{\pi N}^{(2)}$ read

$$\begin{aligned} \mathcal{L}_{\pi N}^{(2)} = & \bar{H} \left\{ \frac{(v \cdot D)^2}{2m} - \frac{D^2}{2m} - \frac{ig_A}{2m} \{S \cdot D, v \cdot u\} + c_1 \langle \chi_+ \rangle \right. \\ & \left. + \left(c_2 - \frac{g_A^2}{2m} \right) (v \cdot u)^2 + c_3 u \cdot u + \left(c_4 + \frac{1}{4m} \right) [S^\mu, S^\nu] u_\mu u_\nu + \dots \right\} H. \end{aligned} \quad (2.9)$$

^{#5}Throughout we will work in the isospin limit apart from kinematical corrections to be discussed later.

^{#6}The role of v_μ is to single out a particular reference frame, here the $\pi^a N$ center-of-mass frame.

^{#7}We do not display explicitly the “ \circ ” commonly used to denote quantities in the chiral limit. The difference between the physical and the chiral limit values has to be kept in mind since it enters the renormalization discussed below.

All terms in $\mathcal{L}_{\pi N}^{(2)}$ are finite. The corresponding LECs have been determined in refs.[16, 21, 10]. A physical interpretation of their numerical values can be found in ref.[16], where it is shown that resonance saturation (mostly due to the Δ -resonance) can indeed explain the size of these LECs. The first divergences appear at $\mathcal{O}(q^3)$ in HBCHPT, the corresponding determinant has been worked out by Ecker [23]. We use here the minimal form of the dimension three πN Lagrangian as constructed in ref.[10]

$$\begin{aligned}\mathcal{L}_{\pi N}^{(3)} &= \mathcal{L}_{\pi N}^{(3), \text{fixed}} + \sum_{i=1}^{23} d_i \bar{H} O_i H + \sum_{i=24}^{31} \tilde{d}_i \bar{H} \tilde{O}_i^{\text{div}} H , \\ &= \bar{H} \left\{ \mathcal{O}_{\text{fixed}}^{(3)} + \mathcal{O}_{\text{ct}}^{(3)} + \mathcal{O}_{\text{div}}^{(3)} \right\} H ,\end{aligned}\tag{2.10}$$

The first set contains terms which stem from the $1/m$ expansion of the various dimension one and two operators and thus have fixed coefficients. Then there are 23 terms, from which 14 are divergent. For our calculation, we need the following dimension three operators $O_i^{(3)}$,

$$\begin{aligned}\mathcal{O}_{\text{ct}}^{(3)} &= i d_1(\lambda) [u_\mu, [v \cdot D, u^\mu]] + i \left(d_2(\lambda) - \frac{1 + 8m c_4}{32m^2} \right) [u_\mu, [D^\mu, v \cdot u]] \\ &+ i \left(d_3(\lambda) + \frac{g_A^2}{32m^2} \right) [v \cdot u, [v \cdot D, v \cdot u]] + i \left(d_4(\lambda) - \frac{g_A}{64m^2} \right) \epsilon^{\mu\nu\alpha\beta} v_\alpha \langle u_\mu u_\nu u_\beta \rangle \\ &+ d_5(\lambda) [\chi_-, v \cdot u] + d_{10}(\lambda) S \cdot u \langle u \cdot u \rangle + d_{11}(\lambda) S^\mu u^\nu \langle u_\mu u_\nu \rangle \\ &+ \left(d_{12}(\lambda) - \frac{4g_A(1 + 4m c_4) + g_A^3}{32m^2} \right) S \cdot u \langle (v \cdot u)^2 \rangle \\ &+ \left(d_{13}(\lambda) + \frac{2g_A(1 + 4m c_4) + g_A^3}{16m^2} \right) S^\mu v \cdot u \langle u_\mu v \cdot u \rangle \\ &+ d_{14}(\lambda) \epsilon^{\mu\nu\alpha\beta} v_\alpha S_\beta \langle [v \cdot D, u_\mu] u_\nu \rangle + \left(d_{15} + \frac{g_A^2}{16m^2} \right) \epsilon^{\mu\nu\alpha\beta} v_\alpha S_\beta \langle u_\mu [D_\nu, v \cdot u] \rangle \\ &+ d_{16}(\lambda) S \cdot u \langle \chi_+ \rangle + i d_{18} S^\mu [D_\mu, \chi_-]\end{aligned}\tag{2.11}$$

For these divergent operators, we introduce scale-independent renormalized LECs,

$$\bar{d}_i = d_i - \frac{\kappa_i}{(4\pi F)^2} \left(L(\lambda) + (4\pi)^2 \ln \frac{\lambda}{M} \right) ,\tag{2.12}$$

with

$$L(\lambda) = \frac{\lambda^{d-4}}{16\pi^2} \left\{ \frac{1}{d-4} - \frac{1}{2} \left[\ln(4\pi) + \Gamma'(1) + 1 \right] \right\} .\tag{2.13}$$

Note also that the operators \mathcal{O}_1 and \mathcal{O}_2 (\mathcal{O}_{14} and \mathcal{O}_{15}) appear as a sum (difference) for $\pi N \rightarrow \pi\pi N$. Four combinations of counterterms ($\bar{d}_1 + \bar{d}_2$, \bar{d}_3 , \bar{d}_5 , $\bar{d}_{14} - \bar{d}_{15}$) have already been fixed from pion-nucleon scattering data and \bar{d}_{18} from the so-called Goldberger-Treiman discrepancy. In addition, there are eight terms which are only necessary for the renormalization, and thus do not appear in matrix elements of physical processes. To be precise, these terms stem solely from the divergent part of the one-loop generating functional and have no (finite) counterparts

in the relativistic theory. They read

$$\begin{aligned}
\mathcal{O}_{\text{div}}^{(3)} &= \tilde{d}_{24}(\lambda) i (v \cdot D)^3 + \tilde{d}_{25}(\lambda) v \cdot \overleftarrow{D} S \cdot u v \cdot D + \tilde{d}_{26}(\lambda) (i \langle u \cdot u \rangle v \cdot D + \text{h.c.}) \\
&+ \tilde{d}_{27}(\lambda) (i \langle (v \cdot u)^2 \rangle v \cdot D + \text{h.c.}) + \tilde{d}_{28}(\lambda) (i \langle \chi_+ \rangle v \cdot D + \text{h.c.}) \\
&+ \tilde{d}_{29}(\lambda) (S^\mu [v \cdot D, u_\mu] v \cdot D + \text{h.c.}) + \tilde{d}_{30}(\lambda) (\epsilon^{\mu\nu\alpha\beta} v_\alpha S_\beta [u_\mu, u_\nu] v \cdot D + \text{h.c.}) .
\end{aligned} \tag{2.14}$$

All these terms are proportional to the nucleons equation of motion, $\sim v \cdot D H$, and thus can be transformed away by appropriate field redefinitions. For more details, see ref.[10].

3 Single pion production: Formal aspects

In this section, we outline the basic technical framework for the reaction $\pi N \rightarrow \pi\pi N$ above threshold treating the nucleons as very heavy fields.

3.1 Invariant amplitudes

We seek the T-matrix for the process

$$\pi^a(q_1) + N(mv + p_1) \rightarrow \pi^b(q_2) + \pi^c(q_3) + N(mv + p_2) , \tag{3.1}$$

with N denoting a nucleon (neutron or proton) and π^a a pion of cartesian isospin a . Note that this process is characterized by five independent four-momenta (or five Mandelstam variables). It is most appropriate in terms of the chiral expansion to choose as variables the energies of the out-going pions and the three invariant momentum transfers t_i ($i = 1, 2, 3$) defined below. Since we work in the framework of HBCHPT, the nucleon four-momenta are written in terms of a conserved four-velocity v and small residual momenta $p_{1,2}$, where small means $v \cdot p_{1,2} \ll m$ and m is the nucleon mass. The $\pi N \rightarrow \pi\pi N$ transition matrix element can be expressed in terms of four invariant amplitudes, denoted A , B , C and D [8], which depend on the five momenta p_1, p_2, q_1, q_2 and q_3 ^{#8} as

$$\begin{aligned}
T_{ss'}^{abc} &= \langle N_{s'}(mv + p_2) \pi^b(q_2) \pi^c(q_3) | T | N_s(mv + p_1) \pi^a(q_1) \rangle \\
&= \mathcal{N}_1 \mathcal{N}_2 \chi_{s'} \left[S \cdot q_1 A + S \cdot q_2 B + S \cdot q_3 C + i \epsilon_{\mu\nu\alpha\beta} q_1^\mu q_2^\nu q_3^\alpha v^\beta D \right]^{abc} \chi_s ,
\end{aligned} \tag{3.2}$$

with χ_s the conventional two-spinor and

$$\mathcal{N}_i = \sqrt{\frac{E_i + m}{2m}} , \quad (i = 1, 2) , \tag{3.3}$$

the standard spinor normalization factors which are mandated by the matching to the relativistic theory if one works in the so-called Pauli interpretation of the heavy nucleon fields (a detailed discussion of this topic can be found in ref.[22]). The invariant amplitudes are complex functions of the momentum variables since in some of the one-loop graphs considered here, the

^{#8}In what follows, we will suppress the dependence of the invariant amplitudes on the momenta.

intermediate pion–nucleon state can go on–shell. The pertinent tree graphs lead, of course, to real amplitudes. The isospin decomposition of the invariant amplitudes reads

$$X^{abc} = \tau^a \delta^{bc} X_1 + \tau^b \delta^{ac} X_2 + \tau^c \delta^{ab} X_3 + i\epsilon^{abc} X_4, \quad X \in \{A, B, C, D\}. \quad (3.4)$$

The following calculations can be simplified considerably if one notices that for most diagrams, the amplitudes have the following symmetries under exchange of particles (note that for these equations to hold, the momenta p_1 and q_1 have to be chosen in–coming and q_2 , p_2 and p_3 out–going):

$$\begin{aligned} A_1(q_1, q_2, q_3) &= -B_2(-q_2, -q_1, q_3) \\ &= -C_3(-q_3, q_2, -q_1) \end{aligned} \quad (3.5)$$

$$\begin{aligned} A_2(q_1, q_2, q_3) &= A_3(q_1, q_3, q_2) \\ &= -B_1(-q_2, -q_1, q_3) \\ &= -C_1(-q_3, -q_1, q_2) \end{aligned} \quad (3.6)$$

$$B_3(q_1, q_2, q_3) = C_2(q_1, q_3, q_2) \quad (3.7)$$

$$\begin{aligned} A_4(q_1, q_2, q_3) &= B_4(-q_2, -q_1, q_3) \\ &= -C_4(-q_3, -q_1, q_2) \end{aligned} \quad (3.8)$$

$$\begin{aligned} D_1(q_1, q_2, q_3) &= -D_2(-q_2, -q_1, q_3) \\ &= -D_3(-q_3, q_2, -q_1), \end{aligned} \quad (3.9)$$

and in all these expressions the fixed values of $p_{1,2}$ are not made explicit. Thus for these diagrams it is enough to give the formulae of six amplitudes A_1 , A_2 , A_4 , B_3 , D_1 and D_4 in order to construct the full T–matrix element. However, in the tree graphs with a dimension two or three $\bar{N}N\pi\pi$ vertex, these symmetries are not present. In these cases, there appear expressions proportional to $S \cdot p_1$ and $S \cdot p_2$. In the center–of–mass (cm) frame these equal $-S \cdot q_1$ and $-S \cdot (q_2 + q_3)$ respectively, which obviously leads to an inequivalent role played by the pion momenta q_1 , q_2 and q_3 . For such diagrams the amplitudes B_1 , B_2 , B_4 , D_2 have to be given in addition to the six discussed before in order to fully determine the T–matrix element.

The five experimentally accessible channels follow from the isospin amplitudes,

$$\pi^+ p \rightarrow \pi^+ \pi^+ n : X = \sqrt{2}(X_2 + X_3), \quad (3.10)$$

$$\pi^+ p \rightarrow \pi^+ \pi^0 p : X = X_3 + X_4, \quad (3.11)$$

$$\pi^- p \rightarrow \pi^+ \pi^- n : X = \sqrt{2}(X_1 + X_2), \quad (3.12)$$

$$\pi^- p \rightarrow \pi^0 \pi^0 n : X = \sqrt{2}X_1, \quad (3.13)$$

$$\pi^- p \rightarrow \pi^0 \pi^- p : X = X_2 + X_4, \quad (3.14)$$

for $X \in \{A, B, C, D\}$. We will calculate the amplitudes X_i in the isospin limit with the charged pion mass ($M_\pi = 139.57$ MeV) and the proton mass ($m = 938.27$ MeV). Isospin breaking is accounted for in a minimal way by shifting the kinetic energy (in the laboratory system) of the incoming pion, called T_π , from the isospin symmetric threshold

$$T_\pi^{\text{thr,iso}} = M_\pi \left(1 + \frac{3M_\pi}{2m} \right) = 170.71 \text{ MeV} \quad (3.15)$$

to the correct threshold of the corresponding reaction. For the five channels given above, the corresponding shift is $\delta T_\pi = +1.68, -5.95, +1.68, -10.21$ and -5.95 MeV in the same order

as in eqs.(3.10-3.14). Finally, we need the expressions of the two threshold quantities $\mathcal{D}_{1,2}$ in terms of the invariant amplitudes defined above. At threshold, $\vec{q}_2 = \vec{q}_3 = 0$ and there are only two amplitudes,

$$\begin{aligned}\mathcal{D}_1 &= -\frac{i}{2} \mathcal{N}_1^{\text{thr}} A_2^{\text{thr}} = -\frac{i}{2} \mathcal{N}_1^{\text{thr}} A_3^{\text{thr}} , \\ \mathcal{D}_2 &= -\frac{i}{2} \mathcal{N}_1^{\text{thr}} A_1^{\text{thr}} ,\end{aligned}\tag{3.16}$$

with $\mathcal{N}_1^{\text{thr}} = 1.006$. The chiral expansion of \mathcal{D}_1 and \mathcal{D}_2 has already been considered to third order, i.e. including all terms of order M_π^2 since the pion mass is the only dimensionful quantity at threshold and the lowest order terms are non-vanishing in the chiral limit. To end this paragraph, we note that from now on we use the energies of the outgoing pions and the three invariant momentum transfers squared as kinematical variables, because $\omega_2 = v \cdot q_2, \omega_3 = v \cdot q_3 = \mathcal{O}(q)$ and $t_1, t_2, t_3 = \mathcal{O}(q^2)$ have the expected chiral dimensions and consequently the residual nucleon energies $v \cdot p_i$ are of second order.

3.2 Observables

To calculate the total (unpolarized) cross section, we need the invariant matrix-element squared multiplied by the appropriate weight functions. It reads

$$\begin{aligned}|\mathcal{M}|^2 &= \frac{1}{2} \sum_{s,s'} T_{ss'}^\dagger T_{ss'} \\ &= \frac{1}{4} \left[A^* A (\omega_1^2 - q_1^2) + B^* B (\omega_2^2 - q_2^2) + C^* C (\omega_3^2 - q_3^2) + (A^* B + A B^*) (\omega_1 \omega_2 - q_1 \cdot q_2) \right. \\ &\quad + (A^* C + A C^*) (\omega_1 \omega_3 - q_1 \cdot q_3) + (B^* C + B C^*) (\omega_2 \omega_3 - q_2 \cdot q_3) \\ &\quad \left. + 4 D^* D (\omega_1^2 - q_1^2)(\omega_2^2 - q_2^2)(\omega_3^2 - q_3^2)(1 - x_1^2)(1 - x_2^2) \left(1 - \frac{(z - x_1 x_2)^2}{(1 - x_1^2)(1 - x_2^2)} \right) \right],\end{aligned}\tag{3.17}$$

where the angular variables $x_{1,2}$ and z are defined below. The formulae for total and the double and triple differential cross sections then become:

$$\sigma_{\text{tot}}(T_\pi) = \frac{4m\mathcal{S}}{(4\pi)^4 \sqrt{T_\pi(T_\pi + 2M_\pi)}} \int \int_{z^2 \leq 1} d\omega_2 d\omega_3 \int_{-1}^1 dx_1 \int_0^\pi d\phi |\mathcal{M}|^2, \tag{3.18}$$

$$\frac{d^2\sigma}{d\omega_2 d\Omega_2} = \frac{8m^2\mathcal{S}}{(4\pi)^5 \sqrt{s} |\vec{q}_1|} \int_{\omega_3^-}^{\omega_3^+} d\omega_3 \int_0^\pi d\phi |\mathcal{M}|^2, \tag{3.19}$$

$$\frac{d^3\sigma}{d\omega_2 d\Omega_2 d\Omega_3} = \frac{4m^2 |\vec{q}_2| |\vec{q}_3| \mathcal{S}}{(4\pi)^5 \sqrt{s} |\vec{q}_1| \tilde{E}_3} |\mathcal{M}|^2, \tag{3.20}$$

with $s = (m + M_\pi)^2 + 2mT_\pi$ the total center-of-mass energy squared and $\omega_i = \sqrt{\vec{q}_i^2 + M_\pi^2}$. \mathcal{S} is a Bose symmetry factor, $\mathcal{S} = 1/2$ for identical pions and $\mathcal{S} = 1$ otherwise. Here, ϕ is the (auxiliary) angle between the planes spanned by \vec{q}_2 and \vec{q}_1 as well as \vec{q}_2 and \vec{q}_3 . In accordance with the experimentalists convention, we have chosen the coordinate frame such

that the incoming pion momentum \vec{q}_1 defines the z-direction, whereas \vec{q}_2 lies in the xz-plane. The polar angles θ_1 and θ_2 of the outgoing pions (with $x_i = \cos \theta_i$) are in general non-vanishing and so is the azimuthal angle φ_2 of π^c . By construction, the azimuthal angle of π^b is zero. Furthermore,

$$\tilde{E}_3 = E_3 \left(1 + \frac{\partial E_3}{\partial \omega_3} \right) = \frac{\omega_3 (\frac{1}{2}(s - m^2) - \sqrt{s} \omega_2) + M_\pi^2 (\omega_2 + \omega_3 - \sqrt{s})}{\omega_3^2 - M_\pi^2}, \quad (3.21)$$

The cosine of the angle between the two three-momenta of the outgoing pions, \vec{q}_2 and \vec{q}_3 , respectively, is given by

$$z = \cos \theta_1 \cos \theta_2 + \sin \theta_1 \sin \theta_2 \cos \varphi_2, \quad (3.22)$$

and it can be used to express the energy ω_3 as

$$\omega_3 = \frac{1}{2[(\sqrt{s} - \omega_1)^2 - z^2 |\vec{q}_2|^2]} \left\{ (\sqrt{s} - \omega_2)(s - 2\sqrt{s} \omega_1 - m^2 + 2M_\pi^2) - z |\vec{q}_2| \sqrt{(s - 2\sqrt{s} \omega_1 - m^2)^2 - 4M_\pi^2(m^2 + (1 - z^2) |\vec{q}_2|^2)} \right\}. \quad (3.23)$$

In the formula for the total cross section, eq.(3.18), the restriction $z^2 \leq 1$ is equivalent to $\omega_2 \in [I_1^-, I_1^+]$, $\omega_3 \in [\omega_3^-, \omega_3^+]$, with

$$I_1^- = M_\pi, \quad I_1^+ = \frac{(\sqrt{s} - M_\pi)^2 - m^2 + M_\pi^2}{2(\sqrt{s} - M_\pi)}, \quad (3.24)$$

$$\omega_3^\pm = \frac{1}{2(s - 2\sqrt{s} \omega_2 + M_\pi^2)} \left[(\sqrt{s} - \omega_2)(s - 2\sqrt{s} \omega_2 - m^2 + 2M_\pi^2) \pm |\vec{q}_2| \sqrt{(s - 2\sqrt{s} \omega_2 - m^2)^2 - 4m^2 M_\pi^2} \right]. \quad (3.25)$$

To compare our calculation to the most recent TRIUMF data, other combinations of differential cross sections are needed. Consider first the differential cross section with respect to the invariant mass of the final dipion system,

$$\frac{d\sigma}{dM_{\pi\pi}^2} = \frac{m\mathcal{S}}{(4\pi)^4 \sqrt{s} |\vec{q}_1| |\vec{q}_2 + \vec{q}_3| \sqrt{T_\pi(T_\pi + 2M_\pi)}} \int dt \int d\omega_2 \int_0^\pi d\phi' |\mathcal{M}|^2. \quad (3.26)$$

The expression for $d^2\sigma/(dM_{\pi\pi}^2 dt)$ can be easily deduced from eq.(3.26). Here, the integration boundaries of t are given by

$$t^\pm = M_\pi^2 + M_{\pi\pi}^2 - 2\omega_1 \omega_{23} \pm 2|\vec{q}_1| |\vec{q}_2 + \vec{q}_3|, \quad (3.27)$$

and ω_{23} is fully determined by $M_{\pi\pi}^2$ via

$$\omega_{23} = \omega_2 + \omega_3 = \frac{M_{\pi\pi}^2 + s - m^2}{2\sqrt{s}}. \quad (3.28)$$

Consequently, ω_2 is restricted to the overlap of the intervals $[I_i^-, I_i^+]$ ($i = 1, 2$) with

$$I_2^\pm = \frac{\omega_{23}}{2} \pm \sqrt{\frac{(\omega_{23}^2 - M_{\pi\pi}^2)(M_{\pi\pi}^2 - 4M_\pi^2)}{4M_{\pi\pi}^2}}. \quad (3.29)$$

Denoting by α the angle between \vec{q}_1 and $\vec{q}_2 + \vec{q}_3$ and by β the one between \vec{q}_2 and $\vec{q}_2 + \vec{q}_3$, the azimuthal angle ϕ' is defined via

$$x_1 = \cos \alpha \cos \beta + \sqrt{(1 - \cos^2 \alpha)(1 - \cos^2 \beta)} \cos \phi' . \quad (3.30)$$

The differential cross section with respect to $t = (q_1 - q_2 - q_3)^2$ reads

$$\frac{d\sigma}{dt} = \frac{mS}{(4\pi)^4 \sqrt{s} |\vec{q}_1| \sqrt{T_\pi(T_\pi + 2M_\pi)}} \int \frac{dM_{\pi\pi}^2}{|\vec{q}_2 + \vec{q}_3|} \int d\omega_2 \int_0^\pi d\phi' |\mathcal{M}|^2 . \quad (3.31)$$

The kinematically allowed region for $M_{\pi\pi}^2$ is

$$M_{\pi\pi}^2 = \frac{1}{m^2} \left\{ t/2 (s + m^2 - M_\pi^2) + m^2 M_\pi^2 \pm |\vec{q}_1| \sqrt{-s t (4m^2 - t)} \right\} , \quad (3.32)$$

and also $M_{\pi\pi}^2 \in (4M_\pi^2, (\sqrt{s} - m)^2)$. Finally, the last measured quantity is the single differential cross section with respect to the scattering angle of the two outgoing pions, in the center-of-mass frame of the outgoing two-pion system:

$$\begin{aligned} \frac{d\sigma}{d\cos\theta} &= \frac{2mS}{(4\pi)^4 \sqrt{T_\pi(T_\pi + 2M_\pi)}} \frac{1}{\sqrt{s} |\vec{q}_1|} \int dM_{\pi\pi}^2 \int d\cos\alpha \int d\omega_2 \frac{|\mathcal{M}|^2}{\sin\phi'} \\ &\quad \times \frac{|\vec{q}_1| |\vec{q}_2|}{|\vec{q}_2| \sqrt{(1 - \cos^2 \alpha)(1 - \cos^2 \beta)}} , \end{aligned} \quad (3.33)$$

with $\vec{q}_1 = (\vec{q}_1)_{\text{CM}}$ and $\vec{q}_2 = (\vec{q}_2)_{\text{CM}}$ the pion momenta in the dipion cms, with magnitude $|\vec{q}_1|^2 = (M_{\pi\pi}^4 - 2M_{\pi\pi}^2(t + M_\pi^2) + (t - M_\pi^2)^2)/4M_{\pi\pi}^2$ and $|\vec{q}_2|^2 = (M_{\pi\pi}^2 - 4M_\pi^2)/4$ respectively. The necessary kinematic constraints are given by the two cosine functions. This completes the necessary formalism for our calculation.

4 Chiral expansion

The effective Lagrangian described in section 2 can now be used to work out the chiral expansion of the invariant amplitudes defined in eq.(3.2). Before discussing the explicit contributions, we first display the general structure of the chiral expansion. All the invariant amplitudes take the form

$$X = X^{\text{tree}} + X^{\text{loop}} , \quad (4.1)$$

where the tree terms are of dimension one, two and three whereas the loop graphs are of third order only. Corrections not calculated here start at order q^4 . The corresponding tree graphs are shown in figs. 1,2. Here, diagram 3p denotes a genuine third order counterterm specific to pion production and the graph 3s embodies the next-to-leading order pion-pion interaction. We note that many of the diagrams are simply elastic pion-nucleon scattering graphs with one additional pion attached in all possible topologies. The one-loop graphs are split into tadpoles (t1-t14 in fig.3) and so-called self-energy diagrams (s1-s35 in figs.4,5). A typical one-loop $\pi\pi$ interaction is e.g. t13. We note again that many diagrams can be split into a πN graph with an additional pion. This leads one to expect that a precise description of elastic pion-nucleon

scattering is an important ingredient to the calculation performed here. As an important check of our calculation we recover the explicit expressions for the two threshold amplitudes worked out to this order in ref.[6]. The contribution from the tree graphs proportional to the dimension three LECs was estimated via resonance saturation in ref.[6]. We are in the position to test this assumption (see below). Of course, many of the loop graphs shown in figs.4,5 simply amount to mass and coupling constant renormalization. This is by now a standard procedure and we refrain from discussing it here in detail (see the appendix). Also, the appearing divergences $\sim 1/(d-4)$, with d the number of space-time dimensions are of course cancelled by the appropriate infinite contributions from the dimension four mesonic LECs and the dimension three pion-nucleon LECs, first given in an overcomplete basis by Ecker [23], see section 2. This procedure closely parallels the calculations described in detail in ref.[6]. It serves of course as an important check of the calculation.

5 Results and discussion

We are now in the position to analyze the existing data within the framework laid out in the previous section. We first discuss the fits which determine the LECs and then show predictions and analyze in detail the chiral expansion, in terms of sensitivity to the $\pi\pi$ and πN interactions, its convergence and related issues.

5.1 The fitting procedure

As stated in section 2, we have to deal in total with 19 independent combinations of LECs. We take the values of the four mesonic LECs from ref.[24],

$$\ell_1^r(1\text{ GeV}) = -5.95, \quad \ell_2^r(1\text{ GeV}) = 4.35, \quad \ell_3^r(1\text{ GeV}) = 1.64, \quad \ell_4^r(1\text{ GeV}) = 2.29, \quad (5.2)$$

in units of 10^{-3} . Although we did not perform a systematic calculation within the framework of generalized CHPT (i.e. assuming a small value of the quark condensate), we can get an idea about that approach by setting $\bar{\ell}_3 \simeq -70$ [18], i.e. $\ell_3^r(1\text{ GeV}) = 117 \cdot 10^{-3}$. Clearly, this is by no means a substitute for a complete calculation but should allow us to discuss some trends. A full analysis based on GCHPT is, however, not the topic of this paper. Turning now to the pion-nucleon sector, we note that the four dimension two LECs as well as five (combinations of) dimension three meson-baryon LECs can e.g. be taken from Fit 2 of ref.[10],

$$\begin{aligned} c_1 &= -1.42, \quad c_2 = 3.13, \quad c_3 = -5.85, \quad c_4 = 3.50, \\ \bar{d}_1 + \bar{d}_2 &= 3.31, \quad \bar{d}_3 = -2.75, \quad \bar{d}_5 = -0.48, \quad \bar{d}_{14} - \bar{d}_{15} = -5.69, \quad \bar{d}_{18} = -0.78. \end{aligned} \quad (5.3)$$

The values for the c_i and \bar{d}_i are in GeV^{-1} and GeV^{-2} , respectively. Therefore, we are left with six genuine LECs which have to be fitted. These are \bar{d}_4 , \bar{d}_{10} , \bar{d}_{11} , \bar{d}_{12} , \bar{d}_{13} and \bar{d}_{16} . For the fitting procedure, we only use data with $T_\pi < 250\text{ MeV}$. This rather large value is mainly motivated by the fact that in the very near threshold region, say in the first 30 MeV above the respective thresholds, there are essentially no data in the two channels $\pi^- p \rightarrow \pi^0 \pi^- p$ and $\pi^+ p \rightarrow \pi^0 \pi^+ p$. The total cross section data are taken from refs.[25]-[46]. Moreover, there exist double differential cross section data from Los Alamos [47, 48] and the Erlangen

group [49, 50, 51].^{#9} In ref.[49], a large amount of angular correlation functions are also given. All these data refer to the $\pi^-p \rightarrow \pi^+\pi^-n$ channel. In addition, there are the recent TRIUMF data listed in the introduction. We have performed a series of fits based on different input material. We refrain from describing all these in detail. What we will present here as results is based on fits to the total (including the recent TRIUMF data) as well as the double differential cross sections of refs.[47, 48]. In that way, we can predict the angular correlation functions of ref.[49], the new TRIUMF data [14] and the total cross sections for $T_\pi > 250$ MeV. In these fits, we have found almost perfect anticorrelations between the values of the LECs \bar{d}_{10} and \bar{d}_{12} as well as \bar{d}_9 and \bar{d}_{11} . Therefore, we can only determine four independent LECs. In table 1, we give the results for various fits with all six LECs free and with one or two of them being fixed. We observe that due to the large anticorrelations, the fit with all six LECs left free leads to

\bar{d}_i	None fixed	$\bar{d}_{11} = -5$	$\bar{d}_{11} = \bar{d}_{10} = -5$
4	0.26 ± 2.29	1.60 ± 2.00	0.97 ± 2.00
10	-3.60 ± 4.52	-12.81 ± 3.11	fixed
11	-20.58 ± 5.90	fixed	fixed
12	4.11 ± 4.32	12.25 ± 3.27	4.28 ± 0.45
13	22.00 ± 5.78	6.60 ± 0.36	6.08 ± 0.32
16	-4.70 ± 0.84	-3.67 ± 0.74	-3.84 ± 0.70
χ^2/dof	2.20	2.25	2.29

Table 1: The dimension three LECs \bar{d}_i in GeV^{-2} from the various fits as described in the text.

rather large values for some of the LECs. If one fixes two to any value of natural size, which in our normalization is of order one, the remaining LECs come out to be of natural size too, compare the last column in table 1. The uncertainties given in that table are the parabolic errors of the MINUIT package and have to be taken with some caution. In what follows, we will always use the values for the \bar{d}_i as given in the first column of table 1. In fig.6 we show the fit to the total cross sections in all five physical channels and in fig.7 the corresponding double differential cross sections. We note that there are some inconsistencies between the older and more recent data, most pronounced in the two channels $\pi^+p \rightarrow \pi^+\pi^+n$ and $\pi^-p \rightarrow \pi^+\pi^-n$. Note also that the data of the OMICRON collaboration [33, 26] have been criticized concerning the normalization. If we perform fits without these data, the χ^2/dof only improves by one permille. The LECs \bar{d}_i change mildly, the only appreciable difference is found for \bar{d}_4 . This LEC only appears in the amplitude D_4 , which contributes to the channels with one neutral pion in the final state. The data from the OMICRON collaboration feature prominently in the process $\pi^-p \rightarrow \pi^0\pi^-p$ which explains the sensitivity of the LEC \bar{d}_4 . In what follows, we keep the data of ref.[33, 26] in our data base. We have also performed fits using the LECs c_i and \bar{d}_i from fits 1 and 3 of ref.[10]. The resulting dimension three LECs only change moderately and the χ^2/dof is 2.21, 2.20 and 2.20 for fits 1,2 and 3, in order. None of the conclusions drawn in the following paragraphs depends on this choice, we always use the values from fit 2 given in eq.(5.3).

^{#9}As described in [7], neither chiral perturbation theory nor any of the resonance models can describe the double differential cross section data at $\sqrt{s} = 1.301$ GeV from ref.[49]. We therefore decided not to use these in the fit. Also, we do not use the unpublished data of refs.[50, 51].

5.2 Predictions, further results and discussion

We now turn to the predictions. In fig.8 we show the total cross sections for incoming pion momenta up to 400 MeV. Despite the large momentum transfers involved, the chiral description works fairly well, in particular in the $\pi^-p \rightarrow \pi^+\pi^-n$ channel. On the other hand, for the two reactions $\pi^+p \rightarrow \pi^+\pi^+n$ and $\pi^-p \rightarrow \pi^0\pi^-p$ the chiral prediction overshoots the data for energies larger than 300 MeV. The angular correlation functions as defined and given in ref.[49] are mostly well described, see figs.9,10, with the exception of the smaller θ_2 values, a trend already observed in ref.[7]. If one insists that these data are also fitted, the χ^2/dof worsens considerably. The comparison to the recent TRIUMF data is shown in fig.11 for $d\sigma/dM_{\pi\pi}^2$ and $d\sigma/dt$. Whereas the data in the π^-p channel are mostly well reproduced, there are some deviations for the π^+p process, most notably in $d\sigma/dM_{\pi\pi}^2$. The description of $d^2\sigma/dtdM_{\pi\pi}^2$ and $d\sigma/d\cos\theta$ is less good, we refrain from showing these. Again, if one includes these data in the fit, the χ^2/dof becomes intolerably large. This means that the presently existing data base shows some inconsistencies, a fact which also limits the precision of our description based on the chiral symmetry of QCD.

We now consider the chiral expansion in more detail. We remark that in three channels the series seems to converge well ($\pi^+p \rightarrow \pi^+\pi^+n$, $\pi^+p \rightarrow \pi^+\pi^0p$ and $\pi^-p \rightarrow \pi^0\pi^-p$), in the two others ($\pi^-p \rightarrow \pi^+\pi^-n$ and $\pi^-p \rightarrow \pi^0\pi^0n$) the third order corrections become large even close to threshold. As two representatives of these classes, we show in the upper part of fig.12 the close to threshold region ($T_\pi \leq 210$ MeV) for $\pi^+p \rightarrow \pi^+\pi^+n$ (good convergence) and $\pi^-p \rightarrow \pi^+\pi^-n$ (poor convergence). However, it is of importance to further analyze these third order contributions. As shown in the lower part of fig.12, in all cases the contributions from the loops and (in most cases) from the terms proportional to the dimension three LECs are small (this holds also for the channels not shown in the figure). If the third order correction is large, it comes entirely from the $1/m$ corrections to the tree graphs proportional to the dimension two LECs c_i and the ones with fixed coefficients. The smallness of the unitarity corrections is a very important result. At first, it appears to be surprising since in elastic pion–nucleon scattering, the loop contributions are sizeable (in some of the invariant amplitudes) already in the threshold region. We note, however, that such terms appear with an additional pion line attached before or after the $\pi N \rightarrow \pi N$ subprocess, which leads to sizeable cancelations in the imaginary parts for the reactions considered here. This finding explains why the relativistic calculation based on dimension one and two tree graphs of ref.[7] worked so well, since in that calculation all imaginary parts were neglected. Similarly, the commonly used resonance models like e.g. the one of the Valencia group [11] only acquire small imaginary parts from the finite width of the resonances, which is built in by modifying the corresponding propagators. Our analysis for the first time gives a reason why such a seemingly ad hoc procedure can work. Another consequence concerns polarization observables, which usually stem from the interference of real and imaginary parts of certain invariant amplitudes. In order to differentiate between different approaches to a given reaction, one often has to analyze polarization data, one prominent example being the multipole separation in pion photoproduction off nucleons. Due to the intrinsic smallness of the imaginary parts for inelastic pion production, one should find out in which polarization observables the small imaginary part is most efficiently amplified by the real part of a large amplitude. In principle, the framework outlined here can be used to do that, but due to the absence of polarization data, we refrain from discussing such an analysis here.

We now consider briefly the threshold amplitudes $\mathcal{D}_{1,2}$, as defined in eq.(3.16). In ref.[6] it was found that no tree graphs with dimension three LECs generated from resonance excitation (via

the dominant Roper resonance) contribute to \mathcal{D}_1 , whereas two distinct terms were considered for \mathcal{D}_2 . The first is linked to the deviation from the Goldberger–Treiman relation and corresponds to our term $\sim \bar{d}_{18}$, the second one was the contribution due to the Roper decay $N^*(1440) \rightarrow N(\pi\pi)_S$, where the two pions are in a relative S-wave. The uncertainty related to this decay in fact was the largest source of theoretical uncertainty for the chiral description of \mathcal{D}_2 . In our more general approach, we also have a contribution from the dimension three LECs to \mathcal{D}_1 . If we convert our central values and errors of the corresponding \bar{d}_i ($i \neq 18$) into the contribution to $\mathcal{D}_{1,2}$, we find

$$\mathcal{D}_1^{\bar{d}_i} = (0.27 \pm 0.07) \text{ fm}^3, \quad \mathcal{D}_2^{\bar{d}_i} = (-1.60 \pm 0.15) \text{ fm}^3, \quad (5.4)$$

which is within 1.5σ of the result of ref.[6] based on Roper excitation, $\mathcal{D}_2^{N^*} = (-0.40 \pm 0.90) \text{ fm}^3$. In addition, we have a smaller contribution to \mathcal{D}_1 , which is however of the same size as the other contributions from the loops, c_i and the $\bar{\ell}_i$ terms, cf. table 2 of ref.[6]. The theoretical uncertainties in eq.(5.4) have been obtained from the MINUIT uncertainties in the \bar{d}_i taking into account the correlation matrix.

Finally, we consider the sensitivity to the LEC $\bar{\ell}_3$. In fig.13 we show total cross sections for the two channels $\pi^+p \rightarrow \pi^+\pi^+n$ and $\pi^-p \rightarrow \pi^0\pi^0n$ at $T_\pi \leq 220 \text{ MeV}$ (which have already been investigated in the study of the low-energy theorems [5]). In both cases the error bars of the recent data are smaller than the difference in the curves with $\bar{\ell}_3 = 2.9$ (standard case) and -70 (generalized case), in order. A similar trend is observed for the differential cross sections $d\sigma/dt$ (at $T_\pi = 220, 240 \text{ MeV}$), which have been used in ref.[14] to extract a_0^0 by Chew–Low techniques. Our analysis tends to support the finding of ref.[6], namely that one can extract a_0^0 from the threshold data, but with an uncertainty which includes both the standard as well as the generalized scenario. Presumably, a study of polarization observables would give a better handle on this question. In ref.[6], a smaller theoretical uncertainty on a_0^2 was given, based on the observation that there is no $N^*(1440)$ contribution to the threshold amplitude \mathcal{D}_1 . Taking into account the additional contribution given in eq.(5.4), we conclude that the theoretical uncertainty for a_0^2 was underestimated in ref.[6].

6 Summary

We have performed a complete third order calculation of the reaction $\pi N \rightarrow \pi\pi N$ in heavy baryon chiral perturbation theory based on the minimal Lagrangian developed in ref.[10]. We had to consider 26 different tree graphs and 49 one loop topologies as displayed in figs. 1-5. Note that the tree contributions with fixed coefficients are obtained from the $1/m$ expansion of the relativistic amplitudes. The pertinent results of this investigation can be summarized as follows:

- i) We have used the total cross sections in all five physical channels (for $T_\pi \leq 250 \text{ MeV}$, with T_π the kinetic energy of the incoming pion in the laboratory frame) and the older double differential cross sections $d^2\sigma/d\Omega dT$ for the process $\pi^-p \rightarrow \pi^+\pi^-n$ to fit the six new dimension three LECs. The other four dimension two and five (combinations of) dimension three LECs were taken from the study of elastic πN scattering in ref.[10]. We observe that the values of two pairs of these LECs are almost perfectly anticorrelated, so that only four LECs can be determined. They come out of natural size.

- ii) Using this input, we predict the total cross sections for energies up to $T_\pi = 400$ MeV. We find an excellent description of the $\pi^- p \rightarrow \pi^+ \pi^- n$ channel whereas the largest deviations are seen for the process $\pi^+ p \rightarrow \pi^+ \pi^+ n$, see fig.8. The angular correlation functions for $\pi^- p \rightarrow \pi^+ \pi^- n$ can be satisfactorily reproduced, with the exception of the small θ_2 angles, cf. figs.9,10. In addition, most of the recent TRIUMF data on $d\sigma/dM_{\pi\pi}^2$, $d\sigma/dt$, $d\sigma/d\cos\theta$ and $d^2\sigma/dtdM_{\pi\pi}^2$ can also be reproduced.
- iii) At third order, the contribution from the loop graphs is essentially negligible. Unitarity corrections therefore play no role. This allows one to understand why resonance models like in refs.[11, 12] work fairly well even in the threshold region (although these are not as precise as the calculation presented here). The effect of the terms proportional to the dimension three LECs is somewhat more pronounced. By far the largest contribution at this order comes from the $1/m$ corrections to the dimension two LECs c_i and the $1/m^2$ corrections with fixed coefficients. This together with the smallness of the loop contributions explains why the tree calculation in ref.[7] works so well. It also means that by far the most important terms are the pion–nucleon subgraphs with an additional pion added in all possible topologies.
- iv) Our study is based on the standard scenario of chiral symmetry breaking where a quark mass insertion is counted as second order in the chiral expansion. This reflects itself in the natural size of the mesonic LECs $\bar{\ell}_{1,2,3,4}$ used here. The generalized scenario with $m_q \sim \mathcal{O}(q)$ can be modeled by setting $\bar{\ell}_3 \simeq -70$ [18].^{#10} Keeping all other mesonic and baryonic LECs fixed, we have studied the sensitivity of the total and differential cross sections as well as the angular correlation functions to the value of $\bar{\ell}_3$. We conclude that one is not able to pin down the LEC $\bar{\ell}_3$ with sufficient accuracy to discriminate between the two scenarios of chiral symmetry breaking by just comparing the observables directly with chiral analysis (which is of course different from applying Chew–Low techniques). We have also evaluated the dimension three counterterm contributions to the threshold amplitudes and discussed the resonance saturation approximation used in ref.[6].

There are two directions in which the study presented here should be extended. First, it would be interesting to study the sensitivity to polarization. In particular, it is conceivable that some polarization observables will be more sensitive to the pion–pion interaction than the unpolarized observables studied here. Second, a complete one–loop calculation requires to include the fourth order terms. For doing that, one first has to work out elastic pion–nucleon scattering to that order. Such investigations are underway and we hope to report on their results soon.

^{#10}Clearly, this can not substitute for a detailed study within generalized CHPT. Such a procedure should, however, be sufficient for simply getting an idea about the sensitivity to the $\pi\pi$ interaction.

A Contributions to the invariant amplitudes

In this appendix, we explicitly give the contributions from the tree and loop graphs shown in figs 1–5 to the invariant amplitudes A, B, C and D . Only the minimal number of non-vanishing amplitudes as explained in section 3 is given.

The calculation of the Born amplitude with fixed coefficients has been done by $1/m$ expansion of the relativistic amplitude. In this expansion, ω_2 and ω_3 have been treated as quantities of order q , $t_1 = (q_1 - q_2)^2$, $t_2 = (q_1 - q_3)^2$ and $t_3 = (q_2 + q_3)^2 = M_{\pi\pi}^2$ count as $\mathcal{O}(q^2)$. As a consequence,

$$v \cdot p_1 = \frac{(\omega_2 + \omega_3)^2 - M_\pi^2}{2m} + \dots = \mathcal{O}(q^2), \quad (\text{A.1})$$

$$v \cdot p_2 = \frac{(\omega_2 + \omega_3)^2 - t_3}{2m} + \dots = \mathcal{O}(q^2), \quad (\text{A.2})$$

$$\omega_1 = (\omega_2 + \omega_3) + \mathcal{O}(q^2), \quad (\text{A.3})$$

where the ellipsis denotes higher order terms. In diagrams 3a, 3b, 3n and 3o, there appear expressions in $S \cdot p_1 = -S \cdot q_1$ and $S \cdot p_2 = -S \cdot (q_2 + q_3)$. As stated before, for these diagrams the amplitudes B_1, B_2, B_4, D_2 have to be given in addition to the six usual ones, in order to fully determine the T-matrix element.

1. Counterterm amplitudes

Diagrams 2a+2b:

$$\begin{aligned} A_1 &= -i \frac{g_A}{F^3} v \cdot (p_1 + p_2) \left[-\frac{1}{\omega_1^2} (-4c_1 M^2 - 2c_2 \omega_2 \omega_3 - 2c_3 q_2 \cdot q_3) \right. \\ &\quad \left. + c_4 (\omega_2 \omega_3 - q_2 \cdot q_3) \left(\frac{1}{\omega_2^2} + \frac{1}{\omega_3^2} \right) \right] \\ A_2 &= i \frac{g_A}{F^3} c_4 (\omega_2 \omega_3 - q_2 \cdot q_3) \frac{v \cdot (p_1 + p_2)}{\omega_3^2} \\ A_4 &= i \frac{g_A}{F^3} c_4 (\omega_2 \omega_3 - q_2 \cdot q_3) \left[\frac{2}{\omega_2} - \frac{2}{\omega_3} + v \cdot (p_1 - p_2) \left(\frac{1}{\omega_2^2} - \frac{1}{\omega_3^2} \right) \right] \\ B_3 &= i \frac{g_A}{F^3} c_4 (\omega_1 \omega_3 - q_1 \cdot q_3) \frac{v \cdot (p_1 + p_2)}{\omega_1^2} \\ D_1 &= i \frac{g_A}{2F^3} c_4 \left[\frac{2}{\omega_2} - \frac{2}{\omega_3} + v \cdot (p_1 - p_2) \left(\frac{1}{\omega_2^2} - \frac{1}{\omega_3^2} \right) \right] \\ D_4 &= -i \frac{g_A}{2F^3} c_4 v \cdot (p_1 + p_2) \left(\frac{1}{\omega_1^2} + \frac{1}{\omega_2^2} + \frac{1}{\omega_3^2} \right) \end{aligned} \quad (\text{A.4})$$

Diagrams 3a+3b:

$$\begin{aligned} A_1 &= -i \frac{g_A}{mF^3} c_4 [\omega_1 (\omega_2 + \omega_3) - \omega_2^2 - \omega_3^2 - q_1 \cdot (q_2 + q_3) + 2M^2] \\ A_2 &= -i \frac{g_A}{mF^3} [-4c_1 M^2 + 2c_2 \omega_1 \omega_3 + 2c_3 q_1 \cdot q_3 - c_4 (\omega_1 \omega_2 - \omega_2^2 - q_1 \cdot q_2 + M^2)] \end{aligned}$$

$$\begin{aligned}
A_4 &= i \frac{g_A}{mF^3} c_4 [\omega_1(\omega_3 - \omega_2) + \omega_3^2 - \omega_2^2 - q_1 \cdot (q_3 - q_2)] \\
B_1 &= i \frac{g_A}{mF^3} [-4c_1 M^2 - 2c_2 \omega_2 \omega_3 - 2c_3 q_2 \cdot q_3 - c_4(\omega_1 \omega_2 - \omega_1^2 - q_1 \cdot q_2 + M^2)] \\
B_2 &= -i \frac{g_A}{mF^3} c_4 [\omega_2(\omega_3 - \omega_1) + \omega_3^2 + \omega_1^2 - q_2 \cdot (q_3 - q_1) - 2M^2] \\
B_3 &= i \frac{g_A}{mF^3} [-4c_1 M^2 + 2c_2 \omega_1 \omega_2 + 2c_3 q_1 \cdot q_2 + c_4(\omega_2 \omega_3 + \omega_3^2 - q_2 \cdot q_3 - M^2)] \\
B_4 &= i \frac{g_A}{mF^3} c_4 [(\omega_1 + \omega_3)(\omega_1 + \omega_2 + \omega_3) - (q_1 + q_3) \cdot (q_1 + q_2 + q_3)] \\
D_2 &= i \frac{g_A}{mF^3} c_4 \\
D_1 &= D_4 = 0
\end{aligned} \tag{A.5}$$

Diagrams 3c+3d:

$$\begin{aligned}
A_1 &= -i \frac{g_A}{2mF^3} \left[\frac{(\omega_1 + \omega_2 + \omega_3)^2 - (q_1 + q_2 + q_3)^2}{\omega_1^2} (-4c_1 M^2 - 2c_2 \omega_2 \omega_3 - 2c_3 q_2 \cdot q_3) \right. \\
&\quad - c_4(\omega_2 \omega_3 - q_2 \cdot q_3) \left(\frac{(\omega_1 + \omega_2)^2 + \omega_3^2 - (q_1 + q_2)^2 - M^2}{\omega_2^2} \right. \\
&\quad \left. \left. + \frac{(\omega_1 + \omega_3)^2 + \omega_2^2 - (q_1 + q_3)^2 - M^2}{\omega_3^2} \right) \right] \\
A_2 &= -i \frac{g_A}{2mF^3} c_4(\omega_2 \omega_3 - q_2 \cdot q_3) \frac{(\omega_1 + \omega_3)^2 + \omega_2^2 - (q_1 + q_3)^2 - M^2}{\omega_3^2} \\
A_4 &= -i \frac{g_A}{2mF^3} c_4(\omega_2 \omega_3 - q_2 \cdot q_3) \left(\frac{(\omega_1 + \omega_2)^2 - \omega_3^2 - (q_1 + q_2)^2 + M^2}{\omega_2^2} \right. \\
&\quad \left. - \frac{(\omega_1 + \omega_3)^2 - \omega_2^2 - (q_1 + q_3)^2 + M^2}{\omega_3^2} \right) \\
B_3 &= -i \frac{g_A}{2mF^3} c_4(\omega_1 \omega_3 - q_1 \cdot q_3) \frac{(\omega_1 + \omega_2 + \omega_3)^2 - (q_1 + q_2 + q_3)^2}{\omega_1^2} \\
D_1 &= -i \frac{g_A}{4mF^3} c_4 \\
&\quad \left(\frac{(\omega_1 + \omega_2)^2 - \omega_3^2 - (q_1 + q_2)^2 + M^2}{\omega_2^2} - \frac{(\omega_1 + \omega_3)^2 - \omega_2^2 - (q_1 + q_3)^2 + M^2}{\omega_3^2} \right) \\
D_4 &= i \frac{g_A}{4mF^3} c_4 \left(\frac{(\omega_1 + \omega_2 + \omega_3)^2 - (q_1 + q_2 + q_3)^2}{\omega_1^2} \right. \\
&\quad \left. + \frac{(\omega_1 + \omega_2)^2 + \omega_3^2 - (q_1 + q_2)^2 - M^2}{\omega_2^2} + \frac{(\omega_1 + \omega_3)^2 + \omega_2^2 - (q_1 + q_3)^2 - M^2}{\omega_3^2} \right)
\end{aligned} \tag{A.6}$$

Diagrams 3e+3f+3g:

$$A_1 = -i \frac{g_A^2}{2F^3} (\omega_2 \omega_3 - q_2 \cdot q_3)$$

$$\begin{aligned}
& \left[\frac{1}{\omega_1 \omega_3} (12M^2 d_{16}(\lambda) - 6M^2 d_{18} + \tilde{d}_{25}(\lambda) \omega_1 \omega_3 + \tilde{d}_{29}(\lambda) (\omega_1^2 + \omega_2^2 + \omega_3^2)) \right. \\
& - \frac{1}{\omega_2 \omega_3} (12M^2 d_{16}(\lambda) - 6M^2 d_{18} - \tilde{d}_{25}(\lambda) \omega_2 \omega_3 + \tilde{d}_{29}(\lambda) (\omega_1^2 + \omega_2^2 + \omega_3^2)) \\
& \left. + \frac{1}{\omega_1 \omega_2} (12M^2 d_{16}(\lambda) - 6M^2 d_{18} + \tilde{d}_{25}(\lambda) \omega_1 \omega_2 + \tilde{d}_{29}(\lambda) (\omega_1^2 + \omega_2^2 + \omega_3^2)) \right] \\
A_2 &= -i \frac{g_A^2}{2F^3} (\omega_2 \omega_3 - q_2 \cdot q_3) \\
& \left[- \frac{1}{\omega_1 \omega_3} (12M^2 d_{16}(\lambda) - 6M^2 d_{18} + \tilde{d}_{25}(\lambda) \omega_1 \omega_3 + \tilde{d}_{29}(\lambda) (\omega_1^2 + \omega_2^2 + \omega_3^2)) \right. \\
& + \frac{1}{\omega_2 \omega_3} (12M^2 d_{16}(\lambda) - 6M^2 d_{18} - \tilde{d}_{25}(\lambda) \omega_2 \omega_3 + \tilde{d}_{29}(\lambda) (\omega_1^2 + \omega_2^2 + \omega_3^2)) \\
& \left. + \frac{1}{\omega_1 \omega_2} (12M^2 d_{16}(\lambda) - 6M^2 d_{18} + \tilde{d}_{25}(\lambda) \omega_1 \omega_2 + \tilde{d}_{29}(\lambda) (\omega_1^2 + \omega_2^2 + \omega_3^2)) \right] \\
B_3 &= i \frac{g_A^2}{2F^3} (\omega_1 \omega_3 - q_1 \cdot q_3) \\
& \left[\frac{1}{\omega_1 \omega_3} (12M^2 d_{16}(\lambda) - 6M^2 d_{18} + \tilde{d}_{25}(\lambda) \omega_1 \omega_3 + \tilde{d}_{29}(\lambda) (\omega_1^2 + \omega_2^2 + \omega_3^2)) \right. \\
& + \frac{1}{\omega_2 \omega_3} (12M^2 d_{16}(\lambda) - 6M^2 d_{18} - \tilde{d}_{25}(\lambda) \omega_2 \omega_3 + \tilde{d}_{29}(\lambda) (\omega_1^2 + \omega_2^2 + \omega_3^2)) \\
& \left. + \frac{1}{\omega_1 \omega_2} (12M^2 d_{16}(\lambda) - 6M^2 d_{18} + \tilde{d}_{25}(\lambda) \omega_1 \omega_2 + \tilde{d}_{29}(\lambda) (\omega_1^2 + \omega_2^2 + \omega_3^2)) \right] \\
D_4 &= -i \frac{g_A^2}{4F^3} \\
& \left[\frac{1}{\omega_1 \omega_3} (12M^2 d_{16}(\lambda) - 6M^2 d_{18} + \tilde{d}_{25}(\lambda) \omega_1 \omega_3 + \tilde{d}_{29}(\lambda) (\omega_1^2 + \omega_2^2 + \omega_3^2)) \right. \\
& - \frac{1}{\omega_2 \omega_3} (12M^2 d_{16}(\lambda) - 6M^2 d_{18} - \tilde{d}_{25}(\lambda) \omega_2 \omega_3 + \tilde{d}_{29}(\lambda) (\omega_1^2 + \omega_2^2 + \omega_3^2)) \\
& \left. + \frac{1}{\omega_1 \omega_2} (12M^2 d_{16}(\lambda) - 6M^2 d_{18} + \tilde{d}_{25}(\lambda) \omega_1 \omega_2 + \tilde{d}_{29}(\lambda) (\omega_1^2 + \omega_2^2 + \omega_3^2)) \right] \\
A_4 &= D_1 = 0
\end{aligned} \tag{A.7}$$

Diagrams 3h+3i:

$$\begin{aligned}
A_1 &= -i \frac{g_A^3}{2F^3} (\omega_2 \omega_3 - q_2 \cdot q_3) \left[\frac{1}{\omega_1 \omega_3} (\tilde{d}_{24}(\lambda) (\omega_1^2 + \omega_3^2) + 16M^2 \tilde{d}_{28}(\lambda)) \right. \\
& \left. + \frac{1}{\omega_1 \omega_2} (\tilde{d}_{24}(\lambda) (\omega_1^2 + \omega_2^2) + 16M^2 \tilde{d}_{28}(\lambda)) - \frac{1}{\omega_2 \omega_3} (\tilde{d}_{24}(\lambda) (\omega_2^2 + \omega_3^2) + 16M^2 \tilde{d}_{28}(\lambda)) \right] \\
A_2 &= -i \frac{g_A^3}{2F^3} (\omega_2 \omega_3 - q_2 \cdot q_3) \left[- \frac{1}{\omega_1 \omega_3} (\tilde{d}_{24}(\lambda) (\omega_1^2 + \omega_3^2) + 16M^2 \tilde{d}_{28}(\lambda)) \right. \\
& \left. + \frac{1}{\omega_1 \omega_2} (\tilde{d}_{24}(\lambda) (\omega_1^2 + \omega_2^2) + 16M^2 \tilde{d}_{28}(\lambda)) + \frac{1}{\omega_2 \omega_3} (\tilde{d}_{24}(\lambda) (\omega_2^2 + \omega_3^2) + 16M^2 \tilde{d}_{28}(\lambda)) \right]
\end{aligned}$$

$$\begin{aligned}
A_4 &= 0 \\
B_3 &= i \frac{g_A^3}{2F^3} (\omega_1 \omega_3 - q_1 \cdot q_3) \left[\frac{1}{\omega_1 \omega_3} (\tilde{d}_{24}(\lambda)(\omega_1^2 + \omega_3^2) + 16M^2 \tilde{d}_{28}(\lambda)) \right. \\
&\quad \left. + \frac{1}{\omega_1 \omega_2} (\tilde{d}_{24}(\lambda)(\omega_1^2 + \omega_2^2) + 16M^2 \tilde{d}_{28}(\lambda)) + \frac{1}{\omega_2 \omega_3} (\tilde{d}_{24}(\lambda)(\omega_2^2 + \omega_3^2) + 16M^2 \tilde{d}_{28}(\lambda)) \right] \\
D_4 &= -i \frac{g_A^3}{4F^3} \left[\frac{1}{\omega_1 \omega_3} (\tilde{d}_{24}(\lambda)(\omega_1^2 + \omega_3^2) + 16M^2 \tilde{d}_{28}(\lambda)) \right. \\
&\quad \left. + \frac{1}{\omega_1 \omega_2} (\tilde{d}_{24}(\lambda)(\omega_1^2 + \omega_2^2) + 16M^2 \tilde{d}_{28}(\lambda)) - \frac{1}{\omega_2 \omega_3} (\tilde{d}_{24}(\lambda)(\omega_2^2 + \omega_3^2) + 16M^2 \tilde{d}_{28}(\lambda)) \right] \\
D_1 &= 0
\end{aligned} \tag{A.8}$$

Diagrams 3j+3k:

$$\begin{aligned}
A_2 &= -i \frac{1}{2F^3} \frac{\omega_2 - \omega_3}{\omega_1} (4M^2 d_{16}(\lambda) - 2M^2 d_{18}) \\
B_3 &= -i \frac{1}{2F^3} \frac{\omega_1 + \omega_3}{\omega_2} (4M^2 d_{16}(\lambda) - 2M^2 d_{18}) \\
A_1 &= A_4 = D_1 = D_4 = 0
\end{aligned} \tag{A.9}$$

Diagrams 3l+3m:

$$\begin{aligned}
A_2 &= -i \frac{g_A}{2F^3} \frac{\omega_2 - \omega_3}{\omega_1} (\tilde{d}_{24}(\lambda) \omega_1^2 - 8M^2 \tilde{d}_{28}(\lambda)) \\
B_3 &= -i \frac{g_A}{2F^3} \frac{\omega_1 + \omega_3}{\omega_2} (\tilde{d}_{24}(\lambda) \omega_2^2 - 8M^2 \tilde{d}_{28}(\lambda)) \\
A_1 &= A_4 = D_1 = D_4 = 0
\end{aligned} \tag{A.10}$$

Diagrams 3n+3o:

$$\begin{aligned}
A_1 &= i \frac{g_A}{F^3} \left[2 \frac{c_2}{m} \frac{\omega_2 q_1 \cdot q_3 + \omega_3 q_1 \cdot q_2}{\omega_1} - \frac{c_4}{m} \left(\frac{\omega_3(\omega_2^2 - M^2)}{\omega_2} + \frac{\omega_2(\omega_3^2 - M^2)}{\omega_3} \right) \right. \\
&\quad \left. + 8\tilde{d}_{26}(\lambda) q_2 \cdot q_3 + 8\tilde{d}_{27}(\lambda) \omega_2 \omega_3 + 8M^2 \tilde{d}_{28}(\lambda) - 8\tilde{d}_{30}(\lambda) (\omega_2 \omega_3 - q_2 \cdot q_3) \right] \\
A_2 &= i \frac{g_A}{F^3} \left[\frac{c_4}{m} \left(-\frac{(\omega_2 - \omega_3)(q_2 \cdot q_3 + M^2) + \omega_3 q_1 \cdot q_2 - \omega_2 q_1 \cdot q_3}{\omega_1} + \frac{\omega_2(\omega_3^2 - M^2)}{\omega_3} \right) \right. \\
&\quad + 4(d_1(\lambda) + d_2) \frac{(\omega_2 - \omega_3) q_2 \cdot q_3}{\omega_1} + 4d_3(\lambda) \frac{(\omega_2 - \omega_3) \omega_2 \omega_3}{\omega_1} - 8M^2 d_5(\lambda) \frac{(\omega_2 - \omega_3)}{\omega_1} \\
&\quad + 2(d_{14}(\lambda) - d_{15}) \frac{(\omega_1 + \omega_3)(\omega_2 \omega_3 - q_2 \cdot q_3)}{\omega_2} + \frac{1}{2} \tilde{d}_{24}(\lambda) \omega_1 (\omega_2 - \omega_3) \\
&\quad \left. - 4M^2 \tilde{d}_{28}(\lambda) \frac{\omega_2 - \omega_3}{\omega_1} + 4\tilde{d}_{30}(\lambda) (\omega_2 \omega_3 - q_2 \cdot q_3) \right]
\end{aligned}$$

$$\begin{aligned}
A_4 &= i \frac{g_A}{mF^3} c_4 \left[\frac{\omega_3 q_1 \cdot q_2 - \omega_2 q_1 \cdot q_3}{\omega_1} + \frac{(\omega_1 + \omega_3)(\omega_2 \omega_3 - q_2 \cdot q_3) + \omega_3(\omega_2^2 - M^2)}{\omega_2} \right. \\
&\quad \left. - \frac{(\omega_1 + \omega_2)(\omega_2 \omega_3 - q_2 \cdot q_3) + \omega_2(\omega_3^2 - M^2)}{\omega_3} \right] \\
B_1 &= i \frac{g_A}{F^3} \left[\frac{c_4}{m} \left(\frac{-(\omega_1 + \omega_3)(q_1 \cdot q_3 - M^2) - \omega_3 q_1 \cdot q_2 + \omega_1 q_2 \cdot q_3}{\omega_2} + \frac{\omega_1(\omega_3^2 - M^2)}{\omega_3} \right) \right. \\
&\quad + 4(d_1(\lambda) + d_2) \frac{(\omega_1 + \omega_3)q_1 \cdot q_3}{\omega_2} + 4d_3(\lambda) \frac{(\omega_1 + \omega_3)\omega_1 \omega_3}{\omega_2} + 8M^2 d_5(\lambda) \frac{(\omega_1 + \omega_3)}{\omega_2} \\
&\quad + 2(d_{14}(\lambda) - d_{15}) \frac{(\omega_2 - \omega_3)(\omega_1 \omega_3 - q_1 \cdot q_3)}{\omega_1} - \frac{1}{2} \tilde{d}_{24}(\lambda) \omega_2 (\omega_1 + \omega_3) \\
&\quad \left. + 4M^2 \tilde{d}_{28}(\lambda) \frac{\omega_1 + \omega_3}{\omega_2} + 4\tilde{d}_{30}(\lambda)(\omega_1 \omega_3 - q_1 \cdot q_3) \right] \\
B_2 &= i \frac{g_A}{F^3} \left[2 \frac{c_2}{m} \frac{\omega_1 q_2 \cdot q_3 + \omega_3 q_1 \cdot q_2}{\omega_2} - \frac{c_4}{m} \left(\frac{\omega_3(\omega_1^2 - M^2)}{\omega_1} + \frac{\omega_1(\omega_3^2 - M^2)}{\omega_3} \right) \right. \\
&\quad \left. + 8\tilde{d}_{26}(\lambda) q_1 \cdot q_3 + 8\tilde{d}_{27}(\lambda) \omega_1 \omega_3 - 8M^2 \tilde{d}_{28}(\lambda) - 8\tilde{d}_{30}(\lambda)(\omega_1 \omega_3 - q_1 \cdot q_3) \right] \\
B_3 &= i \frac{g_A}{F^3} \left[\frac{c_4}{m} \left(\frac{\omega_3(\omega_1^2 - M^2)}{\omega_1} + \frac{(\omega_1 + \omega_3)(q_1 \cdot q_3 - M^2) + \omega_3 q_1 \cdot q_2 - \omega_1 q_2 \cdot q_3}{\omega_2} \right) \right. \\
&\quad - 4(d_1(\lambda) + d_2) \frac{(\omega_1 + \omega_3)q_1 \cdot q_3}{\omega_2} - 4d_3(\lambda) \frac{(\omega_1 + \omega_3)\omega_1 \omega_3}{\omega_2} - 8M^2 d_5(\lambda) \frac{(\omega_1 + \omega_3)}{\omega_2} \\
&\quad - 2(d_{14}(\lambda) - d_{15}) \frac{(\omega_1 + \omega_2)(\omega_1 \omega_3 - q_1 \cdot q_3)}{\omega_3} + \frac{1}{2} \tilde{d}_{24}(\lambda) \omega_2 (\omega_1 + \omega_3) \\
&\quad \left. - 4M^2 \tilde{d}_{28}(\lambda) \frac{\omega_1 + \omega_3}{\omega_2} + 4\tilde{d}_{30}(\lambda)(\omega_1 \omega_3 - q_1 \cdot q_3) \right] \\
B_4 &= i \frac{g_A}{mF^3} c_4 \left[\frac{(\omega_2 + \omega_3)(\omega_1 \omega_3 - q_1 \cdot q_3) + \omega_3(\omega_1^2 - M^2)}{\omega_1} + \frac{\omega_3 q_1 \cdot q_2 - \omega_1 q_2 \cdot q_3}{\omega_2} \right. \\
&\quad \left. + \frac{(\omega_1 + \omega_2)(\omega_1 \omega_3 - q_1 \cdot q_3) + \omega_1(\omega_3^2 - M^2)}{\omega_3} \right] \\
D_1 &= i \frac{g_A}{2mF^3} c_4 \left[\frac{\omega_1 + \omega_3}{\omega_2} - \frac{\omega_1 + \omega_2}{\omega_3} \right] \\
D_2 &= i \frac{g_A}{2mF^3} c_4 \left[\frac{\omega_2 + \omega_3}{\omega_1} + \frac{\omega_1 + \omega_2}{\omega_3} \right] \\
D_4 &= -6i \frac{g_A}{F^3} \tilde{d}_{30}(\lambda)
\end{aligned} \tag{A.11}$$

Diagram 3p:

$$\begin{aligned}
A_1 &= \frac{i}{F^3} \left[2 \frac{c_4}{m} g_A \omega_2 \omega_3 - 4d_{10}(\lambda) q_2 \cdot q_3 - 4d_{12}(\lambda) \omega_2 \omega_3 - 4M^2 d_{16}(\lambda) + 2M^2 d_{18} \right] \\
A_2 &= \frac{i}{F^3} \left[-\frac{c_4}{m} g_A \omega_2 \omega_3 - 2d_{11}(\lambda) q_2 \cdot q_3 - 2d_{13}(\lambda) \omega_2 \omega_3 + 2M^2 d_{16}(\lambda) - M^2 d_{18} \right]
\end{aligned}$$

$$\begin{aligned}
& + \frac{1}{2} \tilde{d}_{29}(\lambda) (\omega_2^2 - \omega_3^2) \Big] \\
B_3 &= \frac{i}{F^3} \left[-\frac{c_4}{m} g_A \omega_1 \omega_3 - 2d_{11}(\lambda) q_1 \cdot q_3 - 2d_{13}(\lambda) \omega_1 \omega_3 - 2M^2 d_{16}(\lambda) + M^2 d_{18} \right. \\
& \quad \left. + \frac{1}{2} \tilde{d}_{29}(\lambda) (\omega_1^2 - \omega_3^2) \right] \\
D_4 &= \frac{i}{F^3} 12d_4(\lambda) \\
A_4 &= D_1 = 0
\end{aligned} \tag{A.12}$$

Diagram 3q:

$$\begin{aligned}
A_1 &= -\frac{i}{F^3} \frac{1}{(q_1 - q_2 - q_3)^2 - M^2} [4M^2 d_{16}(\lambda) - 2M^2 d_{18}] (t_3 - M^2) \\
A_2 &= -\frac{i}{F^3} \frac{1}{(q_1 - q_2 - q_3)^2 - M^2} [4M^2 d_{16}(\lambda) - 2M^2 d_{18}] (t_2 - M^2) \\
B_3 &= \frac{i}{F^3} \frac{1}{(q_1 - q_2 - q_3)^2 - M^2} [4M^2 d_{16}(\lambda) - 2M^2 d_{18}] (t_1 - M^2) \\
A_4 &= D_1 = D_4 = 0
\end{aligned} \tag{A.13}$$

Diagram 3r: Combine with diagrams R1e and s35.

Diagram 3s:

$$\begin{aligned}
A_1 &= -i \frac{g_A}{F^5} \frac{1}{(q_1 - q_2 - q_3)^2 - M^2} \left[8\ell_1 q_1 \cdot (q_2 + q_3 - q_1) q_2 \cdot q_3 \right. \\
& \quad + 4\ell_2 [q_3 \cdot (q_2 + q_3 - q_1) q_1 \cdot q_2 + q_2 \cdot (q_2 + q_3 - q_1) q_1 \cdot q_3] \\
& \quad \left. + 2M^2 \ell_4 [q_1 \cdot (q_2 + q_3 - q_1) + q_2 \cdot q_3 + (q_2 + q_3)^2] \right] \\
A_2 &= -i \frac{g_A}{F^5} \frac{1}{(q_1 - q_2 - q_3)^2 - M^2} \left[8\ell_1 q_2 \cdot (q_2 + q_3 - q_1) q_1 \cdot q_3 \right. \\
& \quad + 4\ell_2 [q_3 \cdot (q_2 + q_3 - q_1) q_1 \cdot q_2 + q_1 \cdot (q_2 + q_3 - q_1) q_2 \cdot q_3] \\
& \quad \left. - 2M^2 \ell_4 [q_2 \cdot (q_2 + q_3 - q_1) + q_1 \cdot q_3 - (q_1 - q_3)^2] \right] \\
B_3 &= i \frac{g_A}{F^5} \frac{1}{(q_1 - q_2 - q_3)^2 - M^2} \left[8\ell_1 q_3 \cdot (q_2 + q_3 - q_1) q_1 \cdot q_2 \right. \\
& \quad + 4\ell_2 [q_2 \cdot (q_2 + q_3 - q_1) q_1 \cdot q_3 + q_1 \cdot (q_2 + q_3 - q_1) q_2 \cdot q_3] \\
& \quad \left. - 2M^2 \ell_4 [q_3 \cdot (q_2 + q_3 - q_1) + q_1 \cdot q_2 - (q_1 - q_2)^2] \right] \\
A_4 &= D_1 = D_4 = 0
\end{aligned} \tag{A.14}$$

2. Tadpoles

We use the loop functions as defined in ref.[21].

Diagrams t1+t2+t3:

$$\begin{aligned}
A_1 &= -\frac{3i}{4} \frac{g_A^3}{F^5} (\omega_2 \omega_3 - q_2 \cdot q_3) \Delta_\pi \left(\frac{1}{\omega_1 \omega_2} + \frac{1}{\omega_1 \omega_3} - \frac{1}{\omega_2 \omega_3} \right) \\
A_2 &= -\frac{3i}{4} \frac{g_A^3}{F^5} (\omega_2 \omega_3 - q_2 \cdot q_3) \Delta_\pi \left(\frac{1}{\omega_1 \omega_2} - \frac{1}{\omega_1 \omega_3} + \frac{1}{\omega_2 \omega_3} \right) \\
B_3 &= \frac{3i}{4} \frac{g_A^3}{F^5} (\omega_1 \omega_3 - q_1 \cdot q_3) \Delta_\pi \left(\frac{1}{\omega_1 \omega_2} + \frac{1}{\omega_1 \omega_3} + \frac{1}{\omega_2 \omega_3} \right) \\
D_4 &= -\frac{3i}{8} \frac{g_A^3}{F^5} \Delta_\pi \left(\frac{1}{\omega_1 \omega_2} + \frac{1}{\omega_1 \omega_3} - \frac{1}{\omega_2 \omega_3} \right) \\
A_4 &= D_1 = 0
\end{aligned} \tag{A.15}$$

Diagrams t4+t5:

$$\begin{aligned}
A_2 &= -\frac{i}{4} \frac{g_A}{F^5} \Delta_\pi \frac{\omega_2 - \omega_3}{\omega_1} \\
B_3 &= -\frac{i}{4} \frac{g_A}{F^5} \Delta_\pi \frac{\omega_1 + \omega_3}{\omega_2} \\
A_1 &= A_4 = D_1 = D_4 = 0
\end{aligned} \tag{A.16}$$

Diagrams t6+t7:

$$\begin{aligned}
A_2 &= -\frac{5i}{8} \frac{g_A}{F^5} \Delta_\pi \frac{\omega_2 - \omega_3}{\omega_1} \\
B_3 &= -\frac{5i}{8} \frac{g_A}{F^5} \Delta_\pi \frac{\omega_1 + \omega_3}{\omega_2} \\
A_1 &= A_4 = D_1 = D_4 = 0
\end{aligned} \tag{A.17}$$

Diagrams t8+t9:

$$\begin{aligned}
A_2 &= i \frac{g_A}{F^5} \frac{\omega_2 - \omega_3}{\omega_1} I_2(t_3) \\
B_3 &= i \frac{g_A}{F^5} \frac{\omega_1 + \omega_3}{\omega_2} I_2(t_2) \\
A_1 &= A_4 = D_1 = D_4 = 0
\end{aligned} \tag{A.18}$$

Diagram t10:

$$\begin{aligned}
A_1 &= \frac{i}{4} \frac{g_A}{F^5} \left\{ 2(t_3 - M^2) I_0(t_3) \right. \\
&\quad \left. + \frac{1}{3} \left[\left(3q_1 \cdot q_3 - \frac{t_2}{2} + 2M^2 \right) I_0(t_2) - 4\Delta_\pi + \frac{1}{16\pi^2} \left(2M^2 - \frac{t_2}{3} \right) \right] \right\}
\end{aligned}$$

$$\begin{aligned}
& + \frac{1}{3} \left[\left(3q_1 \cdot q_2 - \frac{t_1}{2} + 2M^2 \right) I_0(t_1) - 4\Delta_\pi + \frac{1}{16\pi^2} \left(2M^2 - \frac{t_1}{3} \right) \right] \Big\} \\
A_2 &= \frac{i}{4} \frac{g_A}{F^5} \left\{ (2M^2 - t_3) I_0(t_3) - 2\Delta_\pi + (3t_2 - 2M^2) I_0(t_2) - 2\Delta_\pi \right. \\
& \quad \left. - \frac{1}{3} \left[\left(-3q_1 \cdot q_2 - \frac{t_1}{2} + 2M^2 \right) I_0(t_1) + 2\Delta_\pi + \frac{1}{16\pi^2} \left(2M^2 - \frac{t_1}{3} \right) \right] \right\} \\
B_3 &= \frac{i}{4} \frac{g_A}{F^5} \left\{ \frac{1}{3} \left[\left(3q_2 \cdot q_3 - \frac{t_3}{2} + 2M^2 \right) I_0(t_3) + 2\Delta_\pi + \frac{1}{16\pi^2} \left(2M^2 - \frac{t_3}{3} \right) \right] \right. \\
& \quad \left. - (2M^2 - \frac{t_2}{2}) I_0(t_2) + 2\Delta_\pi - (3t_1 - 2M^2) I_0(t_1) + 2\Delta_\pi \right\} \\
A_4 &= D_1 = D_4 = 0
\end{aligned} \tag{A.19}$$

Diagram t11:

$$\begin{aligned}
A_1 &= \frac{3i}{4} \frac{g_A}{F^5} \Delta_\pi \\
A_2 &= \frac{21i}{8} \frac{g_A}{F^5} \Delta_\pi \\
B_3 &= -\frac{21i}{8} \frac{g_A}{F^5} \Delta_\pi \\
A_4 &= D_1 = D_4 = 0
\end{aligned} \tag{A.20}$$

Diagram t12:

$$\begin{aligned}
A_1 &= -i \frac{g_A}{2F^5} \frac{1}{(q_1 - q_2 - q_3)^2 - M^2} \Delta_\pi (t_3 - M^2) \\
A_2 &= -i \frac{g_A}{2F^5} \frac{1}{(q_1 - q_2 - q_3)^2 - M^2} \Delta_\pi (t_2 - M^2) \\
B_3 &= i \frac{g_A}{2F^5} \frac{1}{(q_1 - q_2 - q_3)^2 - M^2} \Delta_\pi (t_1 - M^2) \\
A_4 &= D_1 = D_4 = 0
\end{aligned} \tag{A.21}$$

Diagram t13:

$$\begin{aligned}
A_1 &= -i \frac{g_A}{2F^5} \frac{1}{(q_1 - q_2 - q_3)^2 - M^2} \\
& \quad \left\{ (t_3 - M^2) [I_0(t_3) (2t_3 + M^2 - 2q_1 \cdot (q_2 + q_3)) - 4\Delta_\pi] \right. \\
& \quad + I_0(t_2) [M^2 (2M^2 - t_2) + \frac{q_1 \cdot q_2}{3} (4t_2 - 10M^2) - \frac{q_2 \cdot q_3}{3} (2t_2 - 2M^2)] \\
& \quad + \Delta_\pi (-4M^2 + \frac{8}{3} q_1 \cdot q_2 - \frac{4}{3} q_2 \cdot q_3) - \frac{1}{72\pi^2} (6M^2 - t_2) q_2 \cdot (q_1 + q_3) \\
& \quad \left. + I_0(t_1) [M^2 (2M^2 - t_1) + \frac{q_1 \cdot q_3}{3} (4t_1 - 10M^2) - \frac{q_2 \cdot q_3}{3} (2t_1 - 2M^2)] \right\}
\end{aligned}$$

$$\begin{aligned}
& +\Delta_\pi(-4M^2 + \frac{8}{3}q_1 \cdot q_3 - \frac{4}{3}q_2 \cdot q_3) - \frac{1}{72\pi^2}(6M^2 - t_1)q_3 \cdot (q_1 + q_2) \Big\} \\
A_2 = & -i \frac{g_A}{2F^5} \frac{1}{(q_1 - q_2 - q_3)^2 - M^2} \\
& \left\{ I_0(t_3)[M^2(2M^2 - t_3) + \frac{q_1 \cdot q_2}{3}(4t_3 - 10M^2) + \frac{q_1 \cdot q_3}{3}(2t_3 - 2M^2)] \right. \\
& +\Delta_\pi(-4M^2 + \frac{8}{3}q_1 \cdot q_2 + \frac{4}{3}q_1 \cdot q_3) - \frac{1}{72\pi^2}(6M^2 - t_3)q_1 \cdot (q_2 - q_3) \\
& + (t_2 - M^2)[I_0(t_2)(2t_2 + M^2 - 2q_2 \cdot (q_1 - q_3)) - 4\Delta_\pi] \\
& + I_0(t_1)[M^2(2M^2 - t_1) - \frac{q_2 \cdot q_3}{3}(4t_1 - 10M^2) + \frac{q_1 \cdot q_3}{3}(2t_1 - 2M^2)] \\
& \left. +\Delta_\pi(-4M^2 - \frac{8}{3}q_2 \cdot q_3 + \frac{4}{3}q_1 \cdot q_3) + \frac{1}{72\pi^2}(6M^2 - t_1)q_3 \cdot (q_1 + q_2) \right\} \\
B_3 = & i \frac{g_A}{2F^5} \frac{1}{(q_1 - q_2 - q_3)^2 - M^2} \\
& \left\{ I_0(t_3)[M^2(2M^2 - t_3) + \frac{q_1 \cdot q_3}{3}(4t_3 - 10M^2) + \frac{q_1 \cdot q_2}{3}(2t_3 - 2M^2)] \right. \\
& +\Delta_\pi(-4M^2 + \frac{8}{3}q_1 \cdot q_3 + \frac{4}{3}q_1 \cdot q_2) - \frac{1}{72\pi^2}(6M^2 - t_3)q_1 \cdot (q_3 - q_2) \\
& + I_0(t_2)[M^2(2M^2 - t_2) - \frac{q_2 \cdot q_3}{3}(4t_2 - 10M^2) + \frac{q_1 \cdot q_2}{3}(2t_2 - 2M^2)] \\
& +\Delta_\pi(-4M^2 - \frac{8}{3}q_2 \cdot q_3 + \frac{4}{3}q_1 \cdot q_2) + \frac{1}{72\pi^2}(6M^2 - t_2)q_2 \cdot (q_1 + q_3) \\
& \left. + (t_1 - M^2)[I_0(t_1)(2t_1 + M^2 - 2q_3 \cdot (q_1 - q_2)) - 4\Delta_\pi] \right\} \\
A_4 = & D_1 = D_4 = 0
\end{aligned} \tag{A.22}$$

Diagram t14:

$$\begin{aligned}
A_1 = & i \frac{g_A}{F^5} \frac{1}{(q_1 - q_2 - q_3)^2 - M^2} \Delta_\pi \left[-5t_3 + \frac{7}{2}M^2 - (q_2 + q_3 - q_1)^2 \right] \\
A_2 = & i \frac{g_A}{F^5} \frac{1}{(q_1 - q_2 - q_3)^2 - M^2} \Delta_\pi \left[-5t_2 + \frac{7}{2}M^2 - (q_2 + q_3 - q_1)^2 \right] \\
B_3 = & -i \frac{g_A}{F^5} \frac{1}{(q_1 - q_2 - q_3)^2 - M^2} \Delta_\pi \left[-5t_1 + \frac{7}{2}M^2 - (q_2 + q_3 - q_1)^2 \right] \\
A_4 = & D_1 = D_4 = 0
\end{aligned} \tag{A.23}$$

3. Self-energies

We use the loop functions as defined in ref.[21].

Diagrams s1+s3:

$$A_1 = -\frac{i}{4} \left(\frac{g_A}{F} \right)^5 (\omega_2 \omega_3 - q_2 \cdot q_3) \left(S^2 + \frac{1}{2} \right) \left[\frac{J_2(\omega_1) - J_2(-\omega_1)}{\omega_1^2} \left(\frac{1}{\omega_2} + \frac{1}{\omega_3} \right) \right]$$

$$\begin{aligned}
& + \frac{J_2(\omega_2) - J_2(-\omega_2)}{\omega_2^2} \left(\frac{1}{\omega_1} - \frac{1}{\omega_3} \right) + \frac{J_2(\omega_3) - J_2(-\omega_3)}{\omega_3^2} \left(\frac{1}{\omega_1} - \frac{1}{\omega_2} \right) \Big] \\
A_2 &= -\frac{i}{4} \left(\frac{g_A}{F} \right)^5 (\omega_2 \omega_3 - q_2 \cdot q_3) \left(S^2 + \frac{1}{2} \right) \left[\frac{J_2(\omega_1) - J_2(-\omega_1)}{\omega_1^2} \left(\frac{1}{\omega_2} - \frac{1}{\omega_3} \right) \right. \\
& \quad \left. + \frac{J_2(\omega_2) - J_2(-\omega_2)}{\omega_2^2} \left(\frac{1}{\omega_1} + \frac{1}{\omega_3} \right) + \frac{J_2(\omega_3) - J_2(-\omega_3)}{\omega_3^2} \left(-\frac{1}{\omega_1} + \frac{1}{\omega_2} \right) \right] \\
A_4 &= -\frac{i}{4} \left(\frac{g_A}{F} \right)^5 (\omega_2 \omega_3 - q_2 \cdot q_3) \left(S^2 + \frac{1}{2} \right) \left[\frac{J_2(\omega_1) + J_2(-\omega_1) - 2J_2(0)}{\omega_1^2} \left(\frac{1}{\omega_2} - \frac{1}{\omega_3} \right) \right. \\
& \quad + \frac{J_2(\omega_2) + J_2(-\omega_2) - 2J_2(0)}{\omega_2^2} \left(\frac{1}{\omega_1} - \frac{1}{\omega_3} \right) \\
& \quad \left. + \frac{J_2(\omega_3) + J_2(-\omega_3) - 2J_2(0)}{\omega_3^2} \left(-\frac{1}{\omega_1} + \frac{1}{\omega_2} \right) \right] \\
B_3 &= \frac{i}{4} \left(\frac{g_A}{F} \right)^5 (\omega_1 \omega_3 - q_1 \cdot q_3) \left(S^2 + \frac{1}{2} \right) \left[\frac{J_2(\omega_1) - J_2(-\omega_1)}{\omega_1^2} \left(\frac{1}{\omega_2} + \frac{1}{\omega_3} \right) \right. \\
& \quad \left. + \frac{J_2(\omega_2) - J_2(-\omega_2)}{\omega_2^2} \left(\frac{1}{\omega_1} + \frac{1}{\omega_3} \right) + \frac{J_2(\omega_3) - J_2(-\omega_3)}{\omega_3^2} \left(\frac{1}{\omega_1} + \frac{1}{\omega_2} \right) \right] \\
D_1 &= -\frac{i}{8} \left(\frac{g_A}{F} \right)^5 \left(S^2 + \frac{1}{2} \right) \left[\frac{J_2(\omega_1) + J_2(-\omega_1) - 2J_2(0)}{\omega_1^2} \left(\frac{1}{\omega_2} - \frac{1}{\omega_3} \right) \right. \\
& \quad + \frac{J_2(\omega_2) + J_2(-\omega_2) - 2J_2(0)}{\omega_2^2} \left(\frac{1}{\omega_1} - \frac{1}{\omega_3} \right) \\
& \quad \left. + \frac{J_2(\omega_3) + J_2(-\omega_3) - 2J_2(0)}{\omega_3^2} \left(-\frac{1}{\omega_1} + \frac{1}{\omega_2} \right) \right] \\
D_4 &= -\frac{i}{8} \left(\frac{g_A}{F} \right)^5 \left(S^2 + \frac{1}{2} \right) \left[\frac{J_2(\omega_1) - J_2(-\omega_1)}{\omega_1^2} \left(\frac{1}{\omega_2} + \frac{1}{\omega_3} \right) \right. \\
& \quad \left. + \frac{J_2(\omega_2) - J_2(-\omega_2)}{\omega_2^2} \left(\frac{1}{\omega_1} - \frac{1}{\omega_3} \right) + \frac{J_2(\omega_3) - J_2(-\omega_3)}{\omega_3^2} \left(\frac{1}{\omega_1} - \frac{1}{\omega_2} \right) \right] \tag{A.24}
\end{aligned}$$

Diagram s2:

$$\begin{aligned}
A_1 &= -\frac{i}{2\omega_1\omega_2\omega_3} \left(\frac{g_A}{F} \right)^5 (\omega_2 \omega_3 - q_2 \cdot q_3) \left(S^2 + \frac{1}{2} \right) \\
& \quad \left[(J_2(\omega_1) - J_2(-\omega_1)) - (J_2(\omega_2) - J_2(-\omega_2)) - (J_2(\omega_3) - J_2(-\omega_3)) \right] \\
A_2 &= -\frac{i}{2\omega_1\omega_2\omega_3} \left(\frac{g_A}{F} \right)^5 (\omega_2 \omega_3 - q_2 \cdot q_3) \left(S^2 + \frac{1}{2} \right) (J_2(\omega_3) - J_2(-\omega_3)) \\
A_4 &= -\frac{i}{2\omega_1\omega_2\omega_3} \left(\frac{g_A}{F} \right)^5 (\omega_2 \omega_3 - q_2 \cdot q_3) \left(S^2 + \frac{1}{2} \right) \\
& \quad \left[- (J_2(\omega_2) + J_2(-\omega_2)) + (J_2(\omega_3) + J_2(-\omega_3)) \right] \\
B_3 &= \frac{i}{2\omega_1\omega_2\omega_3} \left(\frac{g_A}{F} \right)^5 (\omega_1 \omega_3 - q_1 \cdot q_3) \left(S^2 + \frac{1}{2} \right) (J_2(\omega_1) - J_2(-\omega_1))
\end{aligned}$$

$$\begin{aligned}
D_1 &= -\frac{i}{4\omega_1\omega_2\omega_3} \left(\frac{g_A}{F}\right)^5 \left(S^2 + \frac{1}{2}\right) \\
&\quad \left[- (J_2(\omega_2) + J_2(-\omega_2)) + (J_2(\omega_3) + J_2(-\omega_3)) \right] \\
D_4 &= -\frac{i}{4\omega_1\omega_2\omega_3} \left(\frac{g_A}{F}\right)^5 \left(S^2 + \frac{1}{2}\right) \\
&\quad \left[(J_2(\omega_1) - J_2(-\omega_1)) - (J_2(\omega_2) - J_2(-\omega_2)) - (J_2(\omega_3) - J_2(-\omega_3)) \right] \quad (\text{A.25})
\end{aligned}$$

Diagrams s4+s5:

$$\begin{aligned}
A_1 &= \frac{3i}{4} \left(\frac{g_A}{F}\right)^5 S^2(\omega_2\omega_3 - q_2 \cdot q_3) \left[\frac{J_2(\omega_1) - J_2(-\omega_1)}{\omega_1^2} \left(\frac{1}{\omega_2} + \frac{1}{\omega_3}\right) \right. \\
&\quad \left. + \frac{J_2(\omega_2) - J_2(-\omega_2)}{\omega_2^2} \left(\frac{1}{\omega_1} - \frac{1}{\omega_3}\right) + \frac{J_2(\omega_3) - J_2(-\omega_3)}{\omega_3^2} \left(\frac{1}{\omega_1} - \frac{1}{\omega_2}\right) \right] \\
A_2 &= \frac{3i}{4} \left(\frac{g_A}{F}\right)^5 S^2(\omega_2\omega_3 - q_2 \cdot q_3) \left[\frac{J_2(\omega_1) - J_2(-\omega_1)}{\omega_1^2} \left(\frac{1}{\omega_2} - \frac{1}{\omega_3}\right) \right. \\
&\quad \left. + \frac{J_2(\omega_2) - J_2(-\omega_2)}{\omega_2^2} \left(\frac{1}{\omega_1} + \frac{1}{\omega_3}\right) + \frac{J_2(\omega_3) - J_2(-\omega_3)}{\omega_3^2} \left(-\frac{1}{\omega_1} + \frac{1}{\omega_2}\right) \right] \\
A_4 &= \frac{3i}{4} \left(\frac{g_A}{F}\right)^5 S^2(\omega_2\omega_3 - q_2 \cdot q_3) \left[\frac{J_2(\omega_1) + J_2(-\omega_1)}{\omega_1^2} \left(\frac{1}{\omega_2} - \frac{1}{\omega_3}\right) \right. \\
&\quad \left. + \frac{J_2(\omega_2) + J_2(-\omega_2)}{\omega_2^2} \left(\frac{1}{\omega_1} - \frac{1}{\omega_3}\right) + \frac{J_2(\omega_3) + J_2(-\omega_3)}{\omega_3^2} \left(-\frac{1}{\omega_1} + \frac{1}{\omega_2}\right) \right] \\
B_3 &= -\frac{3i}{4} \left(\frac{g_A}{F}\right)^5 S^2(\omega_1\omega_3 - q_1 \cdot q_3) \left[\frac{J_2(\omega_1) - J_2(-\omega_1)}{\omega_1^2} \left(\frac{1}{\omega_2} + \frac{1}{\omega_3}\right) \right. \\
&\quad \left. + \frac{J_2(\omega_2) - J_2(-\omega_2)}{\omega_2^2} \left(\frac{1}{\omega_1} + \frac{1}{\omega_3}\right) + \frac{J_2(\omega_3) - J_2(-\omega_3)}{\omega_3^2} \left(\frac{1}{\omega_1} + \frac{1}{\omega_2}\right) \right] \\
D_1 &= \frac{3i}{8} \left(\frac{g_A}{F}\right)^5 S^2 \left[\frac{J_2(\omega_1) + J_2(-\omega_1)}{\omega_1^2} \left(\frac{1}{\omega_2} - \frac{1}{\omega_3}\right) \right. \\
&\quad \left. + \frac{J_2(\omega_2) + J_2(-\omega_2)}{\omega_2^2} \left(\frac{1}{\omega_1} - \frac{1}{\omega_3}\right) + \frac{J_2(\omega_3) + J_2(-\omega_3)}{\omega_3^2} \left(-\frac{1}{\omega_1} + \frac{1}{\omega_2}\right) \right] \\
D_4 &= \frac{3i}{8} \left(\frac{g_A}{F}\right)^5 S^2 \left[\frac{J_2(\omega_1) - J_2(-\omega_1)}{\omega_1^2} \left(\frac{1}{\omega_2} + \frac{1}{\omega_3}\right) \right. \\
&\quad \left. + \frac{J_2(\omega_2) - J_2(-\omega_2)}{\omega_2^2} \left(\frac{1}{\omega_1} - \frac{1}{\omega_3}\right) + \frac{J_2(\omega_3) - J_2(-\omega_3)}{\omega_3^2} \left(\frac{1}{\omega_1} - \frac{1}{\omega_2}\right) \right] \quad (\text{A.26})
\end{aligned}$$

Diagrams s6+s7:

$$\begin{aligned}
A_1 &= \frac{i}{4\omega_1} \frac{g_A}{F^5} \left[(\omega_2 - \omega_3) (\omega_3 (J_0(\omega_3) - J_0(-\omega_3)) - \omega_2 (J_0(\omega_2) - J_0(-\omega_2))) \right. \\
&\quad \left. - (\omega_2 + \omega_3) \Delta_\pi \right]
\end{aligned}$$

$$\begin{aligned}
A_2 &= -\frac{i}{8\omega_1} \frac{g_A}{F^5} (\omega_2 - \omega_3) \left[\omega_3 (J_0(\omega_3) - J_0(-\omega_3)) + \omega_2 (J_0(\omega_2) - J_0(-\omega_2)) + 3\Delta_\pi \right] \\
A_4 &= -\frac{i}{8\omega_1} \frac{g_A}{F^5} (\omega_2 - \omega_3) \left[\omega_3 (J_0(\omega_3) + J_0(-\omega_3)) + \omega_2 (J_0(\omega_2) + J_0(-\omega_2)) \right] \\
B_3 &= -\frac{i}{8\omega_2} \frac{g_A}{F^5} (\omega_1 + \omega_3) (\omega_3 (J_0(\omega_3) - J_0(-\omega_3)) + \omega_1 (J_0(\omega_1) - J_0(-\omega_1)) + 3\Delta_\pi) \\
D_1 &= D_4 = 0
\end{aligned} \tag{A.27}$$

Diagram s8+s9:

$$\begin{aligned}
A_1 &= \frac{i}{4} \left(\frac{g_A}{F} \right)^5 (\omega_2 \omega_3 - q_2 \cdot q_3) \\
&\quad \left[\frac{J_2(\omega_1) - J_2(-\omega_1)}{\omega_1} \left(\frac{3S^2}{\omega_1 \omega_2} + \frac{3S^2}{\omega_1 \omega_3} - \frac{2(S^2 + 1)}{\omega_2 \omega_3} \right) \right. \\
&\quad - \frac{J_2(\omega_2) - J_2(-\omega_2)}{\omega_2} \left(\frac{S^2 + 1}{\omega_1 \omega_2} - \frac{S^2 + 1}{\omega_2 \omega_3} + \frac{2S^2 - 1}{\omega_1 \omega_3} \right) \\
&\quad \left. - \frac{J_2(\omega_3) - J_2(-\omega_3)}{\omega_3} \left(\frac{S^2 + 1}{\omega_1 \omega_3} - \frac{S^2 + 1}{\omega_2 \omega_3} + \frac{2S^2 - 1}{\omega_1 \omega_2} \right) \right] \\
A_2 &= \frac{i}{4} \left(\frac{g_A}{F} \right)^5 (\omega_2 \omega_3 - q_2 \cdot q_3) \\
&\quad \left[\frac{J_2(\omega_1) - J_2(-\omega_1)}{\omega_1} \left(\frac{S^2}{\omega_1 \omega_2} - \frac{S^2}{\omega_1 \omega_3} + \frac{4(S^2 + 1)}{\omega_2 \omega_3} \right) \right. \\
&\quad - \frac{J_2(\omega_2) - J_2(-\omega_2)}{\omega_2} \left(\frac{3(S^2 + 1)}{\omega_1 \omega_2} + \frac{3(S^2 + 1)}{\omega_2 \omega_3} + \frac{1}{\omega_1 \omega_3} \right) \\
&\quad \left. + \frac{J_2(\omega_3) - J_2(-\omega_3)}{\omega_3} \left(\frac{S^2 + 1}{\omega_1 \omega_3} - \frac{S^2 + 1}{\omega_2 \omega_3} + \frac{2S^2 + 3}{\omega_1 \omega_2} \right) \right] \\
A_4 &= \frac{i}{4} \left(\frac{g_A}{F} \right)^5 (\omega_2 \omega_3 - q_2 \cdot q_3) \\
&\quad \left[\frac{J_2(\omega_1) + J_2(-\omega_1) - 2J_2(0)}{\omega_1} \left(\frac{S^2}{\omega_1 \omega_2} - \frac{S^2}{\omega_1 \omega_3} \right) \right. \\
&\quad - \frac{J_2(\omega_2) + J_2(-\omega_2) - 2J_2(0)}{\omega_2} \left(\frac{S^2 + 1}{\omega_1 \omega_2} - \frac{S^2 + 1}{\omega_2 \omega_3} - \frac{2S^2 + 1}{\omega_1 \omega_3} \right) \\
&\quad \left. + \frac{J_2(\omega_3) + J_2(-\omega_3) - 2J_2(0)}{\omega_3} \left(\frac{S^2 + 1}{\omega_1 \omega_3} - \frac{S^2 + 1}{\omega_2 \omega_3} - \frac{2S^2 + 1}{\omega_1 \omega_2} \right) \right] \\
B_3 &= \frac{i}{4} \left(\frac{g_A}{F} \right)^5 (\omega_1 \omega_3 - q_1 \cdot q_3) \\
&\quad \left[\frac{J_2(\omega_1) - J_2(-\omega_1)}{\omega_1} \left(\frac{S^2 + 1}{\omega_1 \omega_2} + \frac{S^2 + 1}{\omega_1 \omega_3} - \frac{2S^2 + 3}{\omega_2 \omega_3} \right) \right. \\
&\quad - \frac{J_2(\omega_2) - J_2(-\omega_2)}{\omega_2} \left(\frac{S^2}{\omega_1 \omega_2} + \frac{S^2}{\omega_2 \omega_3} + \frac{4(S^2 + 1)}{\omega_1 \omega_3} \right) \\
&\quad \left. + \frac{J_2(\omega_3) - J_2(-\omega_3)}{\omega_3} \left(\frac{3(S^2 + 1)}{\omega_1 \omega_3} + \frac{3(S^2 + 1)}{\omega_2 \omega_3} - \frac{1}{\omega_1 \omega_2} \right) \right]
\end{aligned}$$

$$\begin{aligned}
D_1 &= \frac{i}{8} \left(\frac{g_A}{F} \right)^5 (S^2 + 1) \\
&\quad \left[-\frac{J_2(\omega_1) + J_2(-\omega_1) - 2J_2(0)}{\omega_1} \left(\frac{3}{\omega_1\omega_2} - \frac{3}{\omega_1\omega_3} \right) \right. \\
&\quad - \frac{J_2(\omega_2) + J_2(-\omega_2) - 2J_2(0)}{\omega_2} \left(\frac{1}{\omega_1\omega_2} - \frac{1}{\omega_2\omega_3} + \frac{2}{\omega_1\omega_3} \right) \\
&\quad \left. + \frac{J_2(\omega_3) + J_2(-\omega_3) - 2J_2(0)}{\omega_3} \left(\frac{1}{\omega_1\omega_3} - \frac{1}{\omega_2\omega_3} + \frac{2}{\omega_1\omega_2} \right) \right] \\
D_4 &= \frac{i}{8} \left(\frac{g_A}{F} \right)^5 (S^2 + 1) \\
&\quad \left[-\frac{J_2(\omega_1) - J_2(-\omega_1)}{\omega_1} \left(\frac{1}{\omega_1\omega_2} + \frac{1}{\omega_1\omega_3} + \frac{2}{\omega_2\omega_3} \right) \right. \\
&\quad - \frac{J_2(\omega_2) - J_2(-\omega_2)}{\omega_2} \left(\frac{1}{\omega_1\omega_2} - \frac{1}{\omega_2\omega_3} - \frac{2}{\omega_1\omega_3} \right) \\
&\quad \left. - \frac{J_2(\omega_3) - J_2(-\omega_3)}{\omega_3} \left(\frac{1}{\omega_1\omega_3} - \frac{1}{\omega_2\omega_3} - \frac{2}{\omega_1\omega_2} \right) \right] \tag{A.28}
\end{aligned}$$

Diagram s10:

$$\begin{aligned}
A_2 &= \frac{i}{8\omega_1} \frac{g_A}{F^5} [(\omega_2 - \omega_3) (\omega_3 (J_0(\omega_3) - J_0(-\omega_3)) - \omega_2 (J_0(\omega_2) - J_0(-\omega_2))) \\
&\quad - (\omega_2 + \omega_3) \Delta_\pi] \\
A_4 &= -\frac{i}{8\omega_1} \frac{g_A}{F^5} (\omega_2 - \omega_3) [\omega_3 (J_0(\omega_3) + J_0(-\omega_3)) + \omega_2 (J_0(\omega_2) + J_0(-\omega_2))] \\
B_3 &= \frac{i}{8\omega_2} \frac{g_A}{F^5} [(\omega_1 + \omega_3) (-\omega_3 (J_0(\omega_3) - J_0(-\omega_3)) + \omega_1 (J_0(\omega_1) - J_0(-\omega_1))) \\
&\quad + (\omega_1 - \omega_3) \Delta_\pi] \\
A_1 &= D_1 = D_4 = 0 \tag{A.29}
\end{aligned}$$

Diagram s11:

$$\begin{aligned}
A_1 &= -\frac{i}{4} \left(\frac{g_A}{F} \right)^5 (\omega_2\omega_3 - q_2 \cdot q_3) \left(S^2 + \frac{1}{2} \right) \\
&\quad \left[\frac{J_2(\omega_1) - J_2(0)}{\omega_1^2} \left(\frac{1}{\omega_2} + \frac{1}{\omega_3} \right) - \frac{J_2(-\omega_1) - J_2(-\omega_2)}{\omega_1} \left(\frac{2}{\omega_2\omega_3} - \frac{1}{\omega_1\omega_2} - \frac{1}{\omega_1\omega_3} \right) \right. \\
&\quad - \frac{J_2(\omega_2) - J_2(0)}{\omega_2} \left(\frac{2}{\omega_1\omega_3} + \frac{1}{\omega_1\omega_2} - \frac{1}{\omega_2\omega_3} \right) - \frac{J_2(-\omega_2) - J_2(0)}{\omega_2^2} \left(\frac{1}{\omega_1} - \frac{1}{\omega_3} \right) \\
&\quad - \frac{J_2(\omega_3) - J_2(0)}{\omega_3} \left(\frac{2}{\omega_1\omega_2} + \frac{1}{\omega_1\omega_3} - \frac{1}{\omega_2\omega_3} \right) - \frac{J_2(-\omega_3) - J_2(0)}{\omega_3^2} \left(\frac{1}{\omega_1} - \frac{1}{\omega_2} \right) \\
&\quad \left. + 2J_2'(0) \left(\frac{1}{\omega_1\omega_2} + \frac{1}{\omega_1\omega_3} - \frac{1}{\omega_2\omega_3} \right) \right]
\end{aligned}$$

$$\begin{aligned}
A_2 &= -\frac{i}{4} \left(\frac{g_A}{F} \right)^5 (\omega_2 \omega_3 - q_2 \cdot q_3) \left(S^2 + \frac{1}{2} \right) \\
&\quad \left[-\frac{J_2(\omega_1) - J_2(-\omega_1)}{\omega_1^2} \left(\frac{1}{\omega_2} - \frac{1}{\omega_3} \right) - \frac{J_2(\omega_2) - J_2(0)}{\omega_2^2} \left(\frac{1}{\omega_1} + \frac{1}{\omega_3} \right) \right. \\
&\quad + \frac{J_2(\omega_3) - J_2(0)}{\omega_3} \left(\frac{2}{\omega_1 \omega_2} + \frac{1}{\omega_1 \omega_3} - \frac{1}{\omega_2 \omega_3} \right) + \frac{J_2(-\omega_3) - J_2(0)}{\omega_3^2} \left(\frac{1}{\omega_1} - \frac{1}{\omega_2} \right) \\
&\quad \left. + 2J_2'(0) \left(\frac{1}{\omega_1 \omega_2} - \frac{1}{\omega_1 \omega_3} + \frac{1}{\omega_2 \omega_3} \right) \right] \\
A_4 &= -\frac{3i}{4} \left(\frac{g_A}{F} \right)^5 (\omega_2 \omega_3 - q_2 \cdot q_3) \left(S^2 + \frac{1}{2} \right) \\
&\quad \left[\frac{J_2(\omega_1) + J_2(-\omega_1) - 2J_2(0)}{\omega_1^2} \left(\frac{1}{\omega_2} - \frac{1}{\omega_3} \right) \right. \\
&\quad + \frac{J_2(\omega_2) - J_2(0)}{\omega_2} \left(\frac{2}{\omega_1 \omega_3} + \frac{1}{\omega_1 \omega_2} - \frac{1}{\omega_2 \omega_3} \right) - \frac{J_2(-\omega_2) - J_2(0)}{\omega_2^2} \left(\frac{1}{\omega_1} - \frac{1}{\omega_3} \right) \\
&\quad - \frac{J_2(\omega_3) - J_2(0)}{\omega_3} \left(\frac{2}{\omega_1 \omega_2} + \frac{1}{\omega_1 \omega_3} - \frac{1}{\omega_2 \omega_3} \right) + \frac{J_2(-\omega_3) - J_2(0)}{\omega_3^2} \left(\frac{1}{\omega_1} - \frac{1}{\omega_2} \right) \left. \right] \\
B_3 &= -\frac{i}{4} \left(\frac{g_A}{F} \right)^5 (\omega_2 \omega_3 - q_2 \cdot q_3) \left(S^2 + \frac{1}{2} \right) \\
&\quad \left[-\frac{J_2(\omega_1) - J_2(0)}{\omega_1^2} \left(\frac{1}{\omega_2} + \frac{1}{\omega_3} \right) + \frac{J_2(-\omega_1) - J_2(0)}{\omega_1} \left(\frac{2}{\omega_2 \omega_3} - \frac{1}{\omega_1 \omega_2} - \frac{1}{\omega_1 \omega_3} \right) \right. \\
&\quad + \frac{J_2(\omega_2) - J_2(-\omega_2)}{\omega_2^2} \left(\frac{1}{\omega_1} + \frac{1}{\omega_3} \right) + \frac{J_2(\omega_3) - J_2(-\omega_3)}{\omega_3^2} \left(\frac{1}{\omega_1} + \frac{1}{\omega_2} \right) \\
&\quad \left. - 2J_2'(0) \left(\frac{1}{\omega_1 \omega_2} + \frac{1}{\omega_1 \omega_3} + \frac{1}{\omega_2 \omega_3} \right) \right] \\
D_1 &= -\frac{i}{4} \left(\frac{g_A}{F} \right)^5 \left(S^2 + \frac{3}{2} \right) \\
&\quad \left[-\frac{J_2(\omega_1) + J_2(-\omega_1) - 2J_2(0)}{\omega_1^2} \left(\frac{1}{\omega_2} - \frac{1}{\omega_3} \right) \right. \\
&\quad - \frac{J_2(\omega_2) - J_2(0)}{\omega_2} \left(\frac{2}{\omega_1 \omega_3} + \frac{1}{\omega_1 \omega_2} - \frac{1}{\omega_2 \omega_3} \right) + \frac{J_2(-\omega_2) - J_2(0)}{\omega_2^2} \left(\frac{1}{\omega_1} - \frac{1}{\omega_3} \right) \\
&\quad + \frac{J_2(\omega_3) - J_2(0)}{\omega_3} \left(\frac{2}{\omega_1 \omega_2} + \frac{1}{\omega_1 \omega_3} - \frac{1}{\omega_2 \omega_3} \right) - \frac{J_2(-\omega_3) - J_2(0)}{\omega_3^2} \left(\frac{1}{\omega_1} - \frac{1}{\omega_2} \right) \left. \right] \\
D_4 &= -\frac{3i}{4} \left(\frac{g_A}{F} \right)^5 \left(S^2 + \frac{3}{2} \right) \\
&\quad \left[-\frac{J_2(\omega_1) - J_2(0)}{\omega_1^2} \left(\frac{1}{\omega_2} + \frac{1}{\omega_3} \right) + \frac{J_2(-\omega_1) - J_2(0)}{\omega_1} \left(\frac{2}{\omega_2 \omega_3} - \frac{1}{\omega_1 \omega_2} - \frac{1}{\omega_1 \omega_3} \right) \right. \\
&\quad + \frac{J_2(\omega_2) - J_2(0)}{\omega_2} \left(\frac{2}{\omega_1 \omega_3} + \frac{1}{\omega_1 \omega_2} - \frac{1}{\omega_2 \omega_3} \right) + \frac{J_2(-\omega_2) - J_2(0)}{\omega_2^2} \left(\frac{1}{\omega_1} - \frac{1}{\omega_3} \right) \\
&\quad + \frac{J_2(\omega_3) - J_2(0)}{\omega_3} \left(\frac{2}{\omega_1 \omega_2} + \frac{1}{\omega_1 \omega_3} - \frac{1}{\omega_2 \omega_3} \right) + \frac{J_2(-\omega_3) - J_2(0)}{\omega_3^2} \left(\frac{1}{\omega_1} - \frac{1}{\omega_2} \right) \left. \right]
\end{aligned}$$

$$-2J'_2(0) \left(\frac{1}{\omega_1\omega_2} + \frac{1}{\omega_1\omega_3} - \frac{1}{\omega_2\omega_3} \right) \Big] \quad (\text{A.30})$$

Diagrams s12+s13: add up to 0.

Diagrams s14+s15:

$$\begin{aligned} A_1 &= -i \frac{g_A^3}{F^5} S^2 \frac{J_2(\omega_1) - J_2(-\omega_1)}{\omega_1} \\ A_2 &= A_4 = B_3 = D_1 = D_4 = 0 \end{aligned} \quad (\text{A.31})$$

Diagrams s16+s17:

$$\begin{aligned} A_2 &= \frac{i}{4} \frac{g_A^3}{F^5} S^2 \frac{\omega_2 - \omega_3}{\omega_1^2} (J_2(\omega_1) - J_2(-\omega_1)) \\ A_4 &= \frac{i}{4} \frac{g_A^3}{F^5} S^2 \frac{\omega_2 - \omega_3}{\omega_1^2} (J_2(\omega_1) + J_2(-\omega_1) - 2J_2(0)) \\ B_3 &= \frac{i}{4} \frac{g_A^3}{F^5} S^2 \frac{\omega_1 + \omega_3}{\omega_2^2} (J_2(\omega_2) - J_2(-\omega_2)) \\ A_1 &= D_1 = D_4 = 0 \end{aligned} \quad (\text{A.32})$$

Diagrams s18+s19:

$$\begin{aligned} A_2 &= -\frac{i}{4} \frac{g_A^3}{F^5} \left(S^2 + \frac{1}{2} \right) \frac{\omega_2 - \omega_3}{\omega_1^2} (J_2(\omega_1) - J_2(-\omega_1)) \\ A_4 &= -\frac{i}{4} \frac{g_A^3}{F^5} \left(S^2 + \frac{1}{2} \right) \frac{\omega_2 - \omega_3}{\omega_1^2} (J_2(\omega_1) + J_2(-\omega_1) - 2J_2(0)) \\ B_3 &= -\frac{i}{4} \frac{g_A^3}{F^5} \left(S^2 + \frac{1}{2} \right) \frac{\omega_1 + \omega_3}{\omega_2^2} (J_2(\omega_2) - J_2(-\omega_2)) \\ A_1 &= D_1 = D_4 = 0 \end{aligned} \quad (\text{A.33})$$

Diagrams s20+s21:

$$\begin{aligned} A_2 &= \frac{3i}{4} \frac{g_A^3}{F^5} S^2 \frac{\omega_2 - \omega_3}{\omega_1^2} (J_2(\omega_1) - J_2(-\omega_1)) \\ A_4 &= \frac{3i}{4} \frac{g_A^3}{F^5} S^2 \frac{\omega_2 - \omega_3}{\omega_1^2} (J_2(\omega_1) + J_2(-\omega_1)) \\ B_3 &= \frac{3i}{4} \frac{g_A^3}{F^5} S^2 \frac{\omega_1 + \omega_3}{\omega_2^2} (J_2(\omega_2) - J_2(-\omega_2)) \\ A_1 &= D_1 = D_4 = 0 \end{aligned} \quad (\text{A.34})$$

Diagrams s22+s23:

$$A_1 = -\frac{i}{4} \frac{g_A}{F^5} \left[\omega_2 (J_0(\omega_2) - J_0(-\omega_2)) + \omega_3 (J_0(\omega_3) - J_0(-\omega_3)) + 2\Delta_\pi \right]$$

$$\begin{aligned}
A_2 &= \frac{3i}{4} \frac{g_A}{F^5} [\omega_2 (J_0(\omega_2) - J_0(-\omega_2)) + \Delta_\pi] \\
A_4 &= -\frac{i}{4} \frac{g_A}{F^5} [\omega_2 (J_0(\omega_2) + J_0(-\omega_2)) - \omega_3 (J_0(\omega_3) + J_0(-\omega_3))] \\
B_3 &= -\frac{3i}{4} \frac{g_A}{F^5} [\omega_3 (J_0(\omega_3) - J_0(-\omega_3)) + \Delta_\pi] \\
D_1 &= D_4 = 0
\end{aligned} \tag{A.35}$$

Diagrams s24+s25:

$$\begin{aligned}
A_1 &= i \frac{g_A^3}{F^5} \left(S^2 + \frac{1}{2} \right) \frac{J_2(\omega_1) - J_2(-\omega_1)}{\omega_1} \\
A_2 &= -i \frac{g_A^3}{F^5} \left(S^2 + \frac{1}{2} \right) \frac{J_2(\omega_1) - J_2(-\omega_1)}{\omega_1} \\
B_3 &= i \frac{g_A^3}{F^5} \left(S^2 + \frac{1}{2} \right) \frac{J_2(\omega_2) - J_2(-\omega_2)}{\omega_2} \\
A_4 &= D_1 = D_4 = 0
\end{aligned} \tag{A.36}$$

Diagram s26+s27:

$$\begin{aligned}
A_2 &= \frac{i}{4} \frac{g_A^3}{F^5} \left(S^2 + \frac{1}{2} \right) \frac{\omega_2 - \omega_3}{\omega_1} \left[\frac{J_2(\omega_1) - J_2(-\omega_1)}{\omega_1} - 2J_2'(0) \right] \\
A_4 &= -\frac{3i}{4} \frac{g_A^3}{F^5} \left(S^2 + \frac{1}{2} \right) \frac{\omega_2 - \omega_3}{\omega_1^2} [J_2(\omega_1) + J_2(-\omega_1) - 2J_2(0)] \\
B_3 &= \frac{i}{4} \frac{g_A^3}{F^5} \left(S^2 + \frac{1}{2} \right) \frac{\omega_1 + \omega_3}{\omega_2} \left[\frac{J_2(\omega_2) - J_2(-\omega_2)}{\omega_2} - 2J_2'(0) \right] \\
A_1 &= D_1 = D_4 = 0
\end{aligned} \tag{A.37}$$

Diagrams s28+s29:

$$\begin{aligned}
A_1 &= i \frac{g_A^3}{F^5} \left\{ \frac{K_0(t_3, \omega_1) - K_0(t_3, -\omega_1)}{8\omega_1} (2t_3^2 - 5M^2 t_3 + 2M^4) \right. \\
&\quad + \frac{J_0(\omega_1) - J_0(-\omega_1)}{8\omega_1} (-2t_3 + 2\omega_1^2 - M^2) + I_0(t_3) \frac{-2t_3 + M^2}{4} + \frac{\Delta_\pi}{2} \\
&\quad + \frac{\omega_2 \omega_3 - q_2 \cdot q_3}{t_2 - \omega_2^2} \left[-\frac{K_0(t_2, \omega_2) - K_0(t_2, -\omega_2)}{8\omega_2} (t_2^2 - 4M^2 t_2 + 4M^2 \omega_2^2) \right. \\
&\quad \left. + \frac{J_0(\omega_2) - J_0(-\omega_2)}{8\omega_2} (t_2 - 2\omega_2^2) + I_0(t_2) \frac{t_2}{2} + \frac{t_2 - \omega_2^2}{16\pi^2} \right] \\
&\quad + \frac{\omega_2 \omega_3 - q_2 \cdot q_2}{t_1 - \omega_3^2} \left[-\frac{K_0(t_1, \omega_3) - K_0(t_1, -\omega_3)}{8\omega_3} (t_1^2 - 4M^2 t_1 + 4M^2 \omega_3^2) \right. \\
&\quad \left. + \frac{J_0(\omega_3) - J_0(-\omega_3)}{8\omega_3} (t_1 - 2\omega_3^2) + I_0(t_1) \frac{t_1}{2} + \frac{t_1 - \omega_3^2}{16\pi^2} \right] \Big\}
\end{aligned}$$

$$\begin{aligned}
A_2 &= i \frac{g_A^3}{F^5} \left\{ \frac{\omega_2 - \omega_3}{8(t_3 - \omega_1^2)} \left[(K_0(t_3, \omega_1) - K_0(t_3, -\omega_1)) t_3 (t_3 - 2M^2) \right. \right. \\
&\quad - (J_0(\omega_1) - J_0(-\omega_1))(t_3 + 2M^2 - 2\omega_1^2) - \frac{20}{3\omega_1} \Delta_\pi \\
&\quad - I_0(t_3) \frac{2}{3\omega_1} (5t_3^2 - 8M^2 t_3 + \omega_1^2 t_3 - 4M^2 \omega_1^2) \\
&\quad \left. \left. - \frac{1}{36\pi^2 \omega_1} (6M^2 - t_3)(t_3 - \omega_1^2) \right] \right. \\
&\quad \left. - \frac{\omega_2 \omega_3 - q_2 \cdot q_3}{t_1 - \omega_3^2} \left[-\frac{K_0(t_1, \omega_3) - K_0(t_1, -\omega_3)}{8\omega_3} (t_1^2 - 4M^2 t_1 + 4M^2 \omega_3^2) \right. \right. \\
&\quad \left. \left. + \frac{J_0(\omega_3) - J_0(-\omega_3)}{8\omega_3} (t_1 - 2\omega_3^2) + I_0(t_1) \frac{t_1}{2} + \frac{t_1 - \omega_3^2}{16\pi^2} \right] \right\} \\
A_4 &= i \frac{g_A^3}{F^5} \left\{ \frac{(\omega_2 - \omega_3)}{8(t_3 - \omega_1^2)} \left[(K_0(t_3, \omega_1) + K_0(t_3, -\omega_1)) t_3 (t_3 - 2M^2) \right. \right. \\
&\quad - (J_0(\omega_1) + J_0(-\omega_1))(t_3 + 2M^2 - 2\omega_1^2) - J_0(0) 2(t_3 - 2M^2) \left. \right] \\
&\quad + \frac{(\omega_2 \omega_3 - q_2 \cdot q_3)}{8\omega_2(t_2 - \omega_2^2)} \left[-(K_0(t_2, \omega_2) + K_0(t_2, -\omega_2))(t_2^2 - 4M^2 t_2 + 4M^2 \omega_2^2) \right. \\
&\quad \left. + (J_0(\omega_2) + J_0(-\omega_2))(t_2 - 2\omega_2^2) + J_0(0) 2t_2 \right] \\
&\quad - \frac{(\omega_2 \omega_3 - q_2 \cdot q_3)}{8\omega_3(t_1 - \omega_3^2)} \left[-(K_0(t_1, \omega_3) + K_0(t_1, -\omega_3))(t_1^2 - 4M^2 t_1 + 4M^2 \omega_3^2) \right. \\
&\quad \left. \left. + (J_0(\omega_3) + J_0(-\omega_3))(t_1 - 2\omega_3^2) + J_0(0) 2t_1 \right] \right\} \\
B_3 &= i \frac{g_A^3}{F^5} \left\{ -\frac{\omega_1 \omega_3 - q_1 \cdot q_3}{t_3 - \omega_1^2} \left[-\frac{K_0(t_3, \omega_1) - K_0(t_3, -\omega_1)}{8\omega_1} (t_3^2 - 4M^2 t_3 + 4M^2 \omega_1^2) \right. \right. \\
&\quad \left. \left. + \frac{J_0(\omega_1) - J_0(-\omega_1)}{8\omega_1} (t_3 - 2\omega_1^2) + I_0(t_3) \frac{t_3}{2} + \frac{t_3 - \omega_1^2}{16\pi^2} \right] \right. \\
&\quad \left. + \frac{\omega_1 + \omega_3}{8(t_2 - \omega_2^2)} \left[(K_0(t_2, \omega_2) - K_0(t_2, -\omega_2)) t_2 (t_2 - 2M^2) \right. \right. \\
&\quad \left. \left. - (J_0(\omega_2) - J_0(-\omega_2))(t_2 + 2M^2 - 2\omega_2^2) - \frac{20}{3\omega_2} \Delta_\pi \right. \right. \\
&\quad \left. \left. - I_0(t_2) \frac{2}{3\omega_2} (5t_2^2 - 8M^2 t_2 + \omega_2^2 t_2 - 4M^2 \omega_2^2) \right. \right. \\
&\quad \left. \left. - \frac{1}{36\pi^2 \omega_2} (6M^2 - t_2)(t_2 - \omega_2^2) \right] \right\} \\
D_1 &= i \frac{g_A^3}{F^5} \left\{ -\frac{1}{16\omega_2(t_2 - \omega_2^2)} \left[(K_0(t_2, \omega_2) + K_0(t_2, -\omega_2))(t_2^2 - 4M^2 t_2 + 4M^2 \omega_2^2) \right. \right. \\
&\quad \left. \left. - (J_0(\omega_2) + J_0(-\omega_2))(t_2 - 2\omega_2^2) - 2J_0(0) t_2 \right] \right. \\
&\quad \left. + \frac{1}{16\omega_3(t_1 - \omega_3^2)} \left[(K_0(t_1, \omega_3) + K_0(t_1, -\omega_3))(t_1^2 - 4M^2 t_1 + 4M^2 \omega_3^2) \right. \right.
\end{aligned}$$

$$\begin{aligned}
D_4 = & i \frac{g_A^3}{16F^5} \left\{ \frac{1}{t_3 - \omega_1^2} \left[-\frac{K_0(t_3, \omega_1) - K_0(t_2, -\omega_2)}{\omega_1} (t_3^2 - 4M^2 t_3 + 4M^2 \omega_1^2) \right. \right. \\
& + \frac{J_0(\omega_1) - J_0(-\omega_1)}{\omega_1} (t_3 - 2\omega_1^2) + I_0(t_3) 4t_3 + \frac{t_3 - \omega_1^2}{2\pi^2} \Big] \\
& + \frac{1}{t_2 - \omega_2^2} \left[-\frac{K_0(t_2, \omega_2) - K_0(t_2, -\omega_2)}{\omega_2} (t_2^2 - 4M^2 t_2 + 4M^2 \omega_2^2) \right. \\
& + \frac{J_0(\omega_2) - J_0(-\omega_2)}{\omega_2} (t_2 - 2\omega_2^2) + I_0(t_2) 4t_2 + \frac{t_2 - \omega_2^2}{2\pi^2} \Big] \\
& + \frac{1}{t_1 - \omega_3^2} \left[-\frac{K_0(t_1, \omega_3) - K_0(t_1, -\omega_3)}{\omega_3} (t_1^2 - 4M^2 t_1 + 4M^2 \omega_3^2) \right. \\
& + \frac{J_0(\omega_3) - J_0(-\omega_3)}{\omega_3} (t_1 - 2\omega_3^2) + I_0(t_1) 4t_1 + \frac{t_1 - \omega_3^2}{2\pi^2} \Big] \Big\} \quad (A.38)
\end{aligned}$$

Diagrams s30+s31:

$$\begin{aligned}
A_1 = & i \frac{g_A}{4F^5} \left\{ \frac{1}{(t_2 - \omega_2^2)^2} \left(\frac{\omega_2(K_0(t_2, \omega_2) - K_0(t_2, -\omega_2))}{2} \right. \right. \\
& \left[(q_1 \cdot (q_1 - q_3) - \omega_1 \omega_2)(-4t_2 M^2 + 4M^2 \omega_2^2 + 3t_2^2) \right. \\
& \left. \left. - (t_2 - \omega_2^2)(3t_2^2 - 6t_2 M^2 + 4M^2 \omega_2^2) \right] \right. \\
& + \frac{\omega_2(J_0(\omega_2) - J_0(-\omega_2))}{2} \left[(q_1 \cdot (q_1 - q_3) - \omega_1 \omega_2)(5t_2 - 2\omega_2^2) \right. \\
& \left. \left. - (t_2 - \omega_2^2)(t_2 - 2M^2 + 2\omega_2^2) \right] \right. \\
& + I_0(t_2) \left[2\omega_1 \omega_2 t_2 (2t_2 + \omega_2^2) + \frac{t_2 - \omega_2^2}{3} (4t_2^2 - 7t_2 M^2 + 14t_2 \omega_2^2 - 5M^2 \omega_2^2) \right. \\
& \left. \left. - \frac{2}{3t_2} q_1 \cdot (q_1 - q_3) (11t_2^2 \omega_2^2 - 4t_2 \omega_2^4 - 2M^2 t_2^2 + 4M^2 t_2 \omega_2^2 - 2M^2 \omega_2^4 + 2t_2^3) \right] \right. \\
& + \Delta_\pi (t_2 - \omega_2)^2 \left[\frac{4}{3t_2} q_1 \cdot (q_1 - q_3) + \frac{2}{3} \right] \\
& + \frac{t_2 - \omega_2^2}{16\pi^2} \left[-\frac{2}{9t_2} q_1 \cdot (q_1 - q_3) (t_2^2 - 6t_2 M^2 + 17t_2 \omega_2^2 + 6M^2 \omega_2^2) + 4\omega_1 \omega_2^3 \right. \\
& \left. \left. + \frac{2(t_2 - \omega_2^2)}{9} (t_2 - 6M^2 + 18\omega_2^2) \right] \right) \\
& + \frac{1}{(t_1 - \omega_3^2)^2} \left(\frac{\omega_3(K_0(t_1, \omega_3) - K_0(t_1, -\omega_3))}{2} \right. \\
& \left[(q_1 \cdot (q_1 - q_2) - \omega_1 \omega_3)(-4t_1 M^2 + 4M^2 \omega_3^2 + 3t_1^2) \right. \\
& \left. \left. - (t_1 - \omega_3^2)(3t_1^2 - 6t_1 M^2 + 4M^2 \omega_3^2) \right] \right. \\
& + \frac{\omega_3(J_0(\omega_3) - J_0(-\omega_3))}{2} \left[(q_1 \cdot (q_1 - q_2) - \omega_1 \omega_3)(5t_1 - 2\omega_3^2) \right.
\end{aligned}$$

$$\begin{aligned}
& -(t_1 - \omega_3^2)(t_1 - 2M^2 + 2\omega_3^2) \Big] \\
& + I_0(t_1) \left[2\omega_1\omega_3t_1(2t_1 + \omega_3^2) + \frac{t_1 - \omega_3^2}{3}(4t_1^2 - 7t_1M^2 + 14t_1\omega_3^2 - 5M^2\omega_3^2) \right. \\
& + -\frac{2}{3t_1}q_1 \cdot (q_1 - q_2)(11t_1^2\omega_3^2 - 4t_1\omega_3^4 - 2M^2t_1^2 + 4M^2t_1\omega_3^2 - 2M^2\omega_3^4 + 2t_1^3) \Big] \\
& + \Delta_\pi(t_1 - \omega_3)^2 \left[\frac{4}{3t_1}q_1 \cdot (q_1 - q_2) + \frac{2}{3} \right] \\
& + \frac{t_1 - \omega_3^2}{16\pi^2} \left[-\frac{2}{9t_1}q_1 \cdot (q_1 - q_2)(t_1^2 - 6t_1M^2 + 17t_1\omega_3^2 + 6M^2\omega_3^2) + 4\omega_1\omega_3^3 \right. \\
& \left. + \frac{2(t_1 - \omega_3^2)}{9}(t_1 - 6M^2 + 18\omega_3^2) \right] \Bigg\} \\
A_2 = & i \frac{g_A}{4F^5} \left\{ \frac{1}{t_2 - \omega_2^2} \left[-(K_0(t_2, \omega_2) - K_0(t_2, -\omega_2))\omega_2t_2^2 \right. \right. \\
& - (J_0(\omega_2) - J_0(-\omega_2))\omega_2(3t_2 - 2\omega_2^2) \\
& + I_0(t_2)t_2(t_2 + 3\omega_2^2) - \Delta_\pi 2(t_2 - \omega_2^2) \Big] \\
& + \frac{1}{(t_1 - \omega_3^2)^2} \left(\frac{\omega_3(K_0(t_1, \omega_3) - K_0(t_1, -\omega_3))}{2} \right. \\
& \left[(-q_2 \cdot (q_1 - q_2) + \omega_2\omega_3)(-4t_1M^2 + 4M^2\omega_3^2 + 3t_1^2) \right. \\
& - 2(t_1 - \omega_3^2)t_1(t_1 - M^2) \Big] \\
& + \frac{\omega_3(J_0(\omega_3) - J_0(-\omega_3))}{2} \left[(-q_2 \cdot (q_1 - q_2) + \omega_2\omega_3)(5t_1 - 2\omega_3^2) \right. \\
& - 2(t_1 - \omega_3^2)(t_1 - M^2) \Big] \\
& + I_0(t_1) \left[\frac{2}{3t_1}q_2 \cdot (q_1 - q_2)(11t_1^2\omega_3^2 - 4t_1\omega_3^4 - 2M^2t_1^2 + 4M^2t_1\omega_3^2 - 2M^2\omega_3^4 + 2t_1^3) \right. \\
& - 2\omega_2\omega_3t_1(2t_1 + \omega_3^2) + 2(t_1 - \omega_3^2)(t_1 - M^2)(t_1 + 3\omega_3^2) \Big] \\
& - \Delta_\pi(t_1 - \omega_3)^2 \frac{4}{3t_1}q_2 \cdot (q_1 - q_2) \\
& \left. + \frac{t_1 - \omega_3^2}{16\pi^2} \left[\frac{2}{9t_1}q_2 \cdot (q_1 - q_2)(t_1^2 - 6t_1M^2 + 17t_1\omega_3^2 + 6M^2\omega_3^2) - 4\omega_2\omega_3^3 \right] \right) \Bigg\} \\
A_4 = & i \frac{g_A}{4F^5} \left\{ \frac{\omega_2}{2(t_2 - \omega_2^2)^2} \left((K_0(t_2, \omega_2) + K_0(t_2, -\omega_2)) \right. \right. \\
& \left[-(\omega_1 + \omega_3)\omega_2(-4t_2M^2 + 4M^2\omega_2^2 + 3t_2^2) - (t_2 - \omega_2^2)(t_2^2 - 4t_2M^2 + 4M^2\omega_2^2) \right] \\
& + (J_0(\omega_2) + J_0(-\omega_2)) \left[-(\omega_1 + \omega_3)\omega_2(5t_2 - 2\omega_2^2) + (t_2 - \omega_2^2)(t_2 - 2\omega_2^2) \right] \\
& + J_0(0)t_2 \left[6(\omega_1 + \omega_3)\omega_2 + 2(t_2 - \omega_2^2) \right] \Big) \\
& + \frac{\omega_3}{2(t_1 - \omega_3^2)^2} \left((K_0(t_1, \omega_3) + K_0(t_1, -\omega_3)) \right.
\end{aligned}$$

$$\begin{aligned}
& \left[(\omega_1 + \omega_2)\omega_3(-4t_1M^2 + 4M^2\omega_3^2 + 3t_1^2) + (t_1 - \omega_3^2)(t_1^2 - 4t_1M^2 + 4M^2\omega_3^2) \right] \\
& + (J_0(\omega_3) + J_0(-\omega_3)) \left[(\omega_1 + \omega_2)\omega_3(5t_1 - 2\omega_3^2) - (t_1 - \omega_3^2)(t_1 - 2\omega_3^2) \right] \\
& - J_0(0)t_1 \left[6(\omega_1 + \omega_2)\omega_3 + 2(t_1 - \omega_3^2) \right] \Bigg\} \\
B_3 = & i \frac{g_A}{4F^5} \left\{ \frac{1}{(t_3 - \omega_1^2)^2} \left(\frac{\omega_1(K_0(t_3, \omega_1) - K_0(t_3, -\omega_1))}{2} \right. \right. \\
& \left[(-q_3 \cdot (q_2 + q_3) + \omega_1\omega_3)(-4t_3M^2 + 4M^2\omega_1^2 + 3t_3^2) + 2(t_3 - \omega_1^2)t_3(t_3 - M^2) \right] \\
& + \frac{\omega_1(J_0(\omega_1) - J_0(-\omega_1))}{2} \left[(-q_3 \cdot (q_2 + q_3) + \omega_1\omega_3)(5t_3 - 2\omega_1^2) \right. \\
& \left. \left. + 2(t_3 - \omega_1^2)(t_3 - M^2) \right] \right. \\
& + I_0(t_3) \left[\frac{2}{3t_3} q_3 \cdot (q_2 + q_3)(11t_3^2\omega_1^2 - 4t_3\omega_1^4 - 2M^2t_3^2 + 4M^2t_3\omega_1^2 - 2M^2\omega_1^4 + 2t_3^3) \right. \\
& \left. - 2\omega_1\omega_3t_3(2t_3 + \omega_1^2) - 2(t_3 - \omega_1^2)(t_3 - M^2)(t_3 + 3\omega_1^2) \right] \\
& - \Delta_\pi(t_3 - \omega_1)^2 \frac{4}{3t_3} q_2 \cdot (q_2 + q_3) \\
& + \frac{t_3 - \omega_1^2}{16\pi^2} \left[\frac{2}{9t_3} q_3 \cdot (q_2 + q_3)(t_3^2 - 6t_3M^2 + 17t_3\omega_1^2 + 6M^2\omega_1^2) - 4\omega_1^3\omega_3 \right] \Bigg) \\
& + \frac{1}{t_1 - \omega_3^2} \left[(K_0(\omega_3) - K_0(-\omega_3))\omega_3t_1^2 + (J_0(\omega_3) - J_0(-\omega_3))\omega_3(3t_1 - 2\omega_3^2) \right. \\
& \left. - I_0(t_1)t_1(t_1 + 3\omega_3^2) + \Delta_\pi 2(t_1 - \omega_3^2) \right] \Bigg\} \\
D_1 = D_4 = 0
\end{aligned} \tag{A.39}$$

Diagram s32:

$$\begin{aligned}
A_2 &= i \frac{g_A^3}{2F^5} \left(S^2 + \frac{1}{2} \right) J_2'(0) \\
B_3 &= -i \frac{g_A^3}{2F^5} \left(S^2 + \frac{1}{2} \right) J_2'(0) \\
A_1 &= A_4 = D_1 = D_4 = 0
\end{aligned} \tag{A.40}$$

Diagram s33:

$$\begin{aligned}
A_1 = & -i \frac{g_A^3}{F^5} \left\{ \frac{1}{\omega_1(t_3 - \omega_1^2)} \left[(K_0(t_3, \omega_1) - K_0(t_3, -\omega_1)) \frac{M^2t_3(t_3 - 2\omega_1^2)}{16} \right. \right. \\
& + (J_0(\omega_1) - J_0(-\omega_1)) \frac{4\omega_1^2t_3 - 7M^2t_3 - 4\omega_1^4 + 4M^2\omega_1^2}{48} + I_0(t_3) \frac{M^2\omega_1^3}{4} \\
& + \Delta_\pi \frac{\omega_1(t_3 - \omega_1^2)}{6} - \frac{\omega_1}{16\pi^2} \frac{-21M^2 + 8\omega_1^2}{18} \Bigg] \\
& - \frac{\omega_2^2 - q_2 \cdot (q_1 - q_3)}{16\omega_2(t_2 - \omega_2^2)^2}
\end{aligned}$$

$$\begin{aligned}
& \left[(K_0(t_2, \omega_2) - K_0(t_2, -\omega_2))(t_2^3 + 2M^2t_2^2 - 4t_2^2\omega_2^2 - 8t_2M^4 + 4M^2\omega_2^2t_2 + 8M^4\omega_2^2) \right. \\
& - (J_0(\omega_2) - J_0(-\omega_2))(t_2^2 - 2M^2t_2 + 2\omega_2^2t_2 - 4M^2\omega_2^2) \\
& \left. + I_0(t_2)4\omega_2(t_2^2 - 2M^2t_2 + 2\omega_2^2t_2 - 4M^2\omega_2^2) + \frac{\omega_2(t_2 - 2M^2)(t_2 - \omega_2^2)}{2\pi^2} \right] \\
& - \frac{\omega_3^2 - q_3 \cdot (q_1 - q_2)}{16\omega_3(t_1 - \omega_3^2)^2} \\
& \left[(K_0(t_1, \omega_3) - K_0(t_1, -\omega_3))(t_1^3 + 2M^2t_1^2 - 4t_1^2\omega_3^2 - 8t_1M^4 + 4M^2\omega_3^2t_1 + 8M^4\omega_3^2) \right. \\
& - (J_0(\omega_3) - J_0(-\omega_3))(t_1^2 - 2M^2t_1 + 2\omega_3^2t_1 - 4M^2\omega_3^2) \\
& \left. + I_0(t_1)4\omega_3(t_1^2 - 2M^2t_1 + 2\omega_3^2t_1 - 4M^2\omega_3^2) + \frac{\omega_3(t_1 - 2M^2)(t_1 - \omega_3^2)}{2\pi^2} \right] \Bigg\} \\
A_2 = & -i\frac{g_A^3}{F^5} \left\{ \frac{1}{\omega_1(t_3 - \omega_1^2)} \left[(K_0(t_3, \omega_1) - K_0(t_3, -\omega_1)) \frac{t_3(t_3^2 - 2\omega_1^2t_3 - 2M^2t_3 + 4M^2\omega_1^2)}{16} \right. \right. \\
& - (J_0(\omega_1) - J_0(-\omega_1)) \frac{3t_3^2 - 10M^2t_3 + 4\omega_1^2t_3 - 4\omega_1^4 + 4M^2\omega_1^2}{48} \\
& \left. + I_0(t_3) \frac{\omega_1^3(t_3 - 2M^2)}{4} - \Delta_\pi \frac{\omega_1(t_3 - \omega_1^2)}{6} + \frac{\omega_1}{16\pi^2} \frac{9t_3 - 30M^2 + 8\omega_1^2}{18} \right] \\
& - \frac{M^2(\omega_2^2 - q_2 \cdot (q_1 - q_3))}{16\omega_2(t_2 - \omega_2^2)^2} \left[- (J_0(\omega_2) - J_0(-\omega_2))(t_2 + 2\omega_2^2) + I_0(t_2)4\omega_2(t_2 + 2\omega_2^2) \right. \\
& \left. + (K_0(t_2, \omega_2) - K_0(t_2, -\omega_2))(-4\omega_2^2t_2 + t_2^2 - 4M^2\omega_2^2 + 4M^2t_2) + \frac{\omega_2(t_2 - \omega_2^2)}{2\pi^2} \right] \\
& - \frac{\omega_3^2 - q_3 \cdot (q_1 - q_2)}{16\omega_3(t_1 - \omega_3^2)^2} \\
& \left[(K_0(t_1, \omega_3) - K_0(t_1, -\omega_3))(t_1^3 + 2M^2t_1^2 - 4t_1^2\omega_3^2 - 8t_1M^4 + 4M^2\omega_3^2t_1 + 8M^4\omega_3^2) \right. \\
& - (J_0(\omega_3) - J_0(-\omega_3))(t_1^2 - 2M^2t_1 + 2\omega_3^2t_1 - 4M^2\omega_3^2) \\
& \left. + I_0(t_1)4\omega_3(t_1^2 - 2M^2t_1 + 2\omega_3^2t_1 - 4M^2\omega_3^2) + \frac{\omega_3(t_1 - 2M^2)(t_1 - \omega_3^2)}{2\pi^2} \right] \Bigg\} \\
A_4 = & -i\frac{g_A^3}{F^5} \left\{ \frac{\omega_2 - \omega_3}{16(t_3 - \omega_1^2)^2} \left[(K_0(t_3, \omega_1) + K_0(t_3, -\omega_1))t_3^2(t_3 - 2\omega_1^2) \right. \right. \\
& - (J_0(\omega_1) + J_0(-\omega_1))\frac{1}{3}(-4\omega_1^2t_3 + 3t_3^2 - 4M^2\omega_1^2 + 4M^2t_3 + 4\omega_1^4) \\
& \left. - J_0(0)\frac{2}{3}(-6\omega_2^2t_3 + 3t_3^2 + 4M^2\omega_1^2 - 4M^2t_3) \right] \\
& + \frac{(\omega_2^2 - q_2 \cdot (q_1 - q_3))(\omega_1 + \omega_3)}{16(t_2 - \omega_2^2)^3} \\
& \left[- (K_0(t_2, \omega_2) + K_0(t_2, -\omega_2))(4M^2\omega_2^2t_2 + 4M^2t_2^2 - 8M^2\omega_2^4 - 6t_2^2\omega_2^2 + t_2^3) \right.
\end{aligned}$$

$$\begin{aligned}
& + (J_0(\omega_2) + J_0(-\omega_2)) \frac{1}{3} (16M^2\omega_2^2 - 16M^2t_2 - 4\omega_2^4 + 16\omega_2^2t_2 + 3t_2^2) \\
& + J_0(0) \frac{2}{3} (-16M^2\omega_2^2 + 16M^2t_2 - 18\omega_2^2t_2 + 3t_2^2) \Big] \\
& + \frac{\omega_1\omega_2 - q_1 \cdot q_2}{24\omega_2(t_2 - \omega_2^2)^2} \left[(K_0(t_2, \omega_2) + K_0(t_2, -\omega_2)) 3\omega_2^2 (4M^2\omega_2^2 + t_2^2 - 4M^2t_2) \right. \\
& + (J_0(\omega_2) + J_0(-\omega_2)) (8M^2\omega_2^2 - 8M^2t_2 + 5\omega_2^2t_2 - 2\omega_2^4) \\
& \left. - J_0(0) 2(-8M^2t_2 + 8M^2\omega_2^2 + 3\omega_2^2t_2) \right] \\
& - \frac{(\omega_3^2 - q_3 \cdot (q_1 - q_2))(\omega_1 + \omega_2)}{16(t_1 - \omega_3^2)^3} \\
& \left[- (K_0(t_1, \omega_3) + K_0(t_1, -\omega_3)) (4M^2\omega_3^2t_1 + 4M^2t_1^2 - 8M^2\omega_3^4 - 6t_1^2\omega_3^2 + t_1^3) \right. \\
& + (J_0(\omega_3) + J_0(-\omega_3)) \frac{1}{3} (16M^2\omega_3^2 - 16M^2t_1 - 4\omega_3^4 + 16\omega_3^2t_1 + 3t_1^2) \\
& + J_0(0) \frac{2}{3} (-16M^2\omega_3^2 + 16M^2t_1 - 18\omega_3^2t_1 + 3t_1^2) \Big] \\
& - \frac{\omega_1\omega_3 - q_1 \cdot q_3}{24\omega_3(t_1 - \omega_3^2)^2} \left[(K_0(t_1, \omega_3) + K_0(t_1, -\omega_3)) 3\omega_3^2 (4M^2\omega_3^2 + t_1^2 - 4M^2t_1) \right. \\
& + (J_0(\omega_3) + J_0(-\omega_3)) (8M^2\omega_3^2 - 8M^2t_1 + 5\omega_3^2t_1 - 2\omega_3^4) \\
& \left. - J_0(0) 2(-8M^2t_1 + 8M^2\omega_3^2 + 3\omega_3^2t_1) \right] \Big\} \\
B_3 = & -i \frac{g_A^3}{F^5} \left\{ \frac{\omega_1^2 - q_1 \cdot (q_2 + q_3)}{16\omega_1(t_3 - \omega_1^2)^2} \right. \\
& \left[(K_0(t_3, \omega_1) - K_0(t_3, -\omega_1)) (t_3^3 + 2M^2t_3^2 - 4t_3^2\omega_1^2 - 8t_3M^4 + 4M^2\omega_1^2t_3 + 8M^4\omega_1^2) \right. \\
& - (J_0(\omega_1) - J_0(-\omega_1)) (t_3^2 - 2M^2t_3 + 2\omega_1^2t_3 - 4M^2\omega_1^2) \\
& \left. + I_0(t_3) 4\omega_1(t_3^2 - 2M^2t_3 + 2\omega_1^2t_3 - 4M^2\omega_1^2) + \frac{\omega_1(t_3 - 2M^2)(t_3 - \omega_1^2)}{2} \right] \\
& - \frac{1}{\omega_2(t_2 - \omega_2^2)} \left[(K_0(t_2, \omega_2) - K_0(t_2, -\omega_2)) \frac{t_2(t_2^2 - 2\omega_2^2t_2 - 2M^2t_2 + 4M^2\omega_2^2)}{16} \right. \\
& - (J_0(\omega_2) - J_0(-\omega_2)) \frac{3t_2^2 - 10M^2t_2 + 4\omega_2^2t_2 - 4\omega_2^4 + 4M^2\omega_2^2}{48} \\
& \left. + I_0(t_2) \frac{\omega_2^3(t_2 - 2M^2)}{4} - \Delta_\pi \frac{\omega_2(t_2 - \omega_2^2)}{6} + \frac{\omega_2}{16\pi^2} \frac{9t_2 - 30M^2 + 8\omega_2^2}{18} \right] \\
& + \frac{M^2(\omega_3^2 - q_3 \cdot (q_1 - q_2))}{16\omega_3(t_1 - \omega_3^2)^2} \left[- (J_0(\omega_3) - J_0(-\omega_3)) (t_1 + 2\omega_3^2) + I_0(t_1) 4\omega_3(t_1 + 2\omega_3^2) \right. \\
& \left. + (K_0(t_1, \omega_3) - K_0(t_1, -\omega_3)) (-4\omega_3^2t_1 + t_1^2 - 4M^2\omega_3^2 + 4M^2t_1) + \frac{\omega_3(t_1 - \omega_3^2)}{2\pi^2} \right] \\
D_1 = & 0
\end{aligned}$$

$$\begin{aligned}
D_4 = & -i \frac{g_A^3}{16F^5} \left\{ \frac{1}{\omega_1(t_3 - \omega_1^2)} \left[- (K_0(t_3, \omega_1) - K_0(t_3, -\omega_1))(4M^2\omega_1^2 + t_3^2 - 4M^2t_3) \right. \right. \\
& + (J_0(\omega_1) - J_0(-\omega_1))(t_3 - 2\omega_1^2) + I_0(t_3)4t_3\omega_1 + \frac{\omega_1(t_3 - \omega_1^2)}{2\pi^2} \Big] \\
& + \frac{1}{\omega_2(t_2 - \omega_2^2)} \left[- (K_0(t_2, \omega_2) - K_0(t_2, -\omega_2))(4M^2\omega_2^2 + t_2^2 - 4M^2t_2) \right. \\
& + (J_0(\omega_2) - J_0(-\omega_2))(t_2 - 2\omega_2^2) + I_0(t_2)4t_2\omega_2 + \frac{\omega_2(t_2 - \omega_2^2)}{2\pi^2} \Big] \\
& + \frac{1}{\omega_3(t_1 - \omega_3^2)} \left[- (K_0(t_1, \omega_3) - K_0(t_1, -\omega_3))(4M^2\omega_3^2 + t_1^2 - 4M^2t_1) \right. \\
& + (J_0(\omega_3) - J_0(-\omega_3))(t_1 - 2\omega_3^2) + I_0(t_1)4t_1\omega_3 + \frac{\omega_3(t_1 - \omega_3^2)}{2\pi^2} \Big] \Big\} \quad (A.41)
\end{aligned}$$

Diagram s34:

$$\begin{aligned}
A_1 &= -i \frac{g_A^3}{F^5} \frac{1}{(q_2 + q_3 - q_1)^2 - M^2} \left(S^2 + \frac{1}{2} \right) J_2'(0)(t_3 - M^2) \\
A_2 &= -i \frac{g_A^3}{F^5} \frac{1}{(q_2 + q_3 - q_1)^2 - M^2} \left(S^2 + \frac{1}{2} \right) J_2'(0)(t_2 - M^2) \\
B_3 &= i \frac{g_A^3}{F^5} \frac{1}{(q_2 + q_3 - q_1)^2 - M^2} \left(S^2 + \frac{1}{2} \right) J_2'(0)(t_1 - M^2) \\
A_4 &= D_1 = D_4 = 0 \quad (A.42)
\end{aligned}$$

Diagram s35: Combine with diagrams R1d and 3r.

4. Renormalization diagrams: We now give those contributions from the first order diagrams, which come in via renormalization and thus cannot be obtained from the $1/m$ expansion of the relativistic amplitude. To third order, the renormalized pion mass, pion Z-factor, decay constant and the axial-vector coupling read:

$$Z_\pi = 1 - \frac{2M^2}{F^2} \ell_4 - \frac{\Delta_\pi}{F^2}, \quad (A.43)$$

$$M_\pi^2 = M^2 \left\{ 1 + \frac{2M^2}{F^2} \ell_3 + \frac{\Delta_\pi}{2F^2} \right\}, \quad (A.44)$$

$$F_\pi = F \left\{ 1 + \frac{M^2}{F^2} \ell_4 - \frac{\Delta_\pi}{F^2} \right\}, \quad (A.45)$$

$$\frac{g_A}{F_\pi} = \left(\frac{g_A}{F} \right)_0 \left\{ 1 - \frac{M^2}{F^2} \ell_4 + \frac{4M^2}{g_A} d_{16}(\lambda) + \frac{g_A^2}{4F^2} \left(\Delta_\pi - \frac{M^2}{4\pi^2} \right) \right\}, \quad (A.46)$$

Here, M , F and $g_{A,0}$ denote the corresponding leading order values in the chiral expansion. Moreover, one has to take care of the renormalization of the nucleon mass when making the heavy baryon transformation:

$$\frac{i}{v \cdot p} \rightarrow \frac{i}{v \cdot p} + \frac{i}{(v \cdot p)^2} \frac{3g_A^2 M^3}{32\pi F^2}. \quad (A.47)$$

The nucleon Z-factor takes the simple form:

$$Z_N = 1 - \frac{g_A^2}{F^2} \frac{3M^2}{32\pi^2}. \quad (\text{A.48})$$

Note that the familiar ln-terms have been treated as described in [22]. With that, we find for the pertinent diagrams:

Diagram R1a:

$$\begin{aligned} A_1 &= -i \left(\frac{g_A}{F} \right)^3 (\omega_2 \omega_3 - q_2 \cdot q_3) \frac{3M^2}{4} \left(\frac{1}{\omega_1 \omega_3} + \frac{1}{\omega_1 \omega_2} - \frac{1}{\omega_2 \omega_3} \right) \\ &\quad \left(\frac{g_A^2}{16\pi^2 F^2} - \frac{8d_{16}(\lambda)}{g_A} - \frac{\Delta_\pi}{2F^2} (g_A^2 + 2) \right) \\ A_2 &= -i \left(\frac{g_A}{F} \right)^3 (\omega_2 \omega_3 - q_2 \cdot q_3) \frac{3M^2}{4} \left(-\frac{1}{\omega_1 \omega_3} + \frac{1}{\omega_1 \omega_2} + \frac{1}{\omega_2 \omega_3} \right) \\ &\quad \left(\frac{g_A^2}{16\pi^2 F^2} - \frac{8d_{16}(\lambda)}{g_A} - \frac{\Delta_\pi}{2F^2} (g_A^2 + 2) \right) \\ A_4 &= -i \left(\frac{g_A}{F} \right)^5 (\omega_2 \omega_3 - q_2 \cdot q_3) \frac{3M^3}{64\pi} \\ &\quad \left[-\frac{1}{\omega_1 \omega_3} \left(\frac{1}{\omega_1} + \frac{1}{\omega_3} \right) + \frac{1}{\omega_1 \omega_2} \left(\frac{1}{\omega_1} + \frac{1}{\omega_2} \right) + \frac{1}{\omega_2 \omega_3} \left(-\frac{1}{\omega_2} + \frac{1}{\omega_3} \right) \right] \\ B_3 &= i \left(\frac{g_A}{F} \right)^3 (\omega_1 \omega_3 - q_1 \cdot q_3) \frac{3M^2}{4} \left(\frac{1}{\omega_1 \omega_3} + \frac{1}{\omega_1 \omega_2} + \frac{1}{\omega_2 \omega_3} \right) \\ &\quad \left(\frac{g_A^2}{16\pi^2 F^2} - \frac{8d_{16}(\lambda)}{g_A} d_{16}(\lambda) - \frac{\Delta_\pi}{2F^2} (g_A^2 + 2) \right) \\ D_1 &= -i \left(\frac{g_A}{F} \right)^5 \frac{3M^3}{128\pi} \\ &\quad \left[-\frac{1}{\omega_1 \omega_3} \left(\frac{1}{\omega_1} + \frac{1}{\omega_3} \right) + \frac{1}{\omega_1 \omega_2} \left(\frac{1}{\omega_1} + \frac{1}{\omega_2} \right) + \frac{1}{\omega_2 \omega_3} \left(-\frac{1}{\omega_2} + \frac{1}{\omega_3} \right) \right] \\ D_4 &= -i \left(\frac{g_A}{F} \right)^3 \frac{3M^2}{8} \left(\frac{1}{\omega_1 \omega_3} + \frac{1}{\omega_1 \omega_2} - \frac{1}{\omega_2 \omega_3} \right) \\ &\quad \left(\frac{g_A^2}{16\pi^2 F^2} - \frac{8d_{16}(\lambda)}{g_A} - \frac{\Delta_\pi}{2F^2} (g_A^2 + 2) \right) \end{aligned} \quad (\text{A.49})$$

Diagrams R1b+R1c:

$$\begin{aligned} A_2 &= i \frac{g_A}{2F^3} \frac{\omega_2 - \omega_3}{\omega_1} \left(\frac{4M^2}{g_A} d_{16}(\lambda) + \frac{g_A^2 M^2}{32\pi^2 F^2} + \frac{\Delta_\pi}{F^2} \left(\frac{7}{2} + \frac{g_A^2}{4} \right) \right) \\ A_4 &= -i \frac{3g_A^3 M^3}{64\pi F^5} \frac{\omega_2 - \omega_3}{\omega_1^2} \\ B_3 &= i \frac{g_A}{2F^3} \frac{\omega_1 + \omega_3}{\omega_2} \left(\frac{4M^2}{g_A} d_{16}(\lambda) + \frac{g_A^2 M^2}{32\pi^2 F^2} + \frac{\Delta_\pi}{F^2} \left(\frac{7}{2} + \frac{g_A^2}{4} \right) \right) \\ A_1 &= D_1 = D_4 = 0 \end{aligned} \quad (\text{A.50})$$

Diagram R1d:

$$\begin{aligned}
A_2 &= -i \frac{g_A}{2F^3} \left(\frac{4M^2}{g_A} d_{16}(\lambda) + \frac{g_A^2 M^2}{32\pi^2 F^2} + \frac{\Delta_\pi}{F^2} \left(\frac{7}{2} + \frac{g_A^2}{4} \right) \right) \\
B_3 &= i \frac{g_A}{2F^3} \left(\frac{4M^2}{g_A} d_{16}(\lambda) + \frac{g_A^2 M^2}{32\pi^2 F^2} + \frac{\Delta_\pi}{F^2} \left(\frac{7}{2} + \frac{g_A^2}{4} \right) \right) \\
A_1 &= A_4 = D_1 = D_4 = 0
\end{aligned} \tag{A.51}$$

Diagrams R1e+3r+s35:

$$\begin{aligned}
A_1 &= i \frac{g_A}{F^3} \frac{1}{(q_1 - q_2 - q_3)^2 - M^2} \left\{ -M^2 \left(\frac{2M^2}{F^2} \ell_3 + \frac{\Delta_\pi}{2F^2} \right) \right. \\
&\quad \left. + (t_3 - M^2) \left(\frac{4M^2}{g_A} d_{16}(\lambda) + \frac{g_A^2 M^2}{32\pi^2 F^2} + \frac{\Delta_\pi}{F^2} \left(\frac{9}{2} + \frac{g_A^2}{4} \right) + \frac{2M^2}{F^2} \ell_4 \right) \right\} \\
A_2 &= i \frac{g_A}{F^3} \frac{1}{(q_1 - q_2 - q_3)^2 - M^2} \left\{ -M^2 \left(\frac{2M^2}{F^2} \ell_3 + \frac{\Delta_\pi}{2F^2} \right) \right. \\
&\quad \left. + (t_2 - M^2) \left(\frac{4M^2}{g_A} d_{16}(\lambda) + \frac{g_A^2 M^2}{32\pi^2 F^2} + \frac{\Delta_\pi}{F^2} \left(\frac{9}{2} + \frac{g_A^2}{4} \right) + \frac{2M^2}{F^2} \ell_4 \right) \right\} \\
B_3 &= -i \frac{g_A}{F^3} \frac{1}{(q_1 - q_2 - q_3)^2 - M^2} \left\{ -M^2 \left(\frac{2M^2}{F^2} \ell_3 + \frac{\Delta_\pi}{2F^2} \right) \right. \\
&\quad \left. + (t_1 - M^2) \left(\frac{4M^2}{g_A} d_{16}(\lambda) + \frac{g_A^2 M^2}{32\pi^2 F^2} + \frac{\Delta_\pi}{F^2} \left(\frac{9}{2} + \frac{g_A^2}{4} \right) + \frac{2M^2}{F^2} \ell_4 \right) \right\} \\
A_4 &= D_1 = D_4 = 0
\end{aligned} \tag{A.52}$$

5. Counterterm amplitude at threshold:

Finally, we spell out the contribution from the various counterterms to the threshold amplitudes. At threshold, $\sqrt{s} = m + 2M_\pi$, $q_2 = q_3 = (M_\pi, 0)$ and $p_2 = (0, 0)$. The energy of the incoming pion and the incoming nucleon can be easily evaluated together with the spinor normalization factor \mathcal{N}_1 . At threshold, the amplitude is fully given by A_1 and A_2 . The contribution from the different diagrams reads:

Diagrams 2a+2b:

$$\begin{aligned}
A_1 &= -2i \frac{g_A}{F^3} \frac{M^2 v \cdot p_1}{\omega_1^2} (2c_1 + c_2 + c_3) \\
A_2 &= 0
\end{aligned} \tag{A.53}$$

Diagrams 3a+3b:

$$\begin{aligned}
A_1 &= 0 \\
A_2 &= i \frac{2g_A M}{m F^3} [2c_1 M - \omega_1 (c_2 + c_3)]
\end{aligned} \tag{A.54}$$

Diagrams 3c+3d:

$$\begin{aligned} A_1 &= i \frac{g_A}{mF^3} \frac{M^2(\omega_1^2 - M^2)}{\omega_1^2} (2c_1 + c_2 + c_3) \\ A_2 &= 0 \end{aligned} \quad (\text{A.55})$$

Diagrams 3n + 3o:

$$\begin{aligned} A_1 &= i \frac{8M^2 g_A}{F^3} \left[\frac{c_2}{2m} + \tilde{d}_{26}(\lambda) + \tilde{d}_{27}(\lambda) + \tilde{d}_{28}(\lambda) \right] \\ A_2 &= 0 \end{aligned} \quad (\text{A.56})$$

Diagram 3p:

$$\begin{aligned} A_1 &= i \frac{4M^2}{F^3} \left[\frac{g_A c_4}{2m} - d_{10}(\lambda) - d_{12}(\lambda) - d_{16}(\lambda) + \frac{1}{2} d_{18} \right] \\ A_2 &= i \frac{2M^2}{F^3} \left[-\frac{g_A c_4}{2m} - d_{11}(\lambda) - d_{13}(\lambda) + d_{16}(\lambda) - \frac{1}{2} d_{18} \right] \end{aligned} \quad (\text{A.57})$$

Diagram 3q:

$$\begin{aligned} A_1 &= i \frac{3M^3}{2F^3(\omega_1 - M)} [2d_{16}(\lambda) - d_{18}] \\ A_2 &= -i \frac{M^2(2\omega_1 - M)}{2F^3(\omega_1 - M)} [2d_{16}(\lambda) - d_{18}] \end{aligned} \quad (\text{A.58})$$

Diagram 3r: Combine with R1e.

Diagram 3s:

$$\begin{aligned} A_1 &= i \frac{g_A}{F^5} \frac{M}{\omega_1 - M} [2\ell_1 M(2\omega_1 - M) + 2\ell_2 \omega_1(2M - \omega_1) + \ell_4 M(2M + \omega_1)] \\ A_2 &= i \frac{g_A}{F^5} \frac{M}{\omega_1 - M} [2\ell_1 \omega_1(2M - \omega_1) + \ell_2(4M\omega_1 - \omega_1^2 - M^2) - \ell_4 M\omega_1] \end{aligned} \quad (\text{A.59})$$

Counterterm contribution at threshold from renormalization diagrams:

Diagram R1d:

$$\begin{aligned} A_1 &= 0 \\ A_2 &= -i \frac{2M^2}{F^3} d_{16}(\lambda) \end{aligned} \quad (\text{A.60})$$

Diagrams R1e+3r:

$$\begin{aligned} A_1 &= -i \frac{g_A}{F^3} \frac{M^3}{2(\omega_1 - M)} \left[\frac{-\ell_3 + 3\ell_4}{F^2} + \frac{6}{g_A} d_{16}(\lambda) \right] \\ A_2 &= i \frac{g_A}{F^3} \frac{M^2}{2(\omega_1 - M)} \left[\frac{M\ell_3 + (2\omega_1 - M)\ell_4}{F^2} + \frac{2(2\omega_1 - M)}{g_A} d_{16}(\lambda) \right] \end{aligned} \quad (\text{A.61})$$

Altogether:

$$\begin{aligned}
A_1 = & \frac{i}{F^3} \left\{ \frac{g_A M^2}{\omega_1^2} (2c_1 + c_2 + c_3) \left(-2v \cdot p_1 + \frac{\omega_1^2 - M^2}{m} \right) + \frac{2M^2 g_A}{m} (2c_2 + c_4) \right. \\
& + 8M^2 g_A (\tilde{d}_{26}(\lambda) + \tilde{d}_{27}(\lambda) + \tilde{d}_{28}(\lambda)) \\
& - 4M^2 (d_{10}(\lambda) + d_{12}(\lambda) + d_{16}(\lambda) - \frac{1}{2}d_{18}) - \frac{3M^3}{2(\omega_1 - M)} d_{18} \\
& + \frac{g_A}{F^2} \frac{M}{\omega_1 - M} [2\ell_1 M (2\omega_1 - M) + 2\ell_2 \omega_1 (2M - \omega_1) \\
& \left. + \ell_4 M \left(\frac{M}{2} + \omega_1 \right) + \frac{M^2}{2} \ell_3 \right] \Big\} ,
\end{aligned} \tag{A.62}$$

$$\begin{aligned}
A_2 = & \frac{i}{F^3} \left\{ \frac{g_A M}{m} (4c_1 M - 2\omega_1 (c_2 + c_3) - c_4 M) \right. \\
& - 2M^2 (d_{11}(\lambda) + d_{13}(\lambda) + \frac{1}{2}d_{18}) + \frac{(2\omega_1 - M)M^2}{2(\omega_1 - M)} d_{18} \\
& + \frac{g_A}{F^2} \frac{M}{\omega_1 - M} \left[2\ell_1 \omega_1 (2M - \omega_1) + \ell_2 (4M\omega_1 - \omega_1^2 - M^2) \right. \\
& \left. \left. + \frac{M^2}{2} (\ell_3 - \ell_4) \right] \right\} .
\end{aligned} \tag{A.63}$$

References

- [1] J. Bijnens et al., Nucl. Phys. B508 (1997) 263; (E) Nucl. Phys. B517 (1998) 639.
- [2] M. Knecht et al., Nucl. Phys. B471 (1996) 445.
- [3] V. Bernard, N. Kaiser, and Ulf-G. Meißner, Int. J. Mod. Phys. E4 (1995) 193.
- [4] J. Beringer, πN Newsletter 7 (1992) 33.
- [5] V. Bernard, N. Kaiser and Ulf-G. Meißner, Phys. Lett. B332 (1994) 415; (E) B338 (1994) 520.
- [6] V. Bernard, N. Kaiser, and Ulf-G. Meißner, Nucl. Phys. B457 (1995) 147.
- [7] V. Bernard, N. Kaiser, and Ulf-G. Meißner, Nucl. Phys. A619 (1997) 261.
- [8] J. Zhang, N. Mobed and M. Benmerrouche, **nucl-th/9806063**.
- [9] G. Ecker and M. Mojžiš, Phys. Lett. B365 (1996) 312.
- [10] N. Fettes, Ulf-G. Meißner and S. Steininger, Nucl. Phys. A640 (1998) 199.
- [11] E. Oset and M.J. Vicente-Vacas, Nucl. Phys. A446 (1985) 584.
- [12] O. Jäkel, H.W. Ortner, M. Dillig and C.A.Z. Vasconcellos, Nucl. Phys. A511 (1990) 733; O. Jäkel, M. Dillig and C.A.Z. Vasconcellos, Nucl. Phys. A541 (1992) 675.
- [13] T.S. Jensen and A. Miranda, Phys. Rev. C55 (1997) 1039.
- [14] M. Kermani et al., Phys. Rev. C58 (1998) 3431.

- [15] J.B. Lange et al., Phys. Rev. Lett. 80 (1998) 1597.
- [16] V. Bernard, N. Kaiser, and Ulf-G. Meißner, Nucl. Phys. A615 (1997) 483.
- [17] M. Kermani et al., Phys. Rev. C58 (1998) 3419.
- [18] J. Gasser and H. Leutwyler, Ann. Phys. (NY) 158 (1984) 142.
- [19] E. Jenkins and A.V. Manohar, Phys. Lett. B255 (1991) 558.
- [20] V. Bernard, N. Kaiser, J. Kambor and Ulf-G. Meißner, Nucl. Phys. B388 (1992) 315.
- [21] M. Mojžiš, Eur. Phys. J. C2 (1998) 181.
- [22] N. Fettes, Ulf-G. Meißner and S. Steininger, JHEP 9809 (1998) 008.
- [23] G. Ecker, Phys. Lett. B336 (1994) 508.
- [24] J. Bijnens, G. Colangelo and J. Gasser, Nucl. Phys. B427 (1994) 417.
- [25] M. Sevier et al., Phys. Rev. Lett. 66 (1991) 2569.
- [26] G. Kernel et al., Z. Phys. C48 (1990) 201.
- [27] A.V. Kratsov et al., Leningrad Institute of Nuclear Physics preprint No. 209, 1976.
- [28] J. Kirz, J. Schwartz and R.D. Tripp, Phys. Rev. 126 (1962) 763.
- [29] D. Počanić et al., Phys. Rev. Lett. 72 (1993) 1156.
- [30] Yu.A. Batsuv et al., Sov. J. Nucl. Phys. 21 (1975) 162.
- [31] M. Arman et al., Phys. Rev. Lett. 29 (1972) 962.
- [32] V. Barnes et al., CERN Report 63-27, 1963.
- [33] G. Kernel et al., Phys. Lett. B216 (1989) 244; *ibid* B225 (1989) 198.
- [34] C.W. Bjork et al., Phys. Rev. Lett. 44 (1980) 62.
- [35] J.A. Jones, W.W.M. Allison and D.H. Saxon, Nucl. Phys. B83 (1974) 93.
- [36] I.M. Blair et al., Phys. Lett. B32 (1970) 528.
- [37] D.H. Saxon, J.H. Mulvey and W. Chinowsky, Phys. Rev. D2 (1970) 1790.
- [38] Yu.A. Batsuv et al., Sov. J. Nucl. Phys. 1 (1965) 374.
- [39] T.D. Blokhintseva et al., Sov. Phys. JETP 17 (1963) 340.
- [40] J. Deahl et al., Phys. Rev. 124 (1961) 1987.
- [41] W.A. Perkins et al., Phys. Rev. 118 (1960) 1364.
- [42] J. Lowe et al., Phys. Rev. C44 (1991) 956.
- [43] A.A. Bel'kov et al., Sov. J. Nucl. Phys. 31 (1980) 96.
- [44] A.A. Bel'kov et al., Sov. J. Nucl. Phys. 28 (1978) 657.
- [45] S.A. Bunyatov et al., Sov. J. Nucl. Phys. 25 (1977) 177.
- [46] A.V. Kratsov et al., Sov. J. Nucl. Phys. 20 (1975) 500.
- [47] M.D. Manley, Phys. Rev. D30 (1984) 536.
- [48] M.D. Manley, Phys. Rev. D30 (1984) 904.
- [49] R. Müller et al., Phys. Rev. C48 (1993) 981.
- [50] U. Bohnert, Thesis, University of Erlangen, 1993.
- [51] D. Malz, Thesis, University of Erlangen, 1989.

Figures

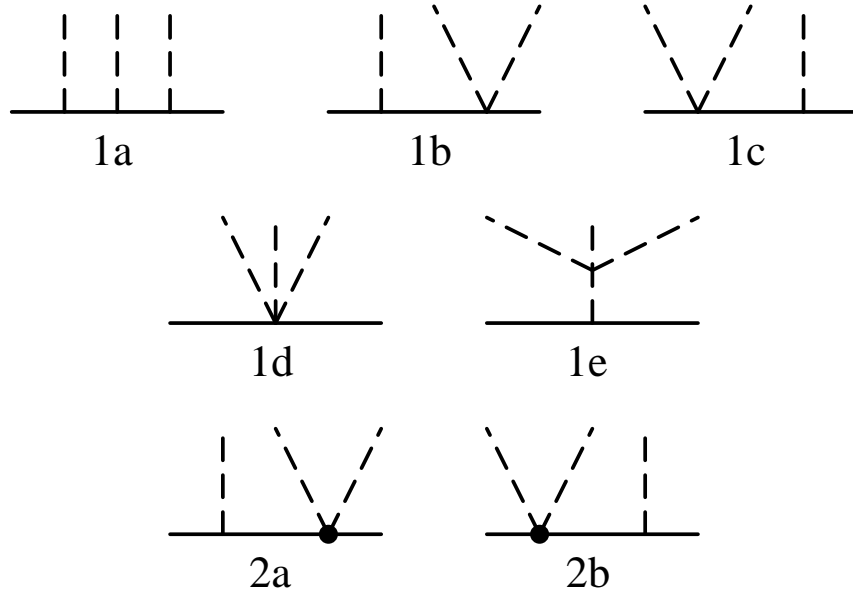


Figure 1: Tree graphs with insertions from the dimension one Lagrangian (1a–1e) and the dimension two Lagrangian as depicted by the dot (2a,b). Solid and dashed lines denote nucleons and pions, respectively.

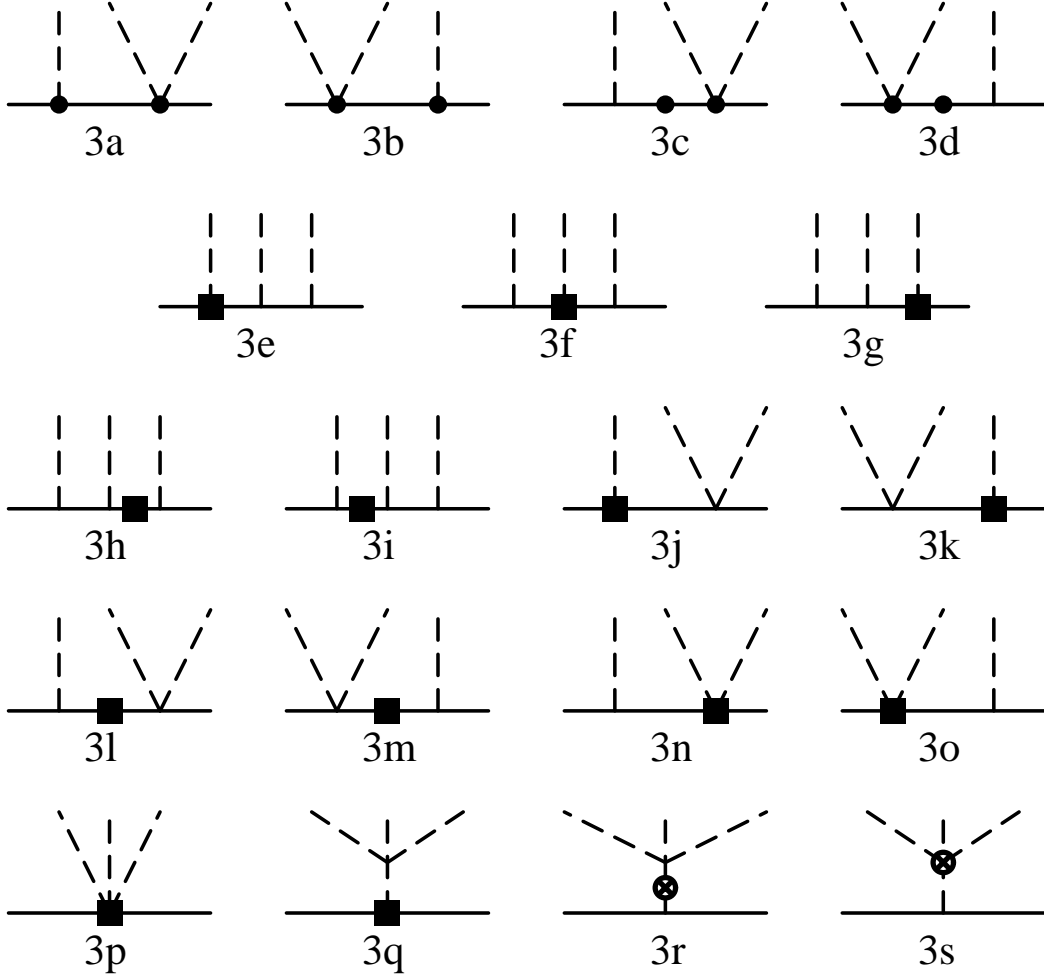


Figure 2: Tree graphs of third order in the chiral expansion. The filled box denotes an insertion from the dimension three pion–nucleon Lagrangian whereas the circle–cross denotes a fourth order mesonic insertion.

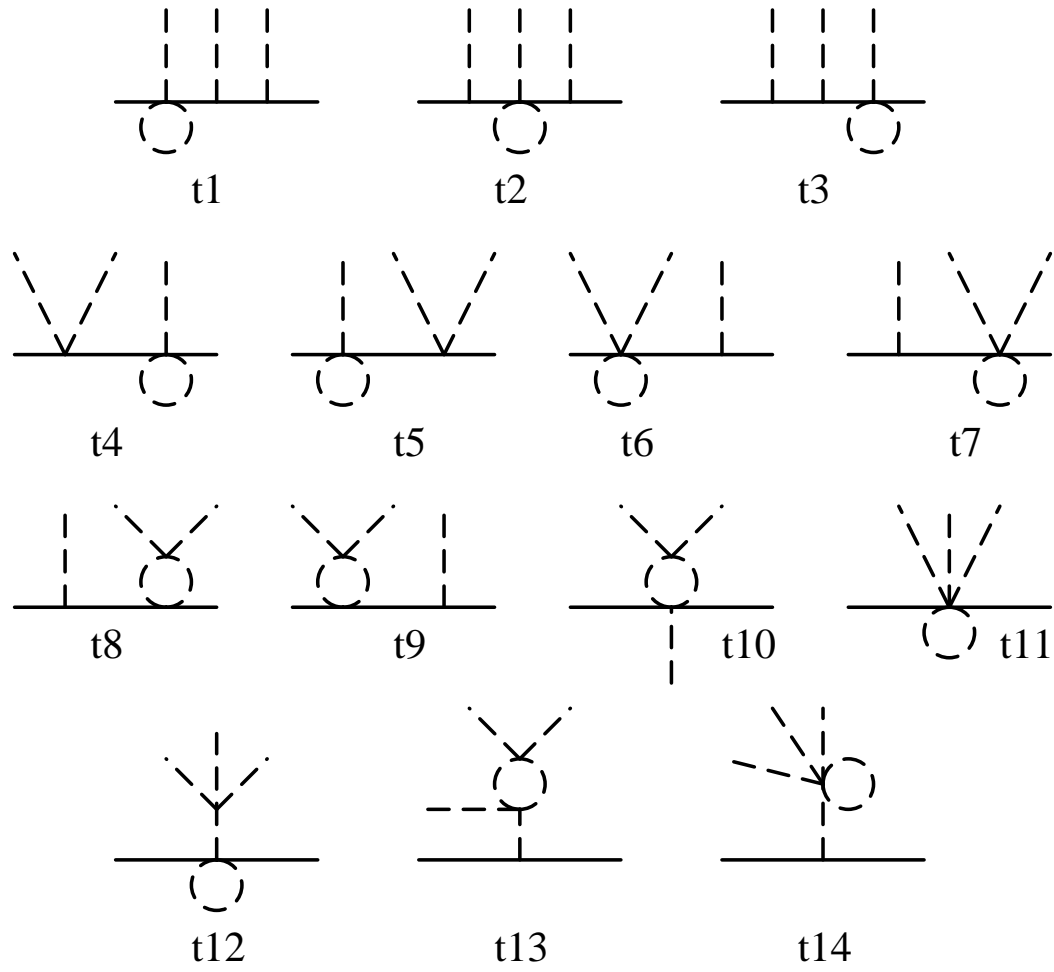


Figure 3: One-loop graphs of the tadpole type.

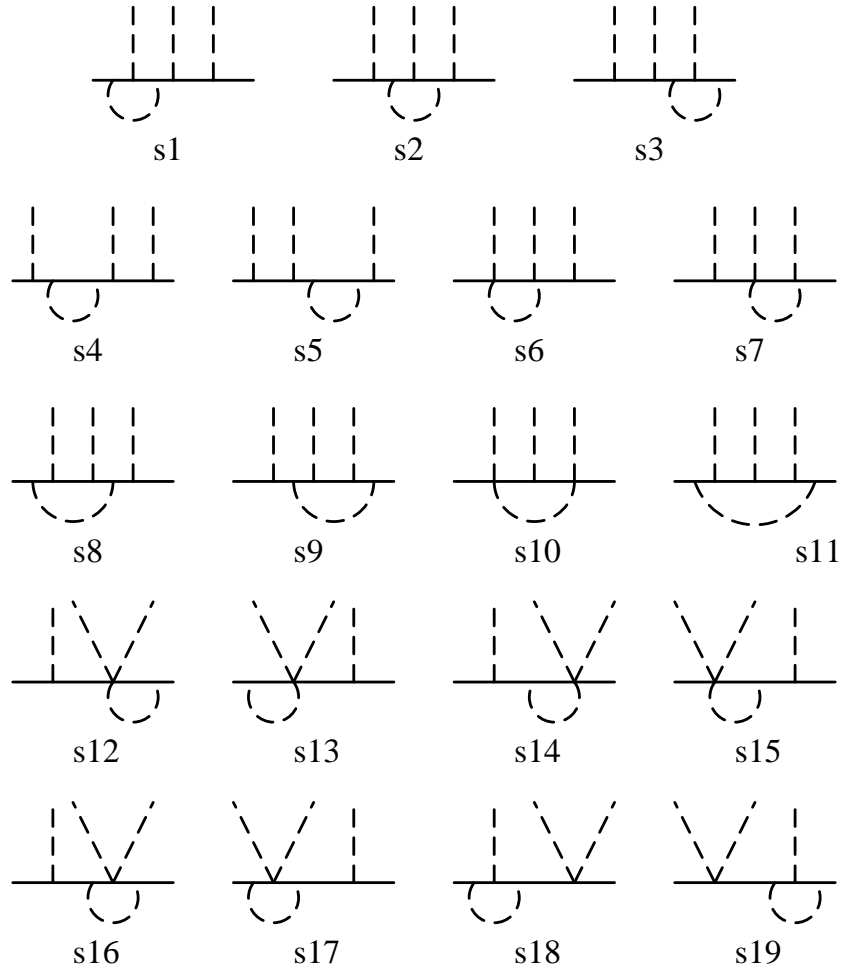


Figure 4: One-loop graphs of the self-energy type.

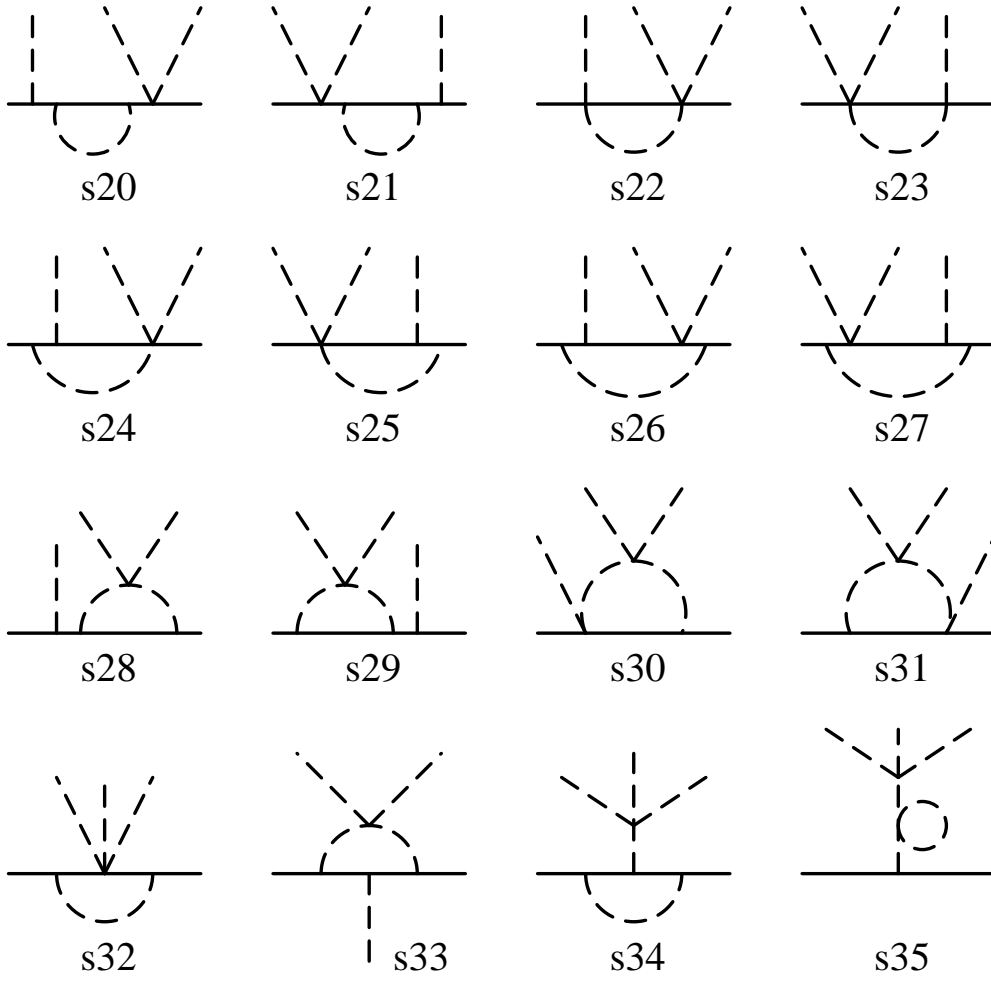


Figure 5: Further one-loop graphs of the self-energy type.

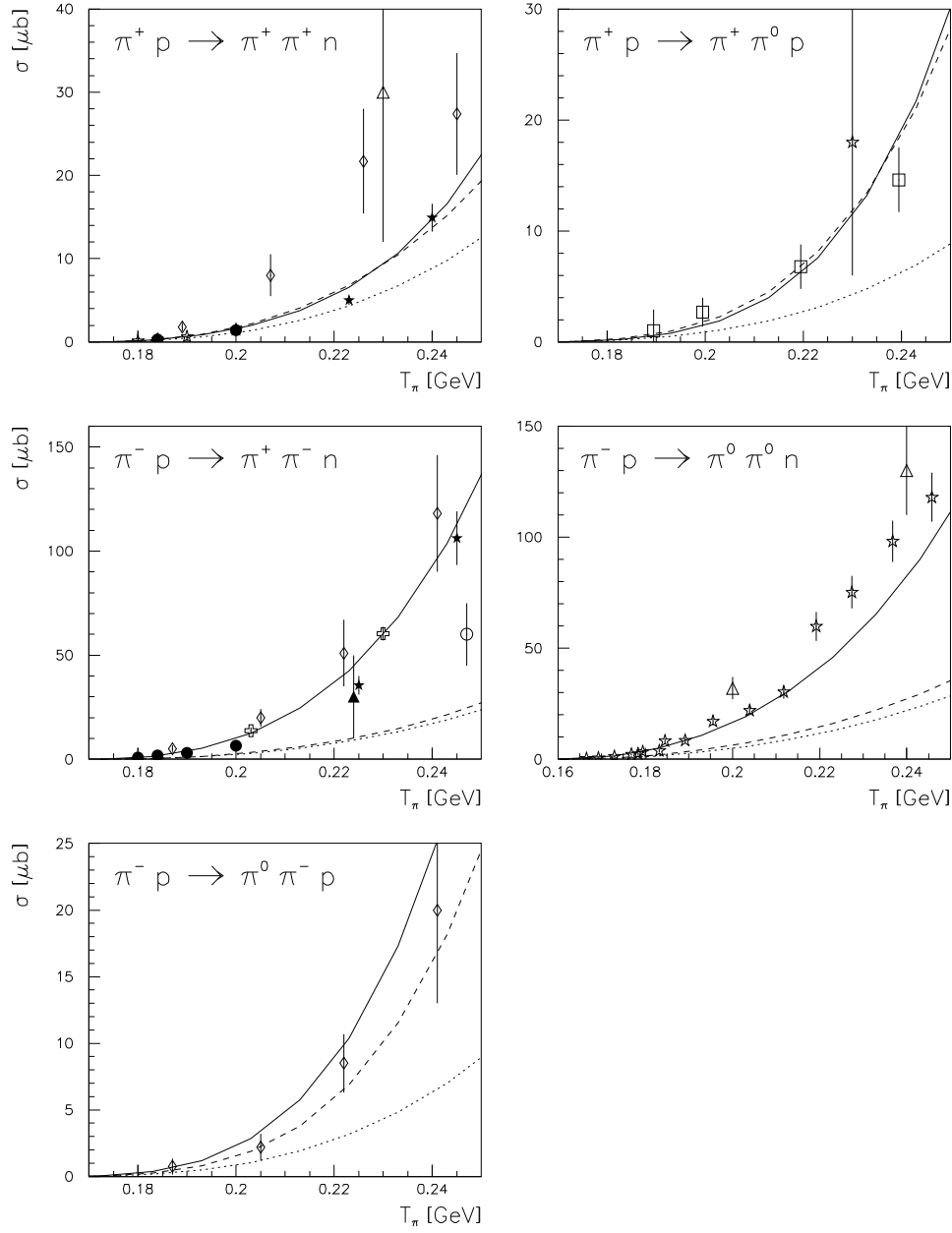


Figure 6: Fits to the total cross sections (solid lines). The dashed and dotted lines refer to the second and first order contributions, respectively.

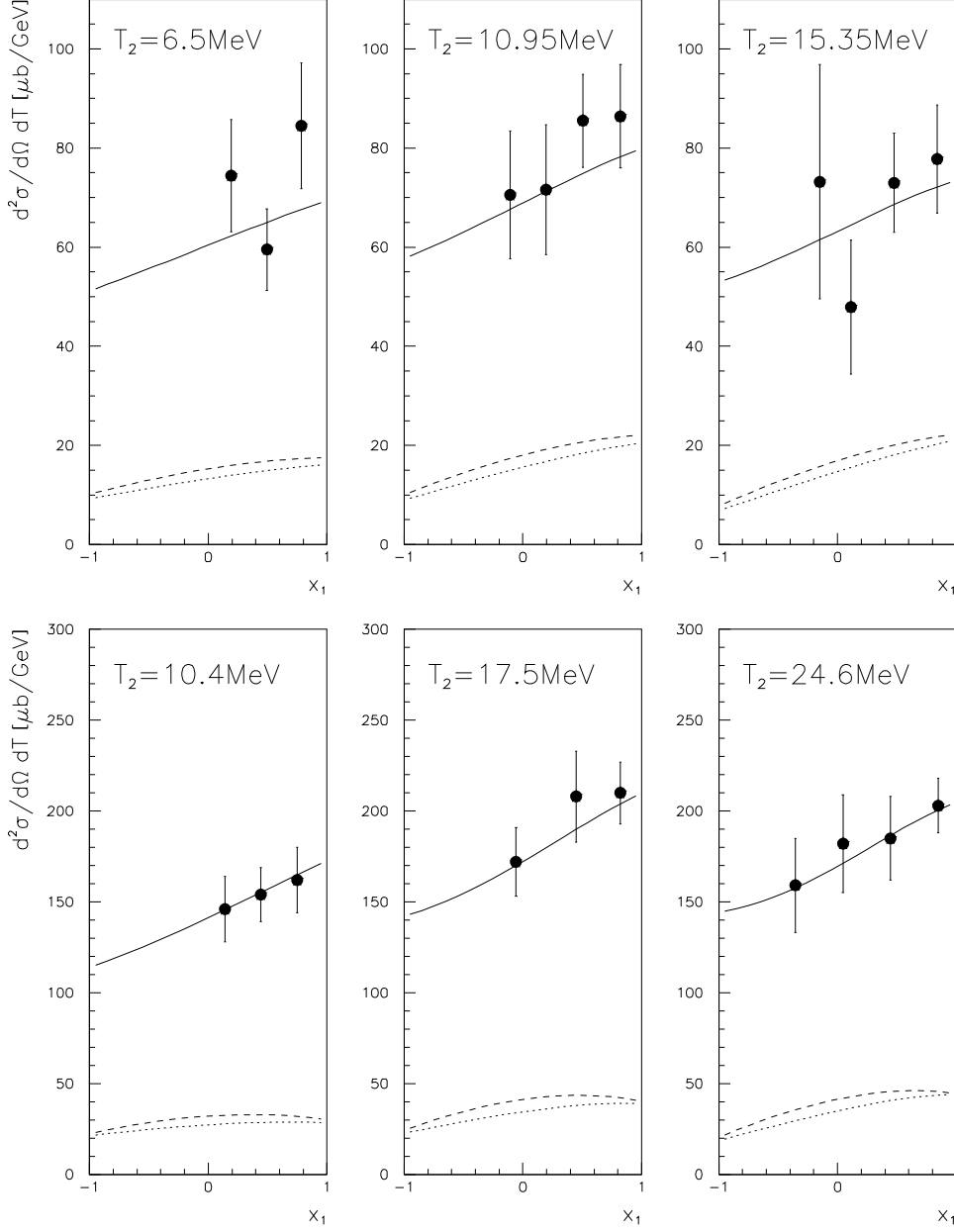


Figure 7: Fits to the differential total cross sections for $\pi^-p \rightarrow \pi^+\pi^-n$ (solid lines) with respect to the kinetic energy and of solid angle the outgoing π^+ . $T_2 = \omega_2 - M_\pi$ refers to the outgoing positively charged pion. For further notations, see fig.6.

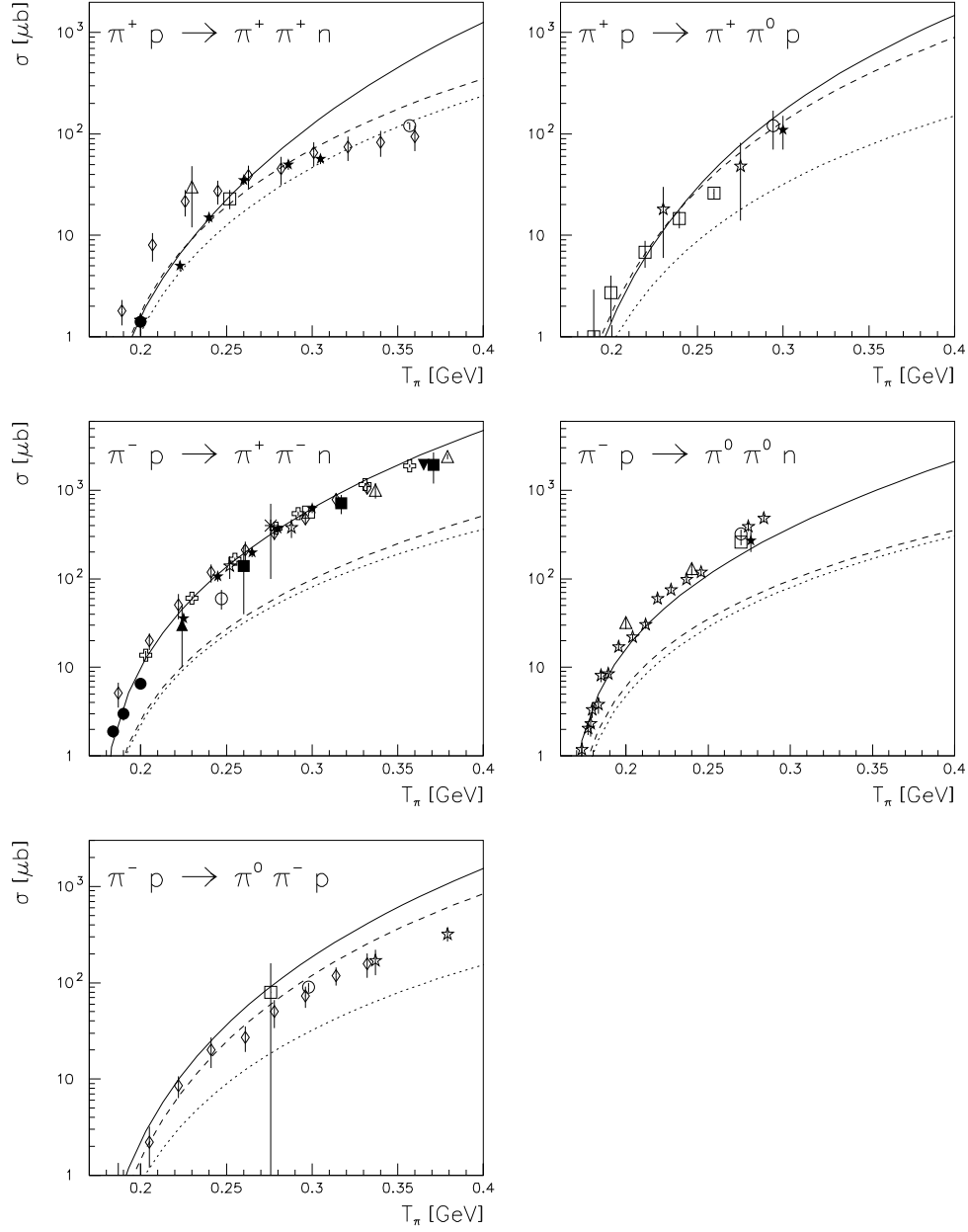


Figure 8: Predictions for the total cross sections up to $T_\pi = 400$ MeV (solid lines). For further notations, see fig.6.

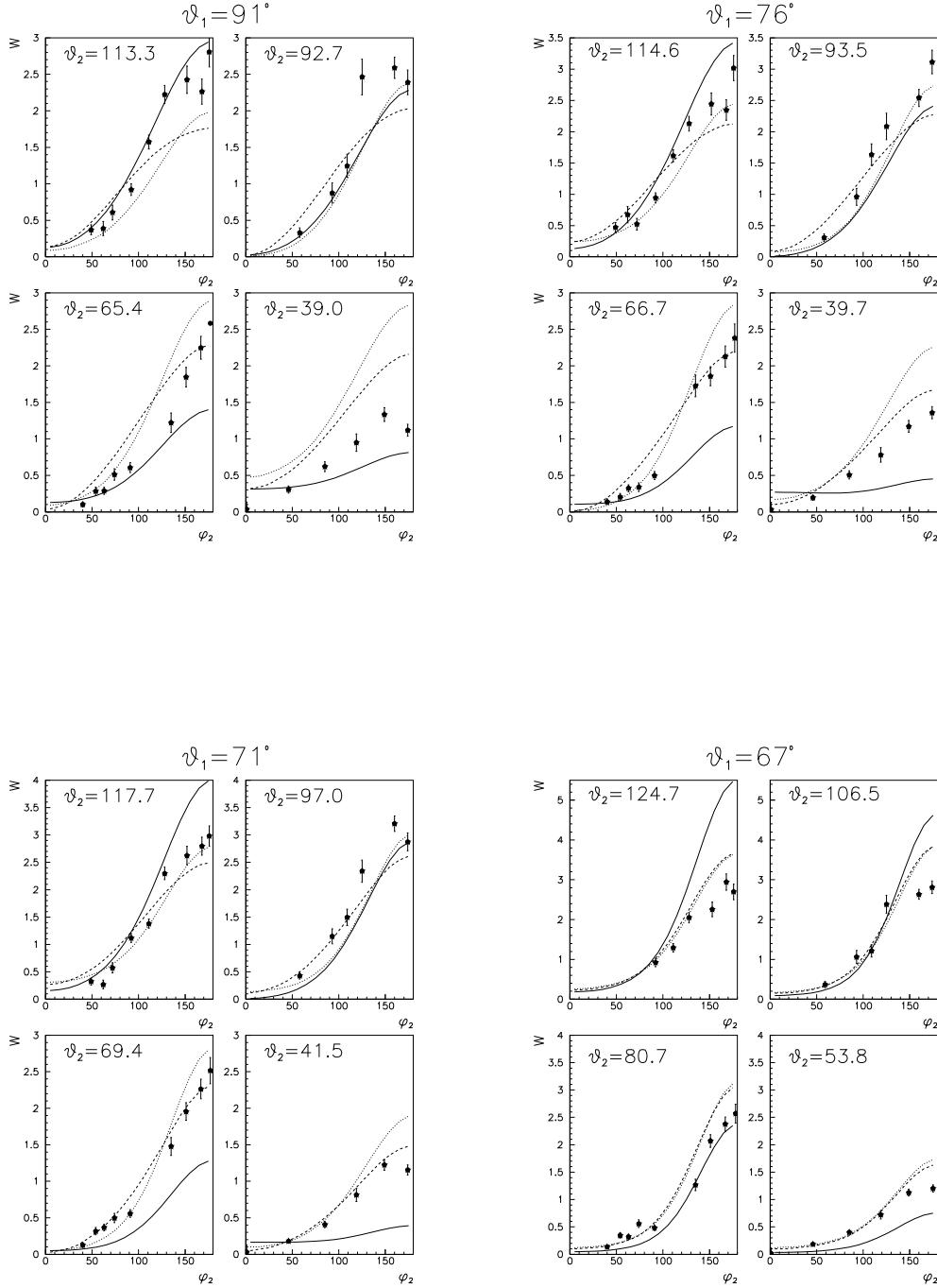


Figure 9: Predictions for the angular correlation functions at fixed θ_2 . For further notations, see fig.6.

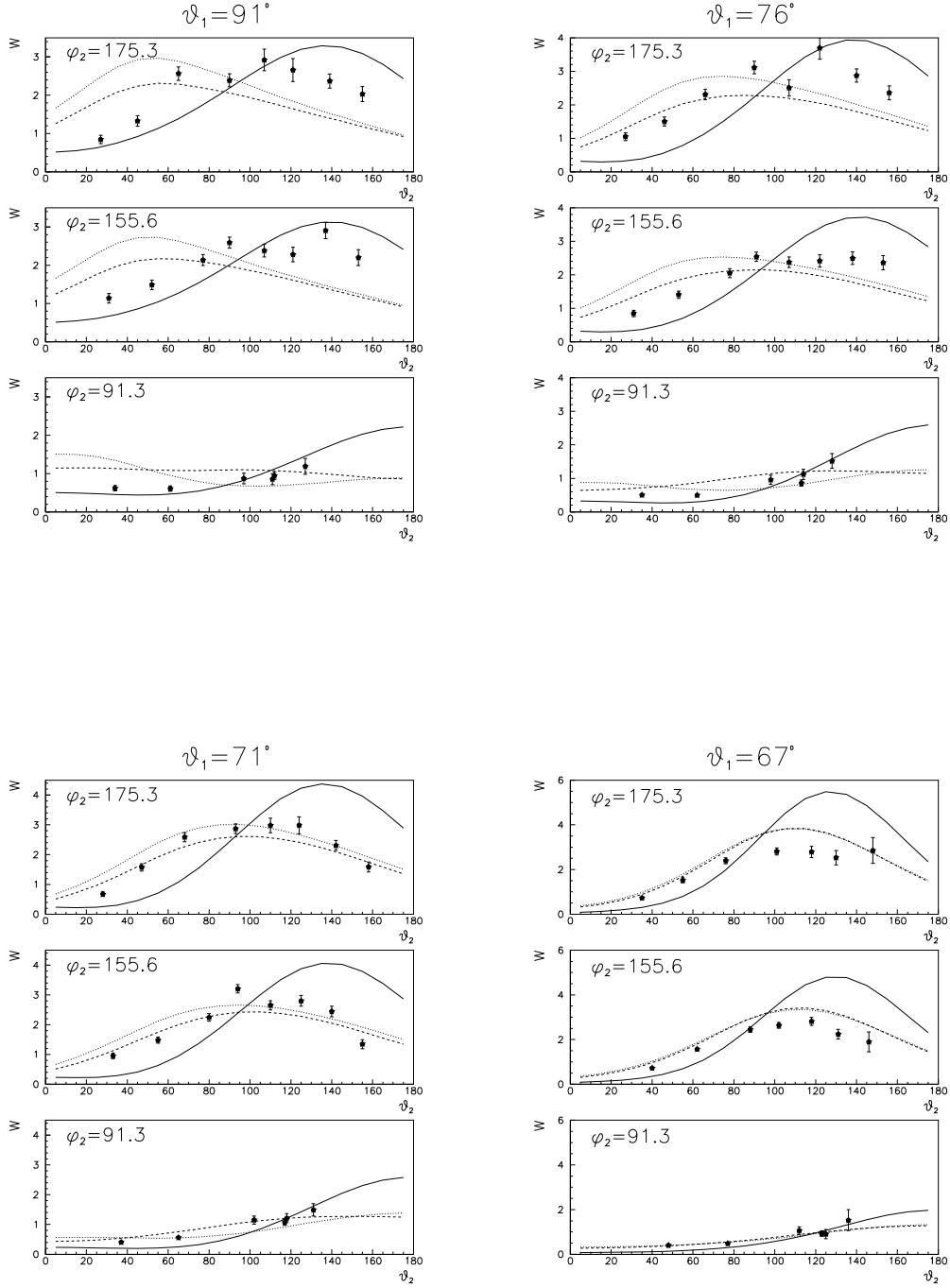


Figure 10: Predictions for the angular correlation functions at fixed φ_2 . For further notations, see fig.6.

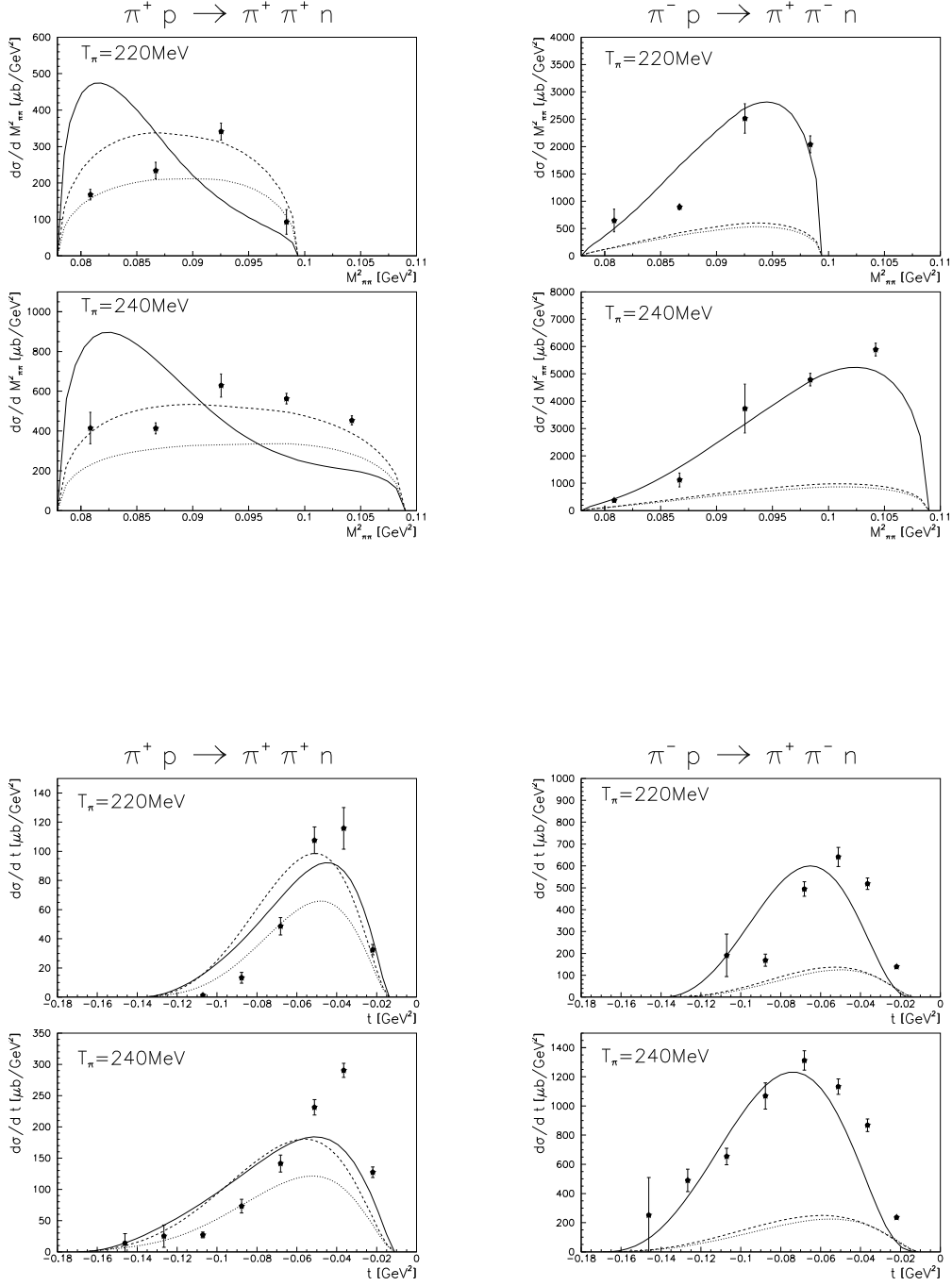


Figure 11: Predictions for the differential cross sections $d\sigma/dM^2_{\pi\pi}$ and $d\sigma/dt$. For further notations, see fig.6.

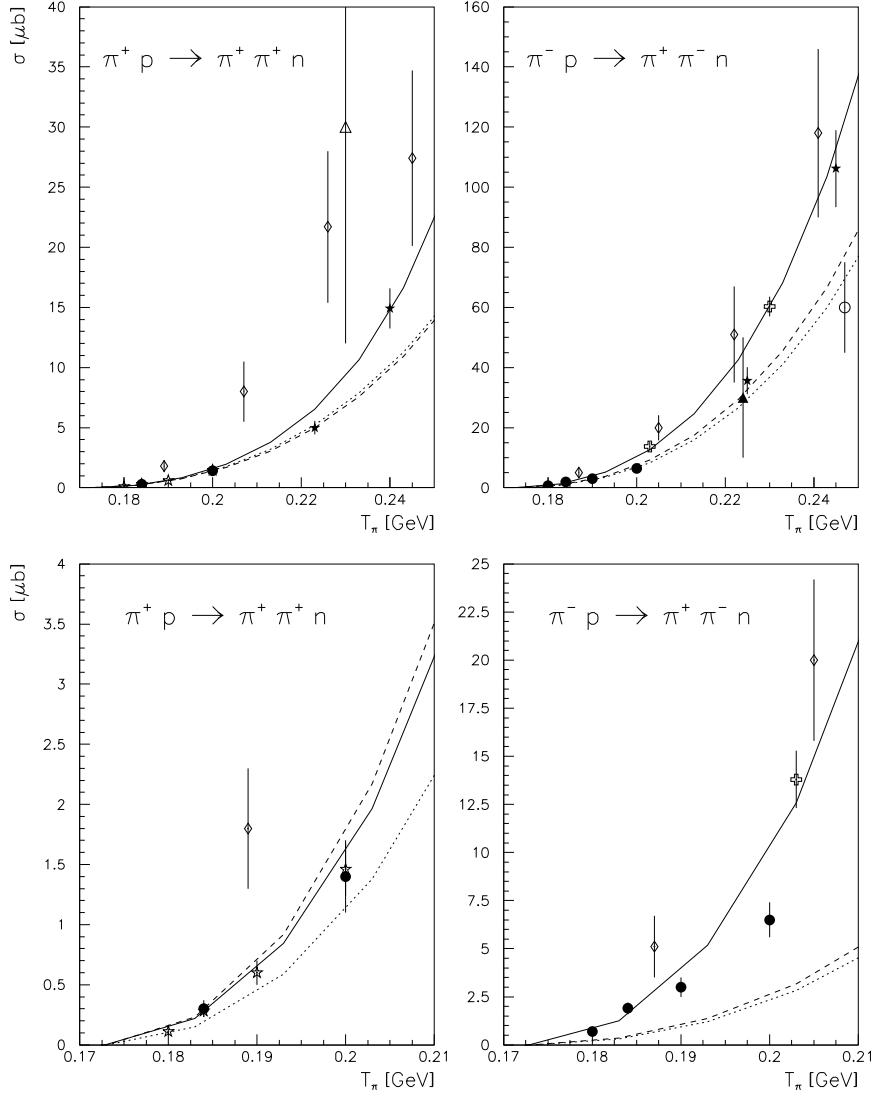


Figure 12: Chiral expansion. In the upper two panels, the solid, dashed and dotted lines refer to the contribution up to third, second and first order respectively. In the lower panels, the dashed lines show the third order contribution minus the ones from the dimension three contact terms. Similarly, for the dotted lines the loop contributions are in addition subtracted.

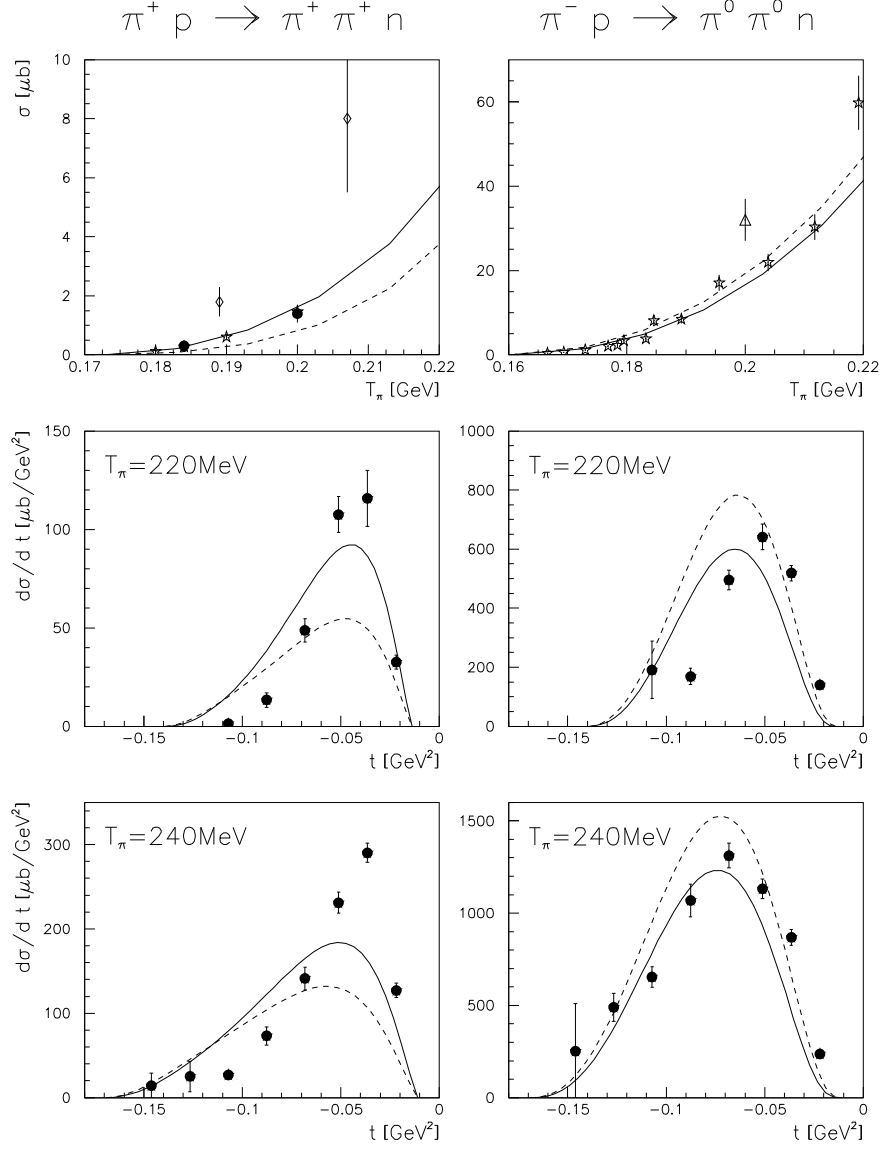


Figure 13: Sensitivity to the pion-pion interaction. Considered are the two channels $\pi^+ p \rightarrow \pi^+ \pi^+ n$ (left) and $\pi^- p \rightarrow \pi^0 \pi^0 n$ (right). Upper panels: Total cross sections in the threshold region. Middle panels: $d\sigma/dt$ at $T_\pi = 220$ MeV. Lower panels: $d\sigma/dt$ at $T_\pi = 240$ MeV. The solid line refers to the standard case, whereas the dashed lines are obtained by setting $\bar{l}_3 = -70$ and keeping all other LECs fixed.